



LIFE+11 ENV/IT/002

CLEAN-ROADS

Action A2: Project Requirements Analysis

D.A2.2

Technological instruments and constraints



Project Coordinating Beneficiary	Provincia di Trento (PAT)
Project Associated Beneficiary n.1	Famas System (FAM)
Project Associated Beneficiary n.2	TIS innovation park (TIS)



PROVINCIA AUTONOMA DI TRENTO





Document history

Date	Document Author(s)	Document Contribution
15/01/2014	Roberto Cavaliere (TIS), Stefano Seppi (TIS), Ilaria Pretto (PAT), Giacomo Merler (PAT), Thomas Tschurschenthaler (Famas), Roberto Apolloni (Famas)	Document finalization

Dissemination level: PU¹

Delivery month: M16

Status: submitted to the EC

¹ **PU** = Public.

CO = Confidential (accessible only by project partners and European Commission).

RE = Restricted Access, i.e. confidential but with a special access to a specific target of stakeholders defined by the project consortium and approved by the European Commission.



Table of Contents

1.	Introduction.....	10
2.	Technologies for mobile and static data sources.....	11
2.1	Overview of parameters and factors influencing road conditions.....	11
2.1.1	Road construction	12
2.1.2	Geographical parameters.....	16
2.1.3	Traffic flows.....	25
2.1.4	Meteorological conditions.....	27
2.2	Road-weather stations.....	35
2.2.1	Power supply.....	37
2.2.2	Remote control and communication unit.....	38
2.2.3	Road conditions measurement technologies.....	39
2.2.4	Roadside weather conditions measurement technologies.....	43
2.2.5	Traffic conditions measurement technologies.....	53
2.3	Mobile probes.....	57
3.	Road-weather models.....	61
3.1	Numerical prediction of weather forecasts.....	62
3.1.1	Forecast models classification.....	63
3.1.2	Data assimilation and parameterization processes.....	64
3.1.3	Ensemble forecasts and nowcasting.....	66
3.1.4	Weather forecasts limitations in mountainous areas.....	66
3.2	Weather forecasts reference models.....	68
3.2.1	ECMWF model.....	69
3.2.1	COSMO N2 RUC model.....	70
3.2.2	WRF model.....	71
3.3	Road-weather reference models.....	72
3.3.1	Zero-dimensional models.....	75
3.3.2	One-dimensional models.....	75
3.3.3	Two/three-dimensional models.....	76
3.4	State-of-art models.....	77
3.4.1	METRo.....	78
3.4.2	FASST.....	86
3.4.3	GeoTop.....	91
3.4.4	Other road weather models.....	93
3.5	Future perspectives in the road weather modeling.....	93
4.	Maintenance Decision Support Systems.....	97
4.1	RWIS-driven advanced winter maintenance methods.....	99



4.1.1	Salting treatments recommendations	100
4.1.2	Dynamic maintenance activities control.....	104
4.1.3	Real-time information services	105
4.2	Best-practices overview	108
4.2.1	Pilot initiatives	108
4.2.2	Research projects	115
5.	A glance to cooperative ITS	120
5.1	Cooperative Vehicle Infrastructure technologies	120
5.2	C-ITS projects in the RWIS domain	121
5.2.1	WiSafeCar.....	121
5.2.2	CoMoSeF	122
5.3	Early commercial connected products for RWIS	123
	Conclusions.....	124
	Bibliography	125

Table of Figures

Figure 1: Four-layers asphalt profiles [2].....	12
Figure 2: Reference geometry considered in the definition of thermal conductivity.	14
Figure 3: Incoming radiation and energy components split.	15
Figure 4: Typical values of albedo for different materials within the road infrastructure scenario [5].....	15
Figure 5: Solar altitude and azimuth: geometrical representation (source: en.wikipedia.com). 16	16
Figure 6: Effective solar radiation at different latitudes(source: geog.ucsb.edu).....	17
Figure 7: Empirical relation between latitude and a winter index calculated in Sweden at a national, regional and county scale [12].....	18
Figure 8: Typical RST variation patterns that can be observed through thermal mapping surveys in case of altitude profile variations [14].....	19
Figure 9: Simple representation of katabatic theory (source: weatheronline.co.uk).....	20
Figure 10: Thermal belt and air temperature variations as a consequence of thermal inversion phenomena (source: weatheronline.co.uk).....	20
Figure 11: Typical RST variation patterns which can be recorded through thermal mapping operations in case of evident screening phenomena [21].	21
Figure 12: Geometrical representation of the calculation of the building angle in the screening factor evaluation process [5].....	22
Figure 13: Simplified representation of different sky-view factors conditions.....	23
Figure 14: A graphical representation of the urban heat island phenomenon.....	23
Figure 15: Sky-view factor measurements in an urban scenario – empirical results example [32].	24
Figure 16: Main contribution to energy balance conditions of RST caused by vehicular transits [37] - [38].....	25
Figure 17: Lane-based comparison between RST measurements and traffic data.	26
Figure 18: Road thermal images and RST – traffic correlation assessment [37].	27
Figure 19: Power density of the solar and terrestrial radiation in the wavelength domain (source: suyts.wordpress.com).....	28
Figure 20: Solar and terrestrial radiation patterns (source: ete.cet.edu).....	29
Figure 21: A graphical representation of the typical effect of cloud cover factor at night.....	30
Figure 23: A graphical representation of the process of formation of snow.....	31
Figure 22: A graphical representation of the process of formation of freezing rain.	31
Figure 24: An overview of all possible road slipperiness situations caused by meteorological factors.	32
Figure 25: Relationship between air temperature (x-axis) and dew point (y-point) in correspondence to different relative humidity conditions (Magnus-Tetens approximation). ...	33
Figure 26: Nocturnal spatial RST variations at road stretches dominated by local topography in different wind conditions [47].	34

Figure 27: The main elements of a complete road weather monitoring system.....	35
Figure 28: High-level architecture of a static RWIS station.	36
Figure 29: The fuel cell based power supply system installed within the ASFINAG highway network [48].....	37
Figure 30: The MotionPower™ energy production system based on the accumulation of the kinematics energy released by the transit vehicles [49].	38
Figure 31: NTC temperature sensor measurement principle.....	40
Figure 32: Reference high-level architecture of a pyrometer (Source: globalspec.com).....	41
Figure 33: Infrared pyrometer camera (Source: testolimited.com).	41
Figure 34: Possible design of an invasive road conditions sensor [51].	42
Figure 35: Remote sensing techniques applied in the road weather application domain for non-invasive road conditions measurements.....	43
Figure 36: The reference geometry of a capacitor.	44
Figure 37: Empirical relationships between capacity and relative humidity in different dielectric sensing elements: (a) standard capacitive element [56]; (b) MWCNTs [55].....	44
Figure 38: Typical layout of a piezoresistive air pressure sensor [57].	45
Figure 39: Absolute air pressure level measurement approach.	45
Figure 40: Typical layout of a capacitive air pressure sensor [58]	46
Figure 41: Principle of functioning of an optical disdrometer (source: thiesclima.com).....	47
Figure 42: Mechanical anemometer example.	49
Figure 43: Reference architecture of an electronic anemometer based on a 2D thermal flow sensor [60].	49
Figure 44: Layout of an electronic anemometer based on ZDT approach [59].....	49
Figure 45: Sonic anemometer.....	50
Figure 46: Principle of functioning of an acoustic-resonance anemometer (Source: FT Technologies).....	50
Figure 47: Principle of functioning of a Laser Doppler Anemometer (Source: dantecdynamics.com).....	51
Figure 48: Principle of functioning of a common visibility meter [60].	52
Figure 49: Principle of functioning of a camera-based visibility meter [60]	52
Figure 50: Principle of an inductive loop (source: auto.howstuffworks.com)	54
Figure 51: Principle of a magnetic traffic detector (source: fhwa.dot.gov)	54
Figure 52: Principle of a piezoelectric traffic detector (source: metrocount.com).....	55
Figure 53: Principle of an active infrared traffic detector (source: fhwa.dot.gov)	55
Figure 54: Ultrasonic vehicle detector (source: global-sei.com).	56
Figure 55: Video image processing techniques applied to traffic detection domain (source: aldridgetrafficcontrollers.com.au).....	56
Figure 56: Traffic jams detection through FCD messages [62].....	57
Figure 57: On-board systems which can provide XFCD that can be potentially used in RWIS [62].	58
Figure 58: Different friction measurement devices mounted on a probe vehicles [64].....	59



Figure 59: Road construction discontinuities detection through GPR [65].....	60
Figure 60: Road weather models reference elaboration chain.....	61
Figure 61: An overall perspective of the atmosphere phenomena which determine the weather conditions [66].....	62
Figure 62: The improvements of ECMWF weather forecasts in the two hemispheres among years (Source: ECMWF).	63
Figure 63: LAM and global models (source: FMI)	64
Figure 64: A complete perspective of different data sources of weather data (source: Met Office).....	65
Figure 65: Space and time scales for convective precipitation phenomena (source: ECMWF). 65	
Figure 66: Example of ensemble forecast output (source: easterbrook.ca).....	66
Figure 67: The orography of the Autonomous Province of Trento in the COSMO NWP model. 67	
Figure 68: The orography of the north of Italy in the ECMWF NWP models.....	68
Figure 69: An example of output of the ECMWF NWP model [70].	70
Figure 69: An example of output of the COSMO N2 RUC model.	71
Figure 71: An example of output of the WRF model run by local company CISMA.	72
Figure 72: A graphical representation of different dimensional road weather models.	73
Figure 72: An example of the route-based forecast output which can be obtained through a XRWIS [74].	74
Figure 73: A possible output of Salting Routing Optimization algorithms [74].	74
Figure 75: The three stages of the METRo forecast process [79].	82
Figure 76: METRo input files – static RWIS station configuration file.....	84
Figure 77: METRo input files – list of surface observation parameters required.....	84
Figure 78: METRo input files – static RWIS station measurements file.....	85
Figure 79: METRo input files – list of forecast parameters required.....	85
Figure 80: METRo input files – forecasts file.	86
Figure 81: The application domain of FASST model.	87
Figure 82: An overview of the interaction between of the flow of FASST model.	88
Figure 83: An example of the FASST input file generated by Met Reader.....	89
Figure 84: Reference soil types details defined by FASST.....	90
Figure 85: An example of FASST input file with the initial conditions and site information.....	90
Figure 86: An example of the spatial outputs of GEOtop.	92
Figure 87: The fuzzy approach of HS4Cast model [87].....	94
Figure 88: The future evolution of road weather models [88].	95
Figure 89: Deterministic road weather forecast [90].....	97
Figure 90: Probabilistic road weather forecast [90].	98
Figure 91: A blueprint of probabilistic RWIS [90].	98
Figure 92: The advanced winter road maintenance model defined by TU Wien [92].....	100



Figure 93: Residual salt quantities in different road conditions - empirical assessments of TU Wien [92].	101
Figure 94: Recommendations' summary to road operators and drivers from TU Wien research study [92].	102
Figure 95: Preventive treatments – reference physical mechanism [92].	103
Figure 96: Delayed treatments – reference physical mechanism [92].	103
Figure 97: Application rates suggested for different road weather conditions [92].	104
Figure 98: Recommendations' summary to road operators and drivers from TU Wien research study [92].	105
Figure 99: Application of WCSA approach to Finland [95].	106
Figure 100: Winter road weather information – potential market in the EU [96].	107
Figure 101: Real-time road weather online service example in Finland [99].	108
Figure 102: Traffic jam predictor based on traffic flows and road weather forecasts [102].	109
Figure 103: The static RWIS stations' network in Latvia [103].	109
Figure 104: The integrated open ITS business model chain in Latvia [103].	110
Figure 105: The static RWIS stations' network in Slovenia [104].	111
Figure 106: The RWIS in use in Slovakia [105].	111
Figure 107: The RWIS used by ASFINAG [106].	112
Figure 108: The MDSS HMI used in ASFINAG RWIS [105].	113
Figure 109: The multiple application domains of the Clarus system (source: http://www.its.dot.gov/clarus/).	113
Figure 110: An example of the elaborated information from the BiFi system [110].	115
Figure 111: The architecture of the SRIS project [111].	116
Figure 112: The evolution of mobile road conditions observations [112].	118
Figure 113: The architecture of a C-ITS system [118].	121
Figure 114: The architecture of the CoMoSeF project [120].	122
Figure 115: A screenshot of the AVL Genius application (source: www.viaesys.com).	123



Table of Tables

Table 1: List of features and factors influencing the conditions of the roads (adapted from [1]). 12	
Table 2: List of all possible road conditions classes and precipitation types.....	31
Table 3: Comprehensive overview of the invasive and non-invasive technologies for the measurement of road conditions parameters.....	39
Table 4: Performances of invasive and non-invasive RST measurement techniques.....	41
Table 5: Performances of invasive and non-invasive water film layer measurement techniques.....	43
Table 6: Overview of the physical principles at the base of state-of-art anemometer classes. 48	
Table 7: Reference measurement ranges and accuracies for different meteorological parameters.....	53
Table 8: NWP models of interest for CLEAN-ROADS – forecasted meteorological parameters.....	69
Table 9: Details of the temporal runs of ECMWF, WRF and COSMO NWP models.....	69
Table 10: Overview of the main features of the ECMWF HRES model.....	70
Table 11: Overview of the main features of the COSMO N2 RUC model.....	71
Table 12: Overview of the main features of the WRF model run by the local company CISMA. 72	
Table 13: A comparison between FASST and METRo models.....	96
Table 14: Detection capabilities of pure static, pure mobile and hybrid RWIS.....	118



1. Introduction

This report summarizes the activities and results carried out within Task A2.2, which is the responsible of the initial technological requirements evaluations. The output of this deliverable is functional to the requirements analysis process which has been reported in the other deliverable produced by Action A2, namely D.A2.1 “*Target users functional requirements*”. For more details concerning the methodology and activities carried out in this preparatory action, please refer to the introduction of this deliverable.

The document is organized in five different chapters. Chapter 2 presents a comprehensive overview of the different physical phenomena that influence the conditions of the road network, in particular during the winter season. Chapter 3 offers an analysis of the reference state-of-art in the fields of numerical prediction of weather forecasts and road weather modeling techniques. Chapter 4 gives a perspective of the basic elements of a Road Weather Information System (RWIS), and in particular of the peculiarities of Maintenance Decision Support System, providing evidence of best-practices and activities carried out all around the world; finally, Chapter 5 provides some final insights about the future evolution of RWIS in the perspective of cooperative intelligent transportation systems (C-ITS).

2. Technologies for mobile and static data sources

2.1 Overview of parameters and factors influencing road conditions

Road surface temperature (RST) is a variable which can vary significantly in time and space as a function of a multitude of *influencing factors* of very different nature: **road construction**; **local geography**; **traffic flows** and **meteorological conditions**. Each of these influencing factors is characterized by a set of specific parameters (“*features*”), which play a certain role in the targeted road weather problem. From a mathematical point of view, this complex and multi-disciplinary dependency can be represented as follows:

$$RST(t) = f(\underline{R}, \underline{G}, T(t), \underline{W}(t)) \quad [1]$$

where \underline{R} indicates a vector of features associated to the road construction influencing factor, \underline{G} a vector of geographical features which take in particular account the position of the road within the network and the orography of the surrounding environment, $T(t)$ the traffic volumes and $\underline{W}(t)$ a vector of meteorological features.

From an engineering point of view, this is a classical problem of *pattern recognition*, in which the goal is to associate to an input multi-dimensional pattern belonging to a certain feature space either a function (e.g. RST) or a thematic class (e.g. the condition of the road) through a regression or classification approach, respectively. In the latter case, the problem can be formulated as follows:

$$\{\underline{R}, \underline{G}, T(t), \underline{W}(t)\} \rightarrow \Omega = \{\omega_1, \omega_2, \omega_3, \omega_4, \omega_5\} \quad [2]$$

where $\Omega = \{\omega_1, \omega_2, \omega_3, \omega_4, \omega_5\}$ is the set of thematic classes, in particular ω_1 indicates dry road conditions, ω_2 wet road conditions, ω_3 is associated with the presence of ice on the road, ω_4 is associated with the presence of frost and ω_5 is associated with the presence of snow. All features belonging to the different influencing factors are summarized in Table 1.

Influencing factor	Feature
Road construction \underline{R}	<ul style="list-style-type: none"> • Depth of construction (R_1) • Thermal conductivity (R_2) • Thermal diffusivity (R_3) • Emissivity (R_4) • Albedo (R_5)
Geography \underline{G}	<ul style="list-style-type: none"> • Latitude (G_1) • Altitude (G_2) • Topography (G_3) • Screening (G_4)

Traffic $T(t)$ Meteorology $W(t)$	<ul style="list-style-type: none"> • Sky-view factor (G_5) • Landuse (G_6) • Topographic exposure (G_7)
	<ul style="list-style-type: none"> • Traffic volumes • Solar radiation ($W_1(t)$) • Terrestrial radiation ($W_2(t)$) • Air temperature ($W_3(t)$) • Cloud cover and type ($W_4(t)$) • Wind speed ($W_5(t)$) • Humidity and dew point ($W_6(t)$) • Precipitation ($W_7(t)$)

Table 1: List of features and factors influencing the conditions of the roads (adapted from [1]).

2.1.1 Road construction

From a purely road construction point of view, a road can be considered as a solid element characterized by different overlapping layers, which guarantee the transmission of the superficial loads on the ground with a minimum of deformability and wear. At present, road construction profiles can be of two different types: (i) **rigid concrete profiles**, which are intrinsically much more resistant and therefore long-lasting, and (ii) **flexible four-layers asphalt profiles** (Figure 1), which are the most used in practice, since they guarantee much more reduced building times and costs.

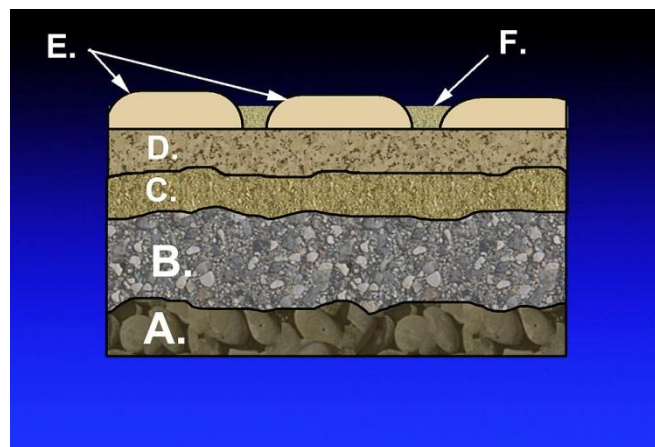


Figure 1: Four-layers asphalt profiles [2].

From a purely road construction point of view, a road can be considered as a solid element characterized by different overlapping layers, which guarantee the transmission of the superficial loads on the ground with a minimum of deformability and wear. At present, road construction profiles can be of two different types: (i) **rigid concrete profiles**, which are intrinsically much more resistant and therefore long-lasting, and (ii) **flexible four-layers asphalt pavements** (Figure 1), which are the most used in practice, since they guarantee much more reduced building times and costs. These layers are [3]:

- the **subsoil layer**, i.e. the deepest part of the terrain on top of which the foundations of the road profile lie. This layer has a typical thickness of 50-100 [cm];

- the **sub-base layer** (indicated in the figure above with “A”), which is typically built as a granular / concrete mixture, with a typical thickness of 15-35 [cm]. This layer is generally more aerated and is often used for drainage purposes.
- the **road base layer** (indicated in the figure above with “A”), the thickest layer in a flexible pavement, which is typically built through a bituminous mixture. Its thickness, which can typically reach up to 30 [cm], is chosen, among others, as a function of the expected traffic flows and climatic conditions.
- the **road pavement**, which is typically built as a bituminous conglomerate and is divided in turn in two sub-layers:
 - the **base course** (indicated in the figure above with “C”), with a thickness of 6-8 [cm];
 - the **wearing course** (indicated in the figure above with “D”), with a thickness of 4-6 [cm];

It is worth noting that it is common on low traffic roads to combine base and wearing courses into a homogeneous layer without any discontinuity in the nature of the bituminous conglomerates. In the case of rigid concrete profiles, layers “B”, “C”, “D” form typically a unique layer made of up of simple concrete plates. The exact nature of road pavement construction profiles can vary quite significantly within a road network. Deeper profiles characterize roads with more intense transit of vehicles, in particular heavy ones, whereas minor roads typically present a shallower construction.

The road construction design choices are important to characterize its **thermal memory**, i.e. its intrinsic ability to maintain the heat accumulated during the daytime solar radiation; indeed, the higher is depth of the road construction profile, the higher is its thermal memory [4]. For this reason, the major roads tend to present, given the same boundary conditions, the warmest sections within a road networks. On the other side, bridges, which present a very shallow profile, have a very limited thermal memory. This phenomena are particularly emphasized during the early and late winter season, when the amount of daytime solar radiation accumulated by the road surface is highest.

The thermal behavior of a specific road stretch can be completely characterized by taking in consideration a specific set of parameters. The first one is the **thermal conductivity** (k), i.e. the intrinsic ability of a certain material to conduct heat. Materials with high thermal conductivity will thus have a minor inclination to maintain heat, and thus a higher attitude to become colder. Thermal conductivity is defined as ():

$$k = \frac{Q \cdot d}{S \cdot (T_2 - T_1)} [W/m \cdot ^\circ K]$$

[3]

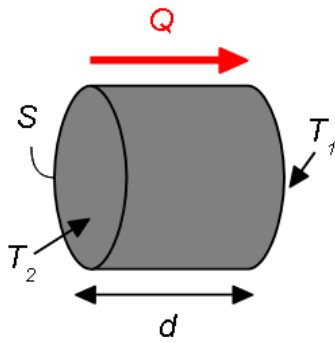


Figure 2: Reference geometry considered in the definition of thermal conductivity.

where Q is the heat conduction speed, which indicates the amount of thermal energy which can flow in the time unit among the section S of the material (measured in $[W]$), d is the length (depth) of the material in the considered geometry, and T_1 and T_2 are the surface temperatures at its boundaries.

Another important parameter which is important to describe the thermal peculiarities of a material is the **thermal diffusivity** (a). This factor is associated with the intrinsic ability of adapting to temperature changes which may occur in the surrounding environment, and is defined as the ratio between its ability to conduct heat and to accumulate it:

$$a = \frac{k}{\rho \cdot c_p} \quad [m^2/s]$$

[4]

where ρ is the density of the material (expressed in $[kg/m^3]$), and c_p is the specific heat, i.e. the amount of heat which is necessary to increase the temperature of a body unit of $1 [^\circ K]$. High values of thermal diffusivity indicate an evident attitude of the material to quickly release heat, while on the contrary low values are an indicator of slow thermal variation processes.

An additional parameter which is important to describe the thermal relationships with the external elements is the **heat transfer coefficient**, which is a marker of the attitude of a material to exchange heat, in particular in correspondence of discontinuity layers. This coefficient is defined as:

$$h = \frac{Q}{S \cdot (T_2 - T_1)} = \frac{k}{d} \quad [W/m^2 \cdot ^\circ K]$$

[5]

and is strictly related to other two parameters that describe the heat transfer exchanges, namely the albedo for the absorption phenomena and the emissivity for the emission ones.

The **albedo** is defined as the percentage of incoming radiation that is reflected by a surface, i.e.:

$$\rho = \frac{E_r}{E_i}$$

[6]

Because of the principle of energy conservation, ρ is related to the absorption coefficient α and the transmission coefficient τ through the equation $\rho + \alpha + \tau = 1$.

Asphalt and concrete profiles are typically dark bodies, and have albedo values in the order of 5-35%; snow-covered roads can on the contrary have very high values, in the order of 90% (Figure 4).

On the other side, the emissivity is defined as the quantity of energy which is radiated by a material, and is typically assumed to be a percentage of the energy radiated by an ideal “black” body, which is in the condition to absorb all the incoming radiation (i.e. $E_r = E_t = 0$; $E_a = E_i$) and is calculated through the following Planck’s equation:

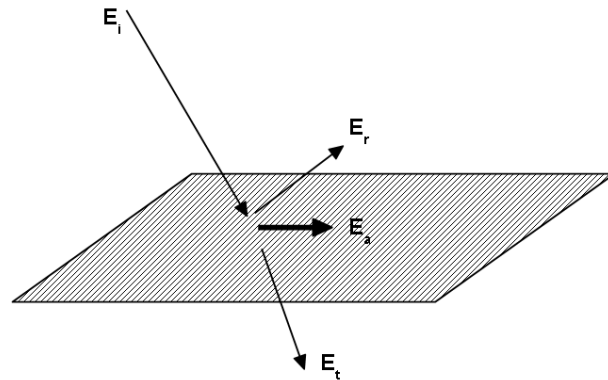


Figure 3: Incoming radiation and energy components split.

$$W_\lambda = \frac{2\pi c^2 h \lambda^{-5}}{e^{\frac{ch}{\lambda k T}} - 1}$$

[7]

where $c \cong 3 \cdot 10^8 [m/s]$ is the speed light in vacuum, $h \cong 6.62 \cdot 10^{-34} [W \cdot s^2]$ is the Planck constant, $k \cong 1.38 \cdot 10^{-23} [W \cdot s/^\circ K]$ is the first Boltzmann constant, λ is the wavelength and T the temperature of the black body.

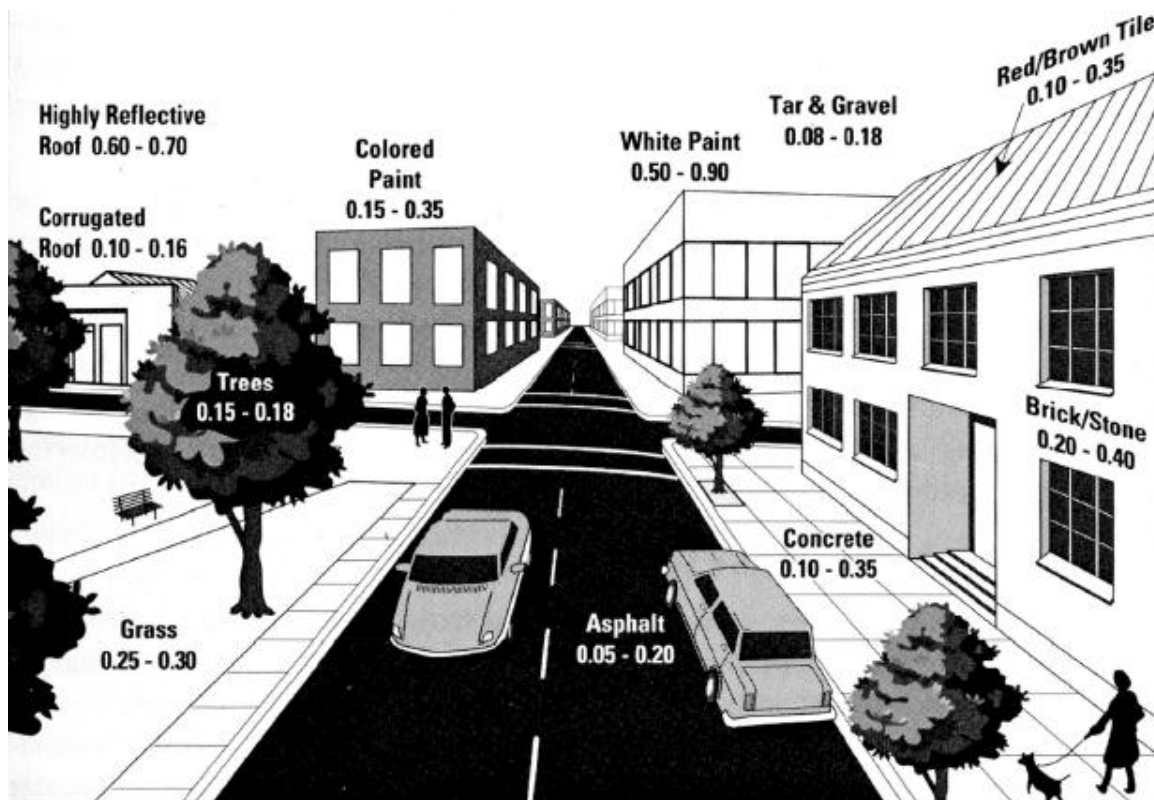


Figure 4: Typical values of albedo for different materials within the road infrastructure scenario [5].

The emissivity ε_λ of a real body is then simply expressed as:

$$\varepsilon_\lambda = \frac{W_{\lambda-gray}}{W_{\lambda-black}}$$

[8]

Furthermore, Kirchhoff demonstrated that the emissivity corresponds exactly to the absorbed energy ($\varepsilon_\lambda = \tau$), with the possibility to link this value directly to the albedo.

The empirical determination of road construction parameters has always been a major issue in the road weather domain, mainly because of a paucity of reliable and accurate data. Even if standard road construction profiles exist, they are subject to change over time, even because of the continuous maintenance activities. High confidence data can therefore only be obtained by (periodically) coring the road section under interest. Because of the current limitations, the current modelling approach is therefore to consider lock-up tables trying to provide reference “standard” values for different types of road construction profiles. Chapman et al. [6] suggested to associate for each road type a specific profile with reference layer depths, materials used, and thermal properties, and to use this information within a spatially-extended RWIS (XRWIS). A possible innovation in this field is the idea to use Ground Penetrating Radars (GPRs) for spatially characterizing the road profile, and to use this accurate data in order to significantly improve the route-based forecasts processed by the road weather models. More details on this technology are described in paragraph 2.3.

2.1.2 Geographical parameters

Road surface temperature (RST) and conditions are strictly related to the particular geographical context in which a road infrastructure is located. The main parameters which play a specific role in this target scenario are the following [1] - [6]:

- latitude
- altitude
- topography
- screening
- sky-view factor
- landuse

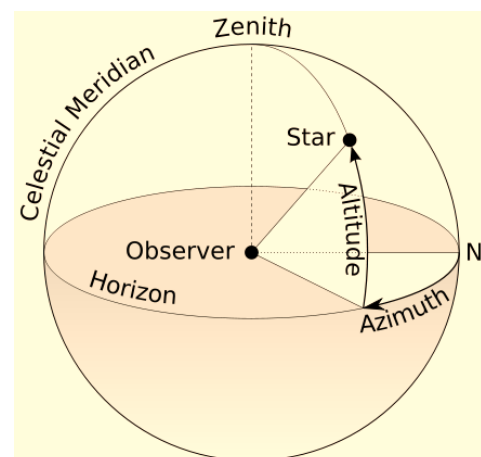


Figure 5: Solar altitude and azimuth: geometrical representation (source: en.wikipedia.com).

Latitude can be considered an initial constraint on the values of RST, since it directly influences the solar direction relative to the local plane of the Earth’s surface and as a consequence the maximum amount of incoming solar radiation that reaches the ground [7] - [8]. In particular, latitude has a direct impact on the values of solar altitude, i.e. the angular elevation of the

Sun above the horizon. This elevation changes either daily and seasonally: it is zero at sunrise each day, increases as the Sun rises and reaches a maximum at solar noon and then decreases again until it reaches zero at sunset.

The maximum daily solar altitude angle, as well the entire daily solar cycle, vary seasonally. All this can be modeled with fundamental solar engineering equations [9]; the main equation of interest for the targeted problem is the following:

$$\sin \alpha = \sin L \sin \delta_s + \cos L \cos \delta_s \cos h_s \quad [9]$$

where α is the **solar altitude**; L is the latitude, δ_s is the solar declination (i.e. the angle between the direction to the Sun and the plane of the Earth's equator) and h_s is the hour angle, which describes how far east or west the Sun is from the local meridian. For this reason, at lower latitudes the solar altitude is higher and the solar energy is less dispersed, while at higher latitudes, the typical altitudes are typically much lower with a more evident distribution of the energy in larger areas (Figure 6).

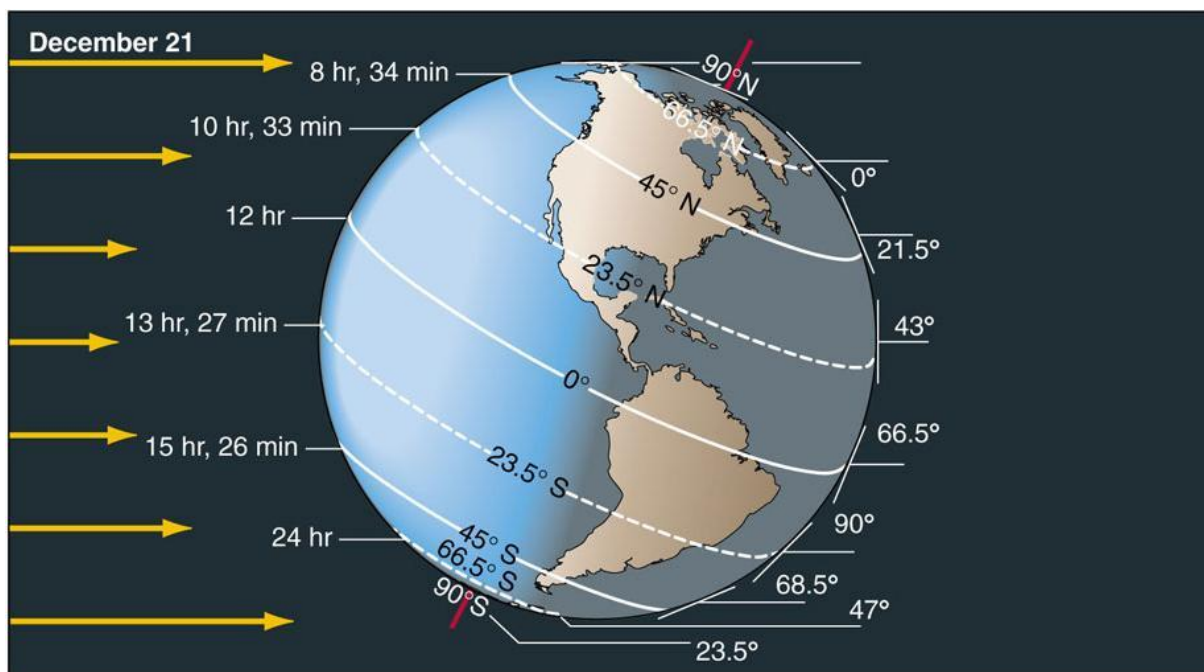


Figure 6: Effective solar radiation at different latitudes(source: geog.ucsb.edu).

Latitude affects as a consequence the duration of winter seasons as well: countries in the northern hemisphere at higher latitudes have to face with longer and more frigid periods, while southern countries present minor ice problems [10]. This is the reason for example, why Scotland has more snow and ice than other parts of the UK, even if their topography is quite similar [7]. Longitude is a parameter that in this context plays a minor role, but is however important in order to determine the “continentality” of a specific region, and more in particular the possible influence that a large body of water can have on it, like for example an ocean [11].

Once of the most specific case studies related to the influence of latitude on the distribution of slipperiness of roads was recently done in Sweden [12], and was studied on different scales (national, regional and county) and as function of a variety of slipperiness types, jointly considered in a unique *winter index* (WI). The result has been that while on the national and regional scales this correlation has showed to be relatively high, with latitude proven to be more the more influencing factor on RST, latitude and more in general all geographical parameters did not manage alone to describe the climate variations at county level, which are in this case more “controlled” by meteorological parameters (Figure 7).

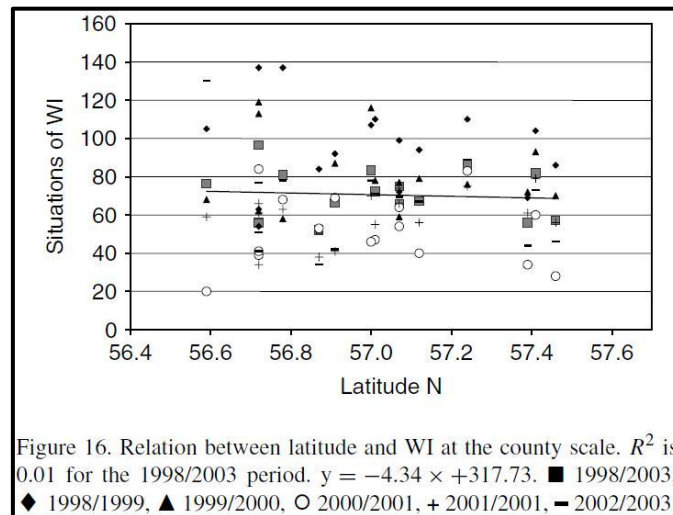
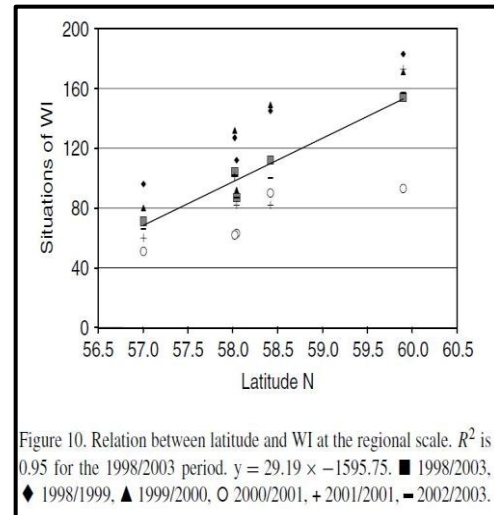
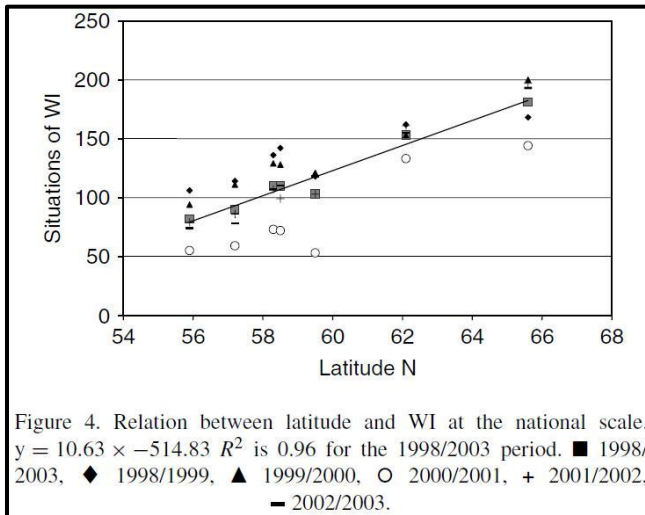


Figure 7: Empirical relation between latitude and a winter index calculated in Sweden at a national, regional and county scale [12].

Altitude has a direct and significant influence on RST, and can well explain the significant variations which may be observed at different road locations in a mountainous region, as can for example in an alpine region like the Autonomous Province of Trento. In this case, the reference index which is directly linked with RST is the *environmental lapse rate* γ , defined as:

$$\gamma = \frac{dT}{dz} \text{ [}^{\circ}\text{C/km]}$$

[10]

Scientific studies have demonstrated since years that typical values for γ are in the order of 6.5 [$^{\circ}\text{C/km}$], with peaks up to a maximum of 9.8 [$^{\circ}\text{C/km}$] [13]. However, the relationship between RST and altitude is complex and non-linear, as specifically analyzed by evaluating and comparing static and mobile RWIS data gathered in Nevada, USA (Figure 8) [14].

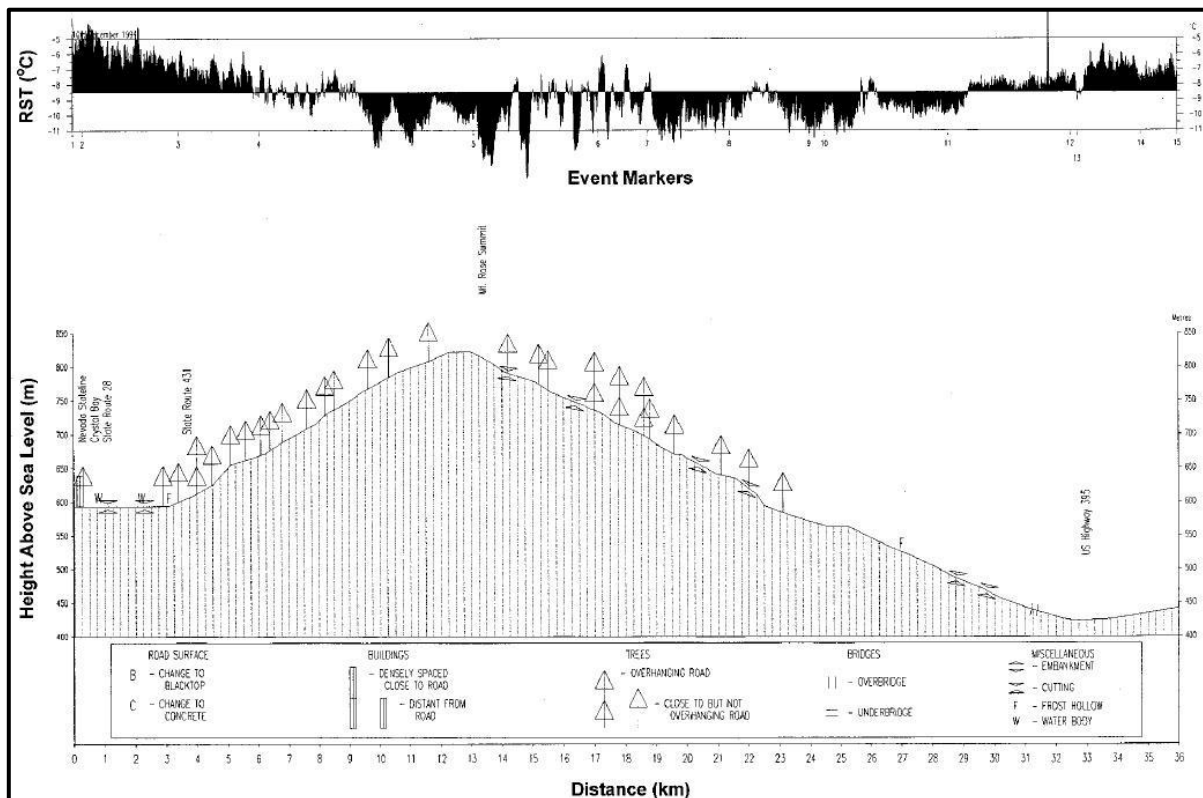


Figure 8: Typical RST variation patterns that can be observed through thermal mapping surveys in case of altitude profile variations [14].

The effects of altitude are more apparent during times of low atmospheric stability, whereas as stability increases, RST tends to present a higher correlation with respect to the topography factor. A common modeling approach is therefore to consider different reference environmental lapse rates as a function of all the possible stability conditions, which are typically parameterized through the **Pasquill-Gifford stability classes** [6]. The present meteorological conditions can be associated to a certain stability class by analyzing both the surface wind speed and the cloud coverage [1]. In case of a temperature inversion, alternative methodologies must be considered in order to properly cope with the presence of negative environmental lapse rates.

Topography is often considered to be the dominant factor causing differences in RST during extreme nights [15]. Large variations in air temperature and RST can be observed even in presence of small differences in topography across the mesoscale landscape.

Several climatology theories have been proposed to explain this complex phenomenon; for example, lower temperatures can be directly associated with the earlier cessation of turbulent heat transfer in sheltered locations [16] or with the production of horizontal isotherms in small-scale sheltered terrain [13]. These consolidated theories can well explain the impact of micro-topography on temperature distribution, while on larger scales the most commonly accepted cause on temperature variations is the katabatic theory. During stable conditions, it is possible to recognize the formation of dense cold air layers at the ground. If the topography is undulating, this layer is induced to move down slope as a katabatic flow, following lines of drainage until a topographic or a thermal barrier is encountered (Figure 9).

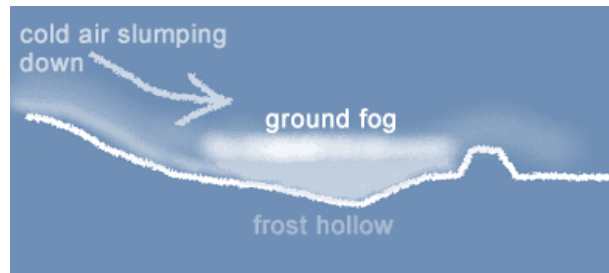


Figure 9: Simple representation of katabatic theory (source: weatheronline.co.uk).

As a consequence, thermal belts are produced, which height may vary as a function of the strength of the katabatic flow and the relative size of surrounding topography [17]. The exposure of a valley becomes in particular a dominant factor especially in case of moderate wind speeds, which are on the contrary more influential in case of environments with exposed sections and located at higher altitudes [18]. The typical result is that sheltered locations may experience significant reduction of RST as a consequence of reduced wind speeds and turbulent heat transfer [19]. Lowest air temperatures measured at valley bottoms are typically recorded when these processes take place, and are in general linear related with RST, even if the latter one is often higher due to the thermal inertia of the road construction.

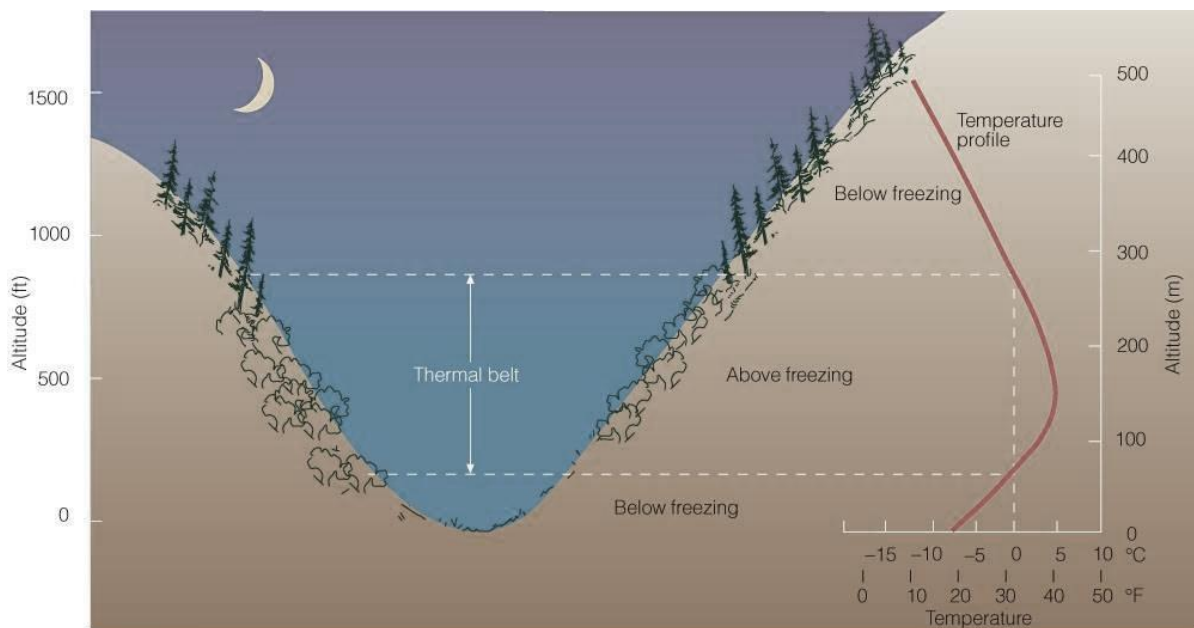


Figure 10: Thermal belt and air temperature variations as a consequence of thermal inversion phenomena (source: weatheronline.co.uk).

RST variations caused by topography and more specifically induced by katabatic flows are typically modeled by considering local biases in the site forecasts, which are defined according to the current stability conditions. A typical approach for this is to associate an index to the estimated Pasquill-Gifford stability class, identified as a function of the surface wind speed and the cloud coverage [1].

Another geographical parameter which can alter the energy budget at the surface is **screening**, i.e. the presence of sheltered environments which may receive only a portion of the incoming daytime short-wave radiation. These effects are typically systematic and can be cause of large daytime RST variations [20]. These deficits were shown to decrease over the afternoon, and to explain specific lag effects which may take place after sunset, in particular at low levels of cloud cover and during early and late winter, when solar input is increased (Figure 11) [21]. Screening effects produced by buildings and forests have the consequence to produce a natural / artificial wind shelter, which lowers RST [22]. Specific validation activities carried out at coniferous sites in Sweden demonstrated the presence of RST differences of up to 3 [°C] between locations in sheltered forests and exposed areas [23] - [24].

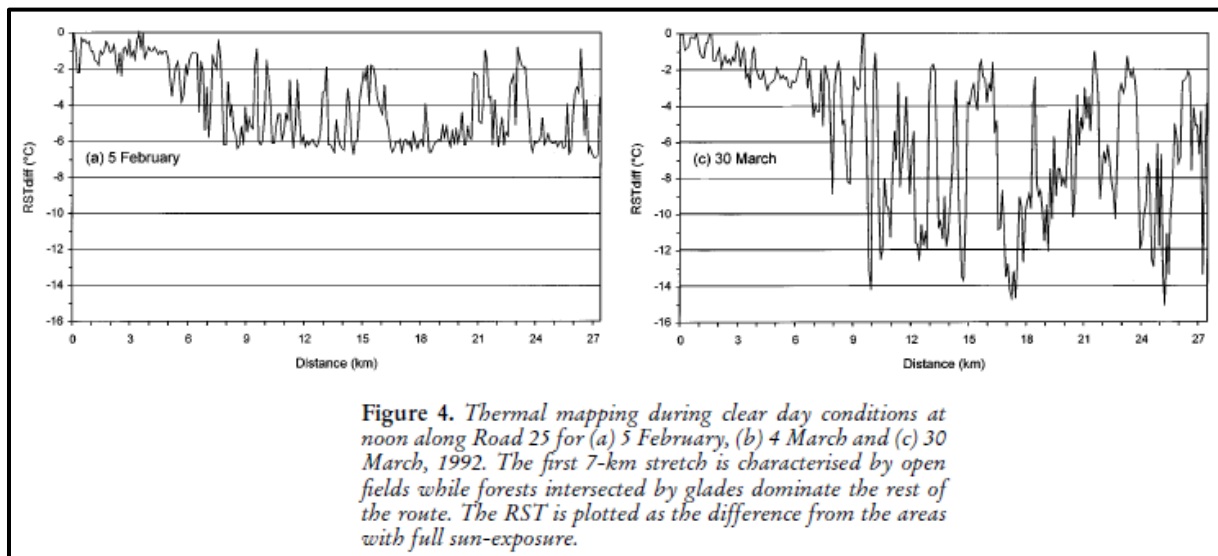


Figure 11: Typical RST variation patterns which can be recorded through thermal mapping operations in case of evident screening phenomena [21].

Screening can be taken into account into energy-balance models by comparing the solar zenith angle with the effective “building” angle, which is representative of the exposure degree of a particular site of interest. In the case the zenith angle is higher, the incoming radiation will be in the form of direct and diffuse radiation, while in the opposite case the solar beam is blocked and the radiation can reach the ground only in a diffuse way. A common way to estimate the “building angle” is to use fish-eye images, which are considered as well in the estimation of the sky-view factor. The reference relationship is [25]:

$$\zeta = \frac{r\pi}{2r_0}$$

[11]

where ζ is the “building” angle, and r and r_0 two parameters as defined in Figure 12 [6].

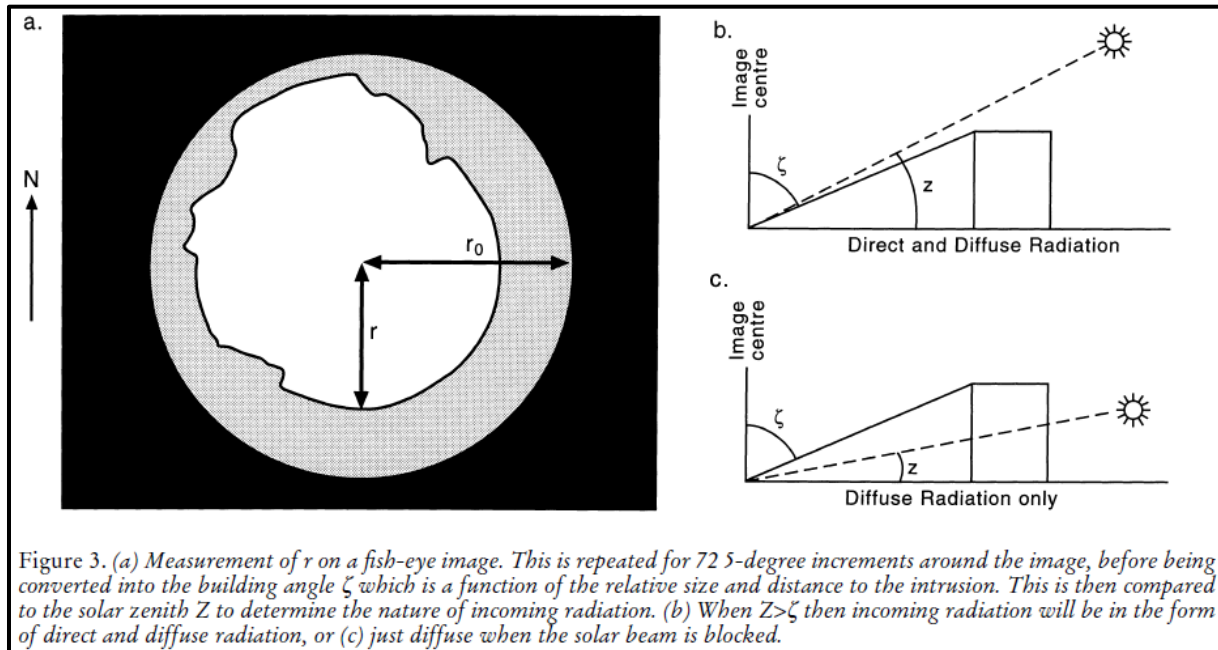


Figure 12: Geometrical representation of the calculation of the building angle in the screening factor evaluation process [5].

A crucial parameter in the spatial variation of RST, which is typically considered in combination with screening, is the **sky-view factor** φ_s . This variable is a dimensionless, normalized quantity which indicates the quantity of visible sky evaluated in correspondence of a specific location, defined as follows:

$$\varphi_s = (\cos \alpha)^2$$

[12]

where α is the medium elevation angle of the topographic horizon [26].

In case $\varphi_s = 1$, the road stretch is located in an “ideal” condition of flat and open terrain, whereas for $\varphi_s < 1$, there are natural and/or human obstructions such as buildings and/or trees which are in the conditions of limiting the arrival of the solar radiation on the ground. Actually, the sky-view factor is very important in the calculation of the nocturnal radiation budget, since such obstructions can significantly limit the loss of long-wave radiation from the ground and thus determine a significant increase of air and road surface temperatures [27] - [28]. Sky-view factor has a dominant role in the application domain of the project. A specific study carried out in Sweden demonstrated that RST variations can be accounted for up to 61% to this parameter [29]. Similar considerations are confirmed also in other several

research works available in the literature [30] - [31] - [32], which clearly show how radiation losses are maximum in case of very high atmospheric stability.

An empirical method to estimate φ_s is through **view factor mapping** (VFM) surveys [1], which are essentially thermal mapping operations which are slightly generalized in order to take into account even this parameter. The sky-view factor is estimated based on a post-processing elaboration chain of digital fish-eye images acquired from a camera mounted on the roof of the mobile probe (Figure 12), which automatically recognizes non-sky pixels from sky ones. This measurement procedure, which was quite expensive in the past but whose costs are becoming more and more affordable, has demonstrated to be very precise, and can produce accuracy values in the order of ± 0.02 . A possible result of such an operation is presented in [33], and demonstrates the large variations that can be obtained within an urban scenario (Figure 15).

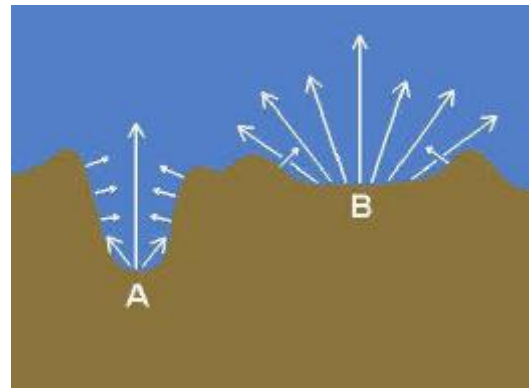


Figure 13: Simplified representation of different sky-view factors conditions

From a modeling point of view, the sky-view factor is very simply taken into account by introducing an additional parameter in the black body emission model of Stefan Boltzmann:

$$W = \varepsilon\sigma\varphi_s T_0^4 \quad [W/cm^2] \quad [13]$$

where ε is the emissivity, $\sigma = 5.67 \cdot 10^{-12} [W/cm^2 \cdot ^\circ K^4]$ is the second Boltzmann constant, and T_0 is the temperature of the radiating body (in our case, the road infrastructure).

The type of **land cover** can finally explain additional road temperature variations. In general, urban areas characterized by a high density of buildings, have a very particular micro-climate, and are generally several degrees warmer than rural areas. For example, empirical measurements carried out in the area of Gothenburg demonstrated that this lag can be in the order of 4 [°C] during stable conditions [31]. This phenomenon is commonly referred as **urban heat islands** [34] - [35], and is explained by the fact that urban climates are particularly influenced by the thermal properties of construction materials and by the anthropogenic heat produced by buildings and traffic [8].



Figure 14: A graphical representation of the urban heat island phenomenon.

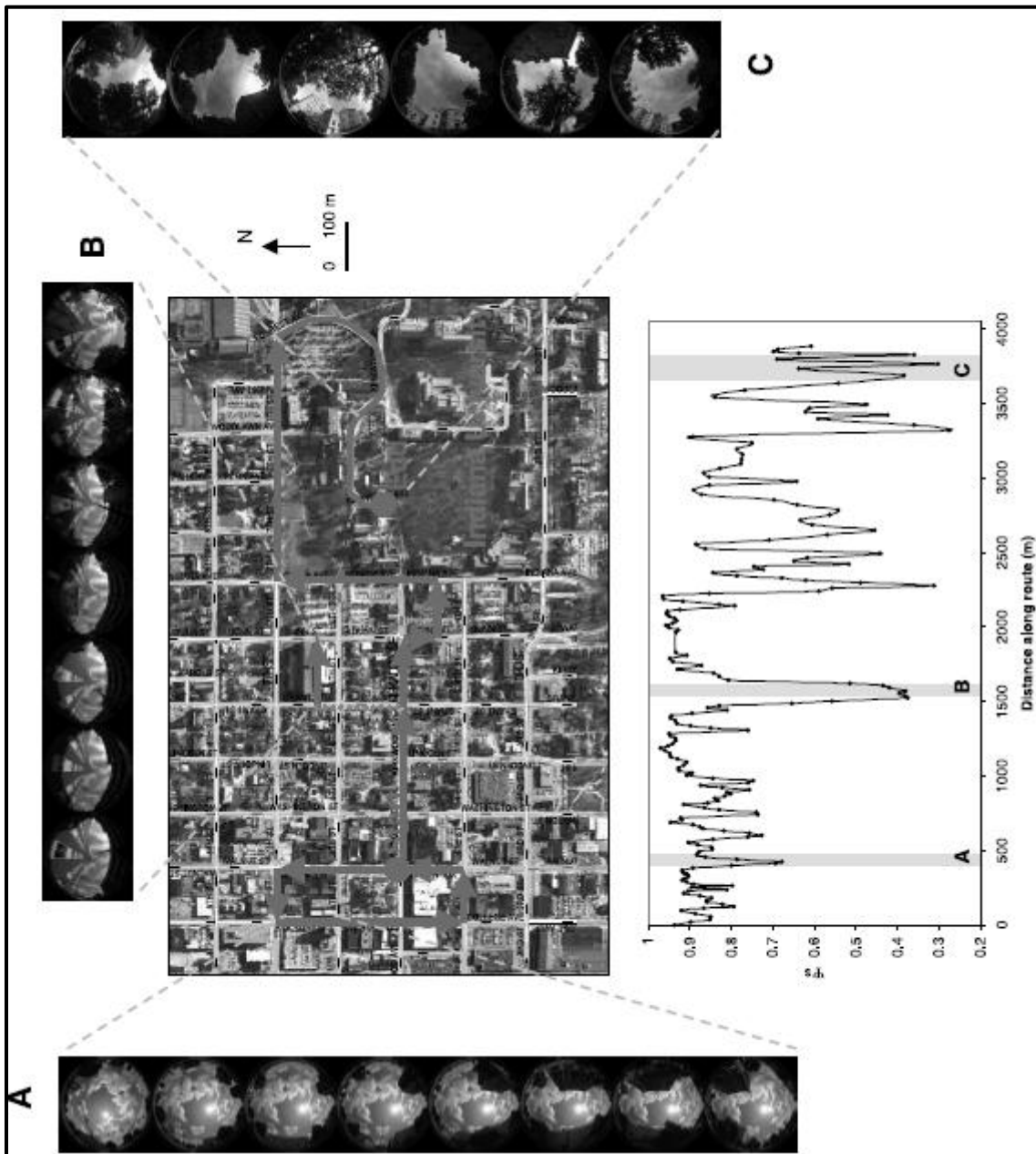


Figure 15: Sky-view factor measurements in an urban scenario – empirical results example [32].

It is worth noting that the canyon geometry which is typical for a urban scenario has also a direct influence on screening and sky-view effects as well, so real variations are typically explained as a function of the combination of all these aspects. The wind can also increase the impact of urban heat island phenomena, since turbulent heat island can significantly be reduced in sheltered areas [27].

Land cover is typically modeled through a particular index, the **roughness length** (Z_0), which is a function of shape, density and height of surface elements. Typical values are of 8 [m] in city centres of large cities and 0.5 [m] for suburban areas [36]. In practice, the dynamics of Z_0 are difficult to estimate because of the complex interaction between surface elements. The common modeling approach is thus to significantly simplify the problem and consider static

reference pick-up tables, which contain values that are representative of specific “ideal” of land-use / road type combinations (e.g. city centre / urban /sub-urban / rural vs motorway / minor road types [6]).

2.1.3 Traffic flows

The above considerations on land cover and urban heat islands phenomena are a perfect introduction for analyzing an additional influencing factor, i.e. traffic. From a physical point of view, traffic is in the condition to influence RST, given the same boundary conditions, because of three different reasons [10]:

- **traffic is an additional anthropogenic heat source**; in particular, heat can be transferred to the road surface from the engine, and from the dissipation caused by tires e frictions during deceleration operations;
- **vehicular transit are in the condition to promote additional turbulent heat fluxes** in correspondence of the road surface.
- during the diurnal periods, **vehicles act as an additional screening element between the road surface and the incoming solar radiation**;

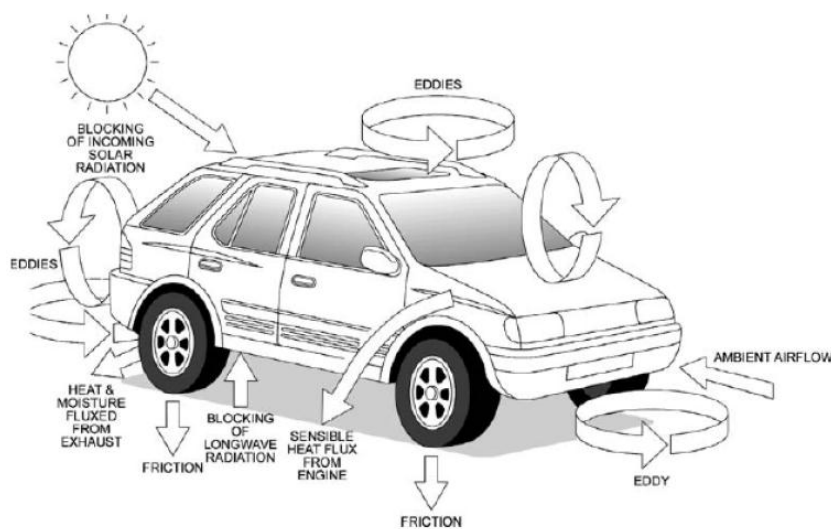
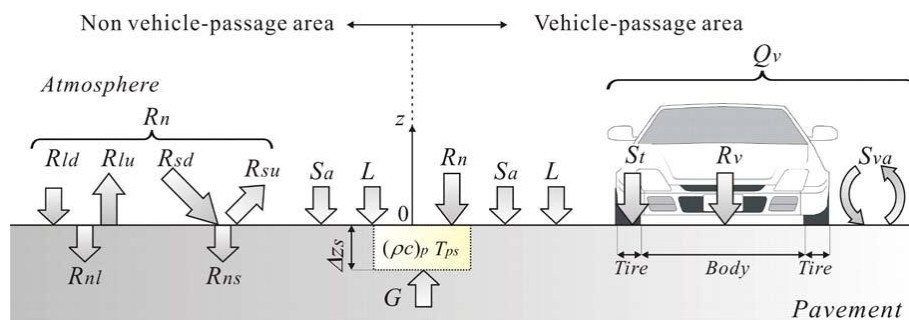


Figure 16: Main contribution to energy balance conditions of RST caused by vehicular transits [37] - [38].

Therefore, the main contribution of traffic on RST are more likely to be noticed on nights, when freezing phenomena have a higher probability to occur and in correspondence of point of the road network where traffic flows can significantly be different (even on a lane base). The largest variations are typically recorded in stable conditions, in correspondence of the highest risk of radiative losses.

Traffic is probably the most difficult parameter to evaluate and model. Despite this, the road weather research has only recently increased its focus on this topic, as a consequence of the consolidation of the first route-based “spatially-enabled” models (i.e. the so called eXtended RWIS, XRWIS).

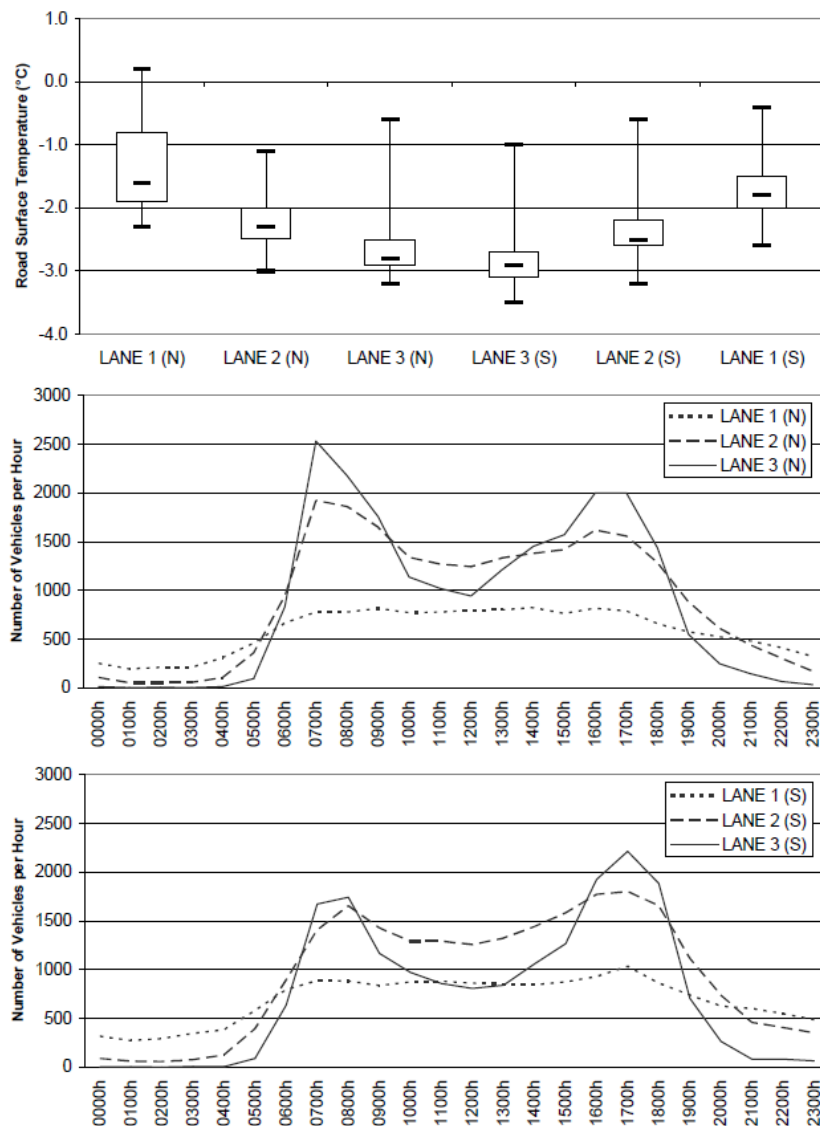


Figure 17: Lane-based comparison between RST measurements and traffic data.

For this reason, available publications concerning this topic in the scientific literature are actually only a few. The first researches done in this field in the '90 years gave an empirical proof of the impact of traffic flows on multi-laned roads, where the different volumes and speed profile of vehicles can be responsible of RST variations of up to 2 [°C] [39]. Similar

results were obtained in [40] where it was empirically assessed a difference of 2 [°C] RST in Stockholm during the early morning peak commuting period time. Differences of 1 [°C] and 2 [°C] are not uncommon between inside and outside lanes, as demonstrated in [41]. Thermal mapping operations have then been started to be carried out with the idea to correlate spatial measurements of RST with traffic data, as suggested in [42] (

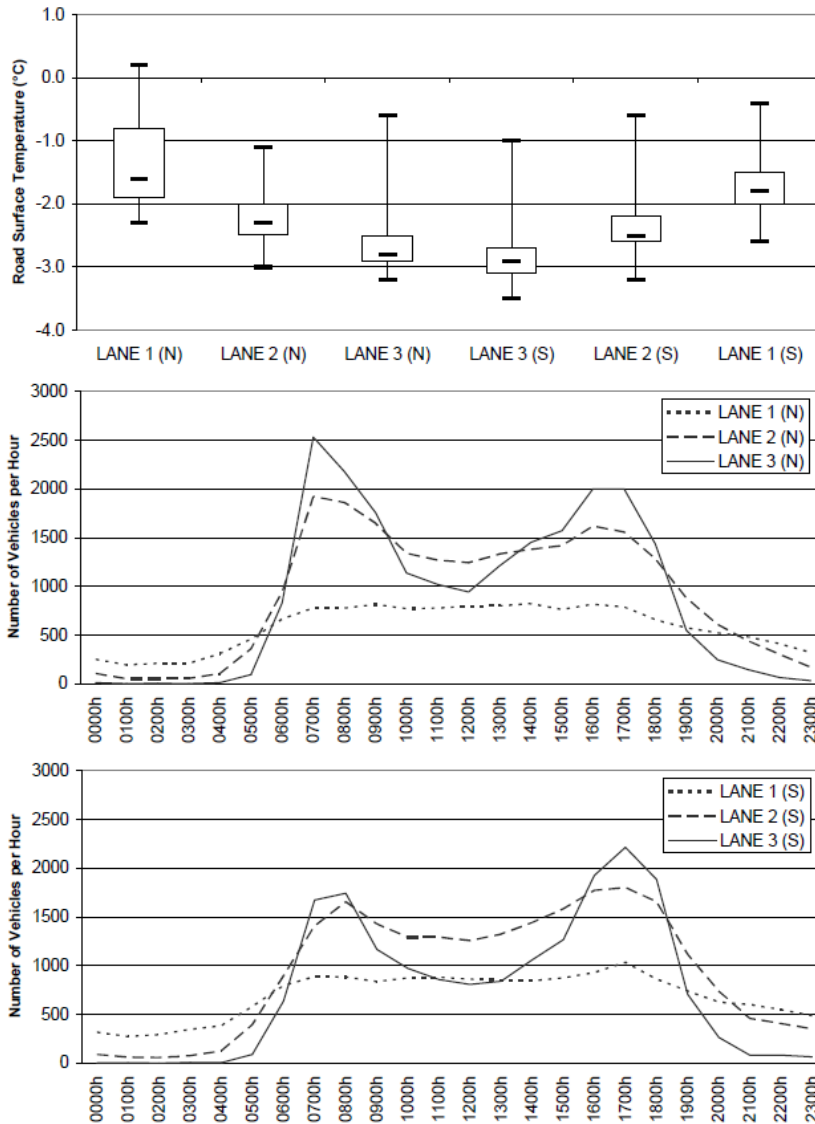


Figure 17). Much more detailed studies of little variations of RST in the “third” spatial dimension (i.e. orthogonal to the transit one), trying to get evidence e.g. of the influence of tyre tracks with respect to the edge of road were started to be carried out by means of thermal imaging camera, which can provide an immediate assessment of the thermal variation of the road profile (Figure 18).

Practical approaches for specifically modeling the impact of traffic on RST as a function of their correspondent variations are therefore even today far from be obtained [43]. The typical approach, very similarly as what is proposed for the roughness length estimation, is to consider static reference pick-up tables, which contain biases that are representative of

specific “ideal” of land-use / road type combinations, which are implicitly associated to particular traffic loads. These biases try to take into account both the contribution of anthropogenic heat as well the long-wave radiation loss from the road surface. Moreover, the additional turbulence phenomena are modeled by considering a particular weight of the wind speed in the energy balance model. In the last couple of years, the research literature has been starting to introduce a new generation of advanced modeling techniques, which try to generalize the traditional zero / one road weather models in the traffic dimension. A relevant example in this direction is the work done by some Japanese researchers [37], who have suggested for the first time the concept of a **Vehicle Road Freezing Forecasting model** (VRFF).

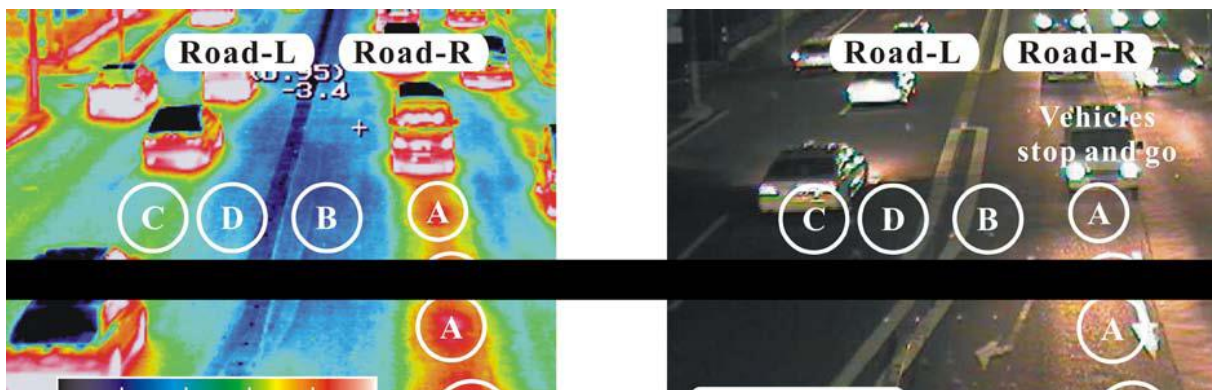


Figure 18: Road thermal images and RST – traffic correlation assessment [37].

2.1.4 Meteorological conditions

Geographical factors are the main responsible of local RST variations which may occur within a road network; on the other side, it is worth noting the dominant role that meteorological conditions have on a more regional level. While, as already mentioned, the first set of factors are typically taken into account by introducing certain modeling parameters and considering static prior values for them, the latter influencing “dimension” is on the contrary evaluated on a dynamic basis by considering field data gathered by a more or less heterogenous monitoring system spread over a certain target area. This data, together with the outputs of mesoscale weather bulletins which are typically provided by trans-national organizations (e.g. ECMWF), is the main input source of road weather forecasting models which are used to predict road surface temperature and conditions, and in some way are responsible for the overall accuracy level of their estimates.

Various meteorological factors have an influence on RST. The most dominant one is probably the incoming **solar radiation**, whose density power can be calculated with reference the Boltzmann equation already presented in equation [13]. The spectral density of this quantity, which can be expressed as $W_{\lambda}(\lambda)$, has a maximum value in correspondence of $\lambda = \lambda_{max}$ which is inversely proportional to its temperature, as described by the Wien's equation:

$$\lambda_{max} = \frac{2898}{T}$$

[14]

By modeling the Sun as a nearly perfect black body with $T = T_s = 5870$ [°K] and $\lambda_{max} \cong 0,50$ [μm], it is possible to obtain a power density of about 6300 [W/cm^2], an enormous value which is about 40% contained within the visible light spectrum (Figure 19).

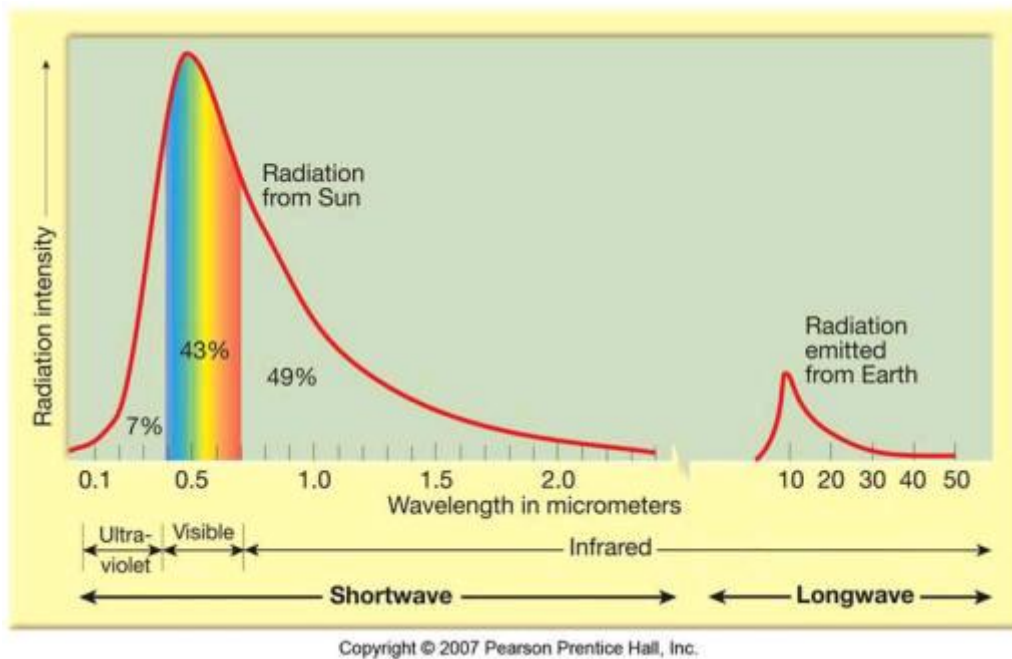


Figure 19: Power density of the solar and terrestrial radiation in the wavelength domain (source: suyts.wordpress.com)

However, the radiation which must be considered in the energy budget equations must consider the portion of it which is able to arrive at the ground level, which can be expressed as:

$$W'_s(\lambda) = W_\lambda(\lambda) \cdot \tau_a(\lambda)$$

[15]

where $\tau_a(\lambda)$ is the transmission coefficient of the atmosphere. Unfortunately, the latter function is described by a very complex relationship, with values which can vary very significantly even in correspondence of very similar wavelengths, and all this by not taking in consideration possible meteorological perturbations. At a first approximation level, however, it is possible to state that $\tau_a(\lambda)$ presents very low values in the ultraviolet spectrum, a certain uniform behavior in the visible spectrum (around the value 0,5), and more complex non-linear relationship in the infrared domain. The atmosphere also causes diffusion phenomena, i.e. dispersion of the incoming radiation due to the impacts with the small particles which are present in its different layers. Diffusion can follow the Rayleigh or the Mie equations,

depending whether the dimension of these particles is smaller or bigger with respect to the associated wavelength, respectively.

Being a body at a temperature higher than zero Kelvin degrees, the Earth itself is a radiating body. A rough estimate of the terrestrial radiation can be done by considering a reference temperature of $T = T_T = 300 [^\circ K]$ and an associate peak wavelength value of $\lambda_{max} \cong 9,66 [\mu m]$, which produces a total power density of $0,046 [W/cm^2]$. This value is significantly lower if compared with the solar radiation one (Figure 19), but is absolutely not negligible in the thermal infrared spectrum, where the maximum radiation intensities are located. The combination of these two radiation sources, well graphically summarized in Figure 20, determine the most important terms when considering the energy balance models at the ground level.

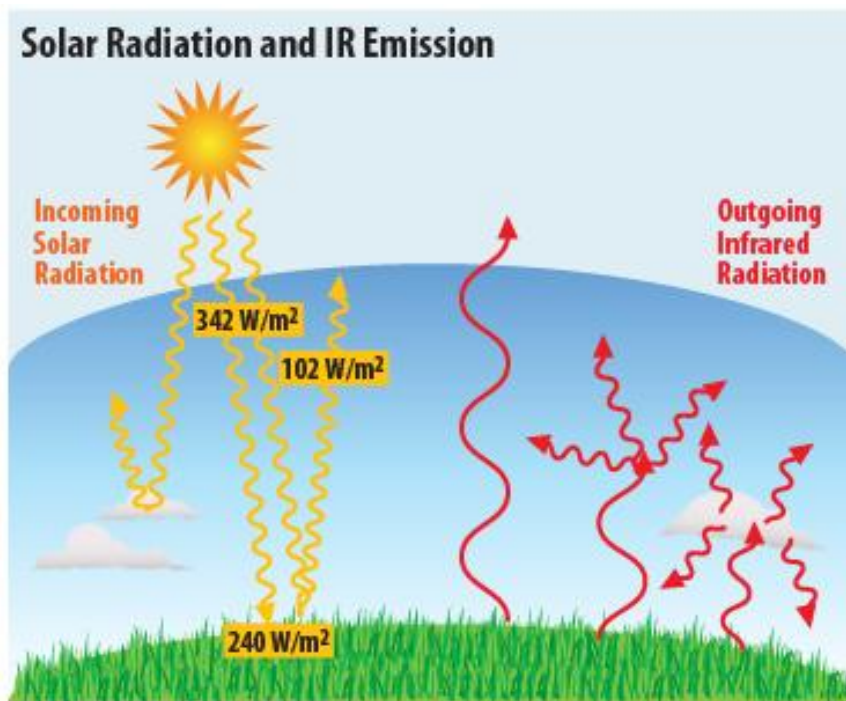


Figure 20: Solar and terrestrial radiation patterns (source: ete.cet.edu)

The incoming solar radiation can be moreover influenced by the **cloud cover** factor. From a modeling point of view, this can be taken into account by introducing an additional transmission factor $\tau_n(\lambda)$, which depends on the dimensions, consistency and physical properties of the clouds. Additionally, one should consider also its kinematics behavior in order to completely describe the incoming radiation $W_s(\lambda, \underline{r}, t)$ in the wavelength / spatial / temporal domain, i.e.:

$$W_s(\lambda, \underline{r}, t) = W_s'(\lambda) \cdot \tau_n(\lambda, \underline{r}, t)$$

[16]

It is worth noting the possibility to combine together atmosphere and cloud cover effects within a unique “equivalent” gray body by considering a unique transmission factor $\tau_{na}(\lambda, \underline{r}, t) = \tau_n(\lambda, \underline{r}, t) \cdot \tau_a(\lambda)$ and put this directly in relationship to the emitted radiation $W_\lambda(\lambda)$, namely $W_s(\lambda, \underline{r}, t) = W_\lambda(\lambda) \cdot \tau_{na}(\lambda, \underline{r}, t)$. In practice, it is at present nearly unfeasible to mathematically represent the cloud cover contribution in great details within road weather models, and this is considered as their main source of errors in the numerical elaborations and predictions they produce as output.

Cloud cover has not only an impact on the amount of solar radiation effectively reaching the ground during the diurnal phase, but has moreover a major role in the way the accumulated heat is released at night. This effect is particularly relevant for the winter maintenance operations: in fact, under the same meteorological conditions, the absence of clouds significantly speeds up the cooling processes of the roads, which is on the contrary smoothed as a function of the overall level of cloud coverage (Figure 21). This physical phenomenon is very critical when conditions change suddenly at night, i.e. when a cloudy situation suddenly changes into a clear-sky one, since this could rapidly bring to the formation of ice on the surface.

Several scientific studies published in the first years of the nineties, in particular [44], tested the sensitivity of individual meteorological parameters on RST. **Air temperature** and **precipitation phenomena** showed to be most influential ones: while the first one is to be easily expected, as air temperature and RST are closely related (as empirically demonstrated in [10], [15] and [45]), the second one has a crucial role on the changes of the road conditions. Both parameters should be considered jointly, since the precipitation type is directly linked to the vertical air temperature profile. On the other side, RST determines whether the falling precipitation is in the condition or not to produce ice formation or snow accumulation on the road. Table 2 provides a comprehensive overview of all different road conditions and precipitation types.

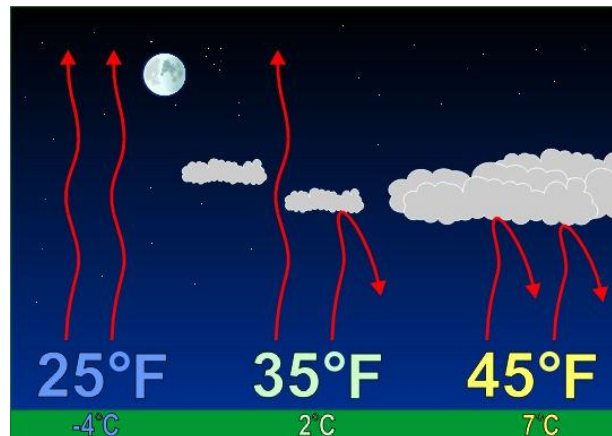


Figure 21: A graphical representation of the typical effect of cloud cover factor at night.

Road conditions classes	Precipitation types
<ul style="list-style-type: none"> • Dry • Wet • Ice on the road • Snow on the road 	<ul style="list-style-type: none"> • Rain • Freezing rain • Sleet • Snow • Hail

Table 2: List of all possible road conditions classes and precipitation types.

The most dangerous precipitation phenomenon which can probably appear on the surface of the road is **freezing rain**, which forms in presence of two layers of cold air (i.e. with air temperature below zero Celsius degrees), where one is a thin blanket over the ground surface, separated by a layer of warm air (i.e. with air temperature above zero Celsius degrees) (Figure 22). In this way, the snow precipitation in the higher cold air layer becomes rain when it enters the warmer air layer; this rain tends to freeze again when it finally meets the lowest cold air layer, but it doesn't have the space to become snow again. However, rain is cooled in such a way that it becomes immediately ice when it enters in contact with a cold surface (i.e. with temperature below zero Celsius degrees).

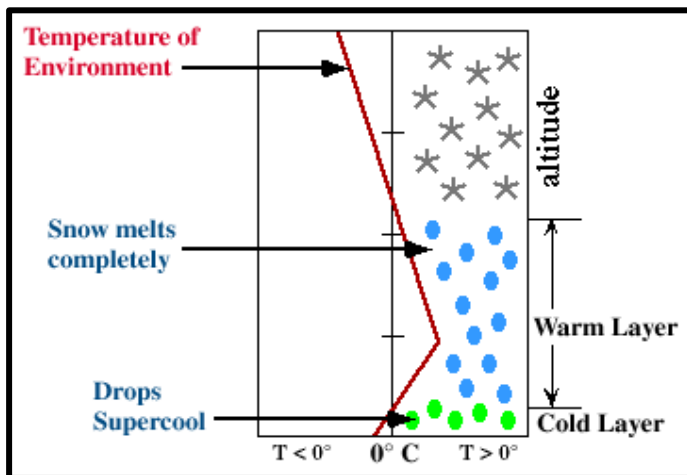


Figure 23: A graphical representation of the process of formation of freezing rain.

Sleet can be somehow considered an intermediate condition which may anticipate a freezing rain phenomenon, and therefore must be properly monitored even if it typically does not produce any relevant issues on the levels of traffic safety. In this case, the layer with warm air is not in the condition to completely melt snow in rain, and the lower cold air layer is not sufficiently wide to produce iced droplets. As far as **snow** phenomena are concerned, the entire air temperature profile is below zero, and there is no possibility to have state solid to liquid changes.

Hails is finally generated by a completely different physical process, and is produced in presence of upward air motions created within thunderstorms that are in the conditions to foster collisions between elementary droplets and to let them grow up in dimensions. Lowered heights of the freezing level finally transform these droplets in hail stones. Despite these meteorological events are typically uncommon for the winter season, they can represent a significant hazard on traffic safety and therefore must be properly considered in road weather applications, since this a very localized phenomenon difficult to predict.

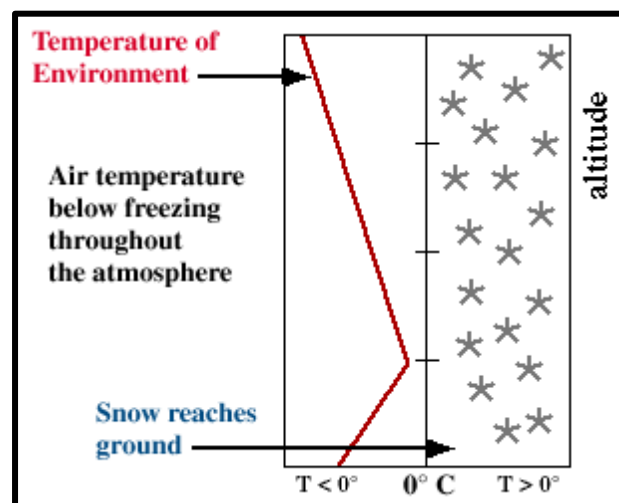


Figure 22: A graphical representation of the process of formation of snow.

In conclusion, the main reference meteorological use cases that need to be addressed by the winter road maintenance

services are all those that have as a direct or indirect consequence the formation of ice on the roads. Ice can appear if (i) a liquid film has accumulated on the road surface after a certain precipitation event, and (ii) the temperature of the water droplets is below the freezing point. The freezing process can take place not only at the road surface level, but also either at a certain layer of the atmosphere (e.g. in case of snow / hail). A holistic overview of all possible road slipperiness situations is graphically illustrated in Figure 24.

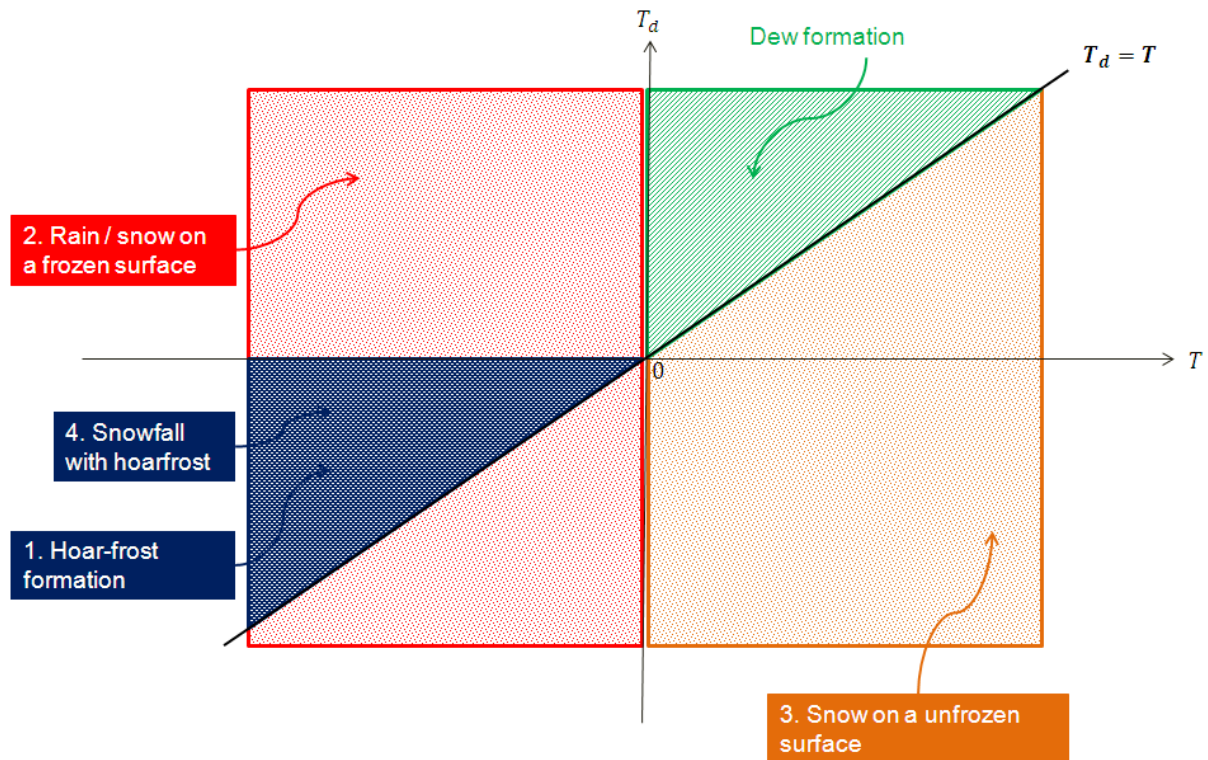


Figure 24: An overview of all possible road slipperiness situations caused by meteorological factors.

A crucial role in all these phenomena is played by the **humidity** factor, which enables the activation of ice formation processes on the road. A contribution to an increase of humidity can be produced by a precipitation event, or through a condensation / sublimation process of the air water vapor, which is at the base for the appearance of dew or **hoarfrost** on the ground, respectively. These processes take place when the air temperature is below a certain threshold value, which is known as **dew point**, which indicates at which temperature the air is overfilled of water vapor. In case the dew point is lower than 0 [°C], a sublimation process take place and hoarfrost can accumulate on the road surface; otherwise, there is only a simple condensation phenomenon and the production of dew. The concentration of humidity, which actually indicates the amount of water vapor present in the atmosphere, is a direct indicator of the relevance of this physical process: at very high concentrations levels, it can also determine the appearance of **fog**, which is another major safety hazard on roads.

The dew point is directly related to the air temperature T and to the relative humidity RH . A reference analytical way to estimate the dew point as a function of these two variables is the Magnus-Tetens approximation [46]:

$$T_d = \frac{b \cdot \left(\frac{aT}{b+T} + \ln RH \right)}{a - \frac{aT}{b+T} - \ln RH}$$

[17]

where a and b are two constant values, namely $a = 17,27$ and $b = 237,7[^\circ\text{C}]$. It is worth noting that in case of maximum relative humidity ($RH = 1$), the dew point corresponds exactly to the air temperature, i.e. $T_d = T$; on the other side, as the relative humidity becomes lower, the dew point is significantly decreased, thus reducing the probability of a hoarfrost event (Figure 25).

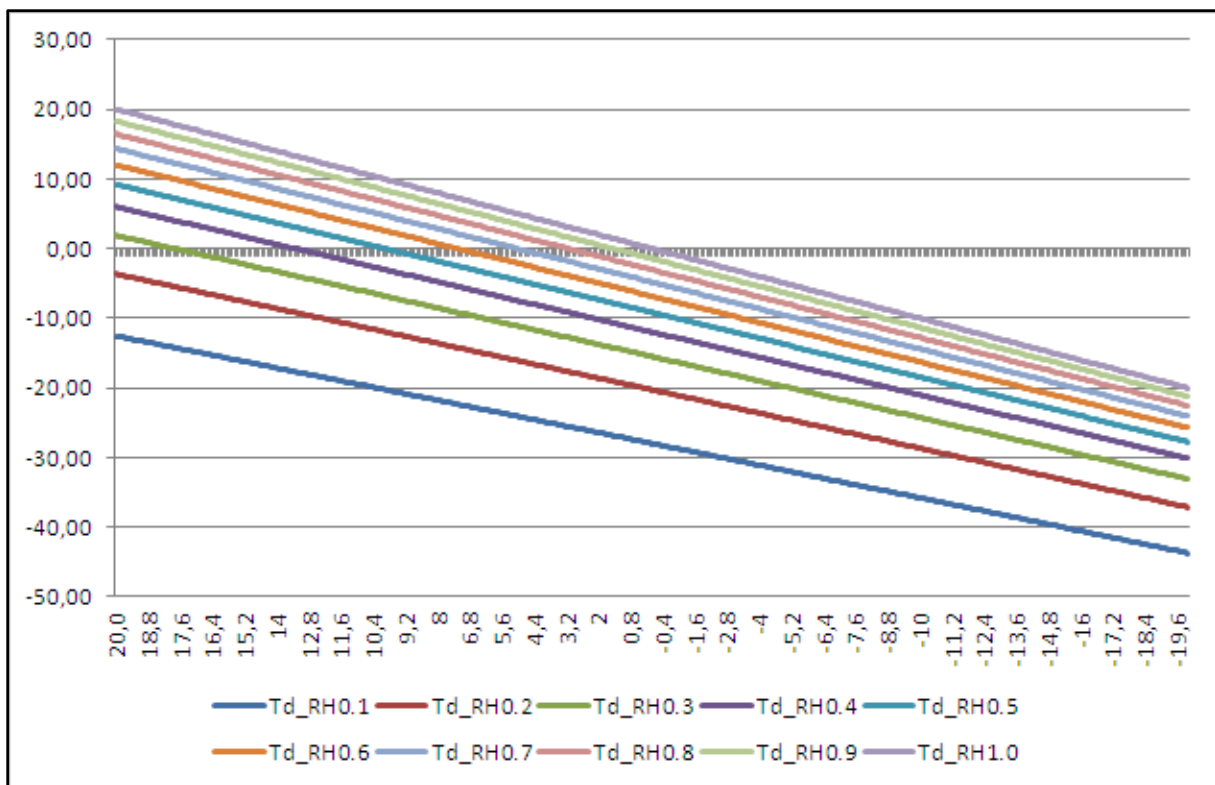


Figure 25: Relationship between air temperature (x-axis) and dew point (y-point) in correspondence to different relative humidity conditions (Magnus-Tetens approximation).

The last meteorological factor which plays an important role in the appearance of road weather events is **wind**, which main contribution is to significantly reduce the radiative cooling effect at night by promoting turbulent mixing, and thus determining higher nocturnal RST values. A reference use scenario for this phenomenon, which fits very well with the topographical patterns of an alpine region like the Autonomous Province of Trento was studied for example in [47], where RST measurements were carried out through thermal mapping operations within a road placed at different altitudes and during different wind conditions (Figure 26). The typical situation is that during clear and calm nights, RST is subjected to relevant spatial variations (e.g. up to five degrees in few hundreds of meters), which follow the local topography in which the road stretch is located. On the other side, in

case of windy and overcast nights, the cooling processes are significantly reduced and the spatial variations of RST are much more smoothed.

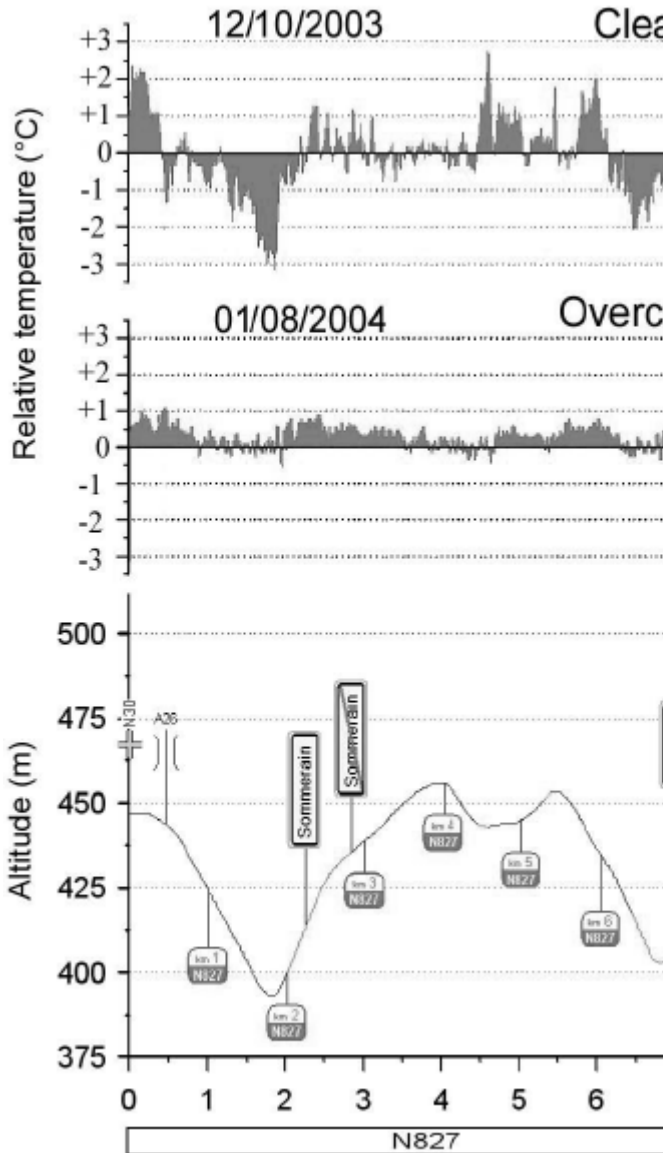


Figure 27: The main elements of a complete road weather monitoring system.

Figure 26: Nocturnal spatial RST variations at road stretches dominated by local topography in different wind conditions [47].

2.2 Road-weather stations

In order to determine in real-time the conditions of the road network, have the ability to compare it with the current and forecasted weather situation, evaluate the potential slipperiness risks that may occur and as a consequence define the treatment operations that need to be carried out in order to avoid them, it is necessary to have a monitoring system able to collect a variety of raw road weather data along the whole area under control. By referring to the mathematical expression proposed in Eq.[1], the influencing factors that

necessitate to be monitored in real-time are basically (i) the **local meteorological conditions** at the road level, and (ii) the **traffic flows**, which may provide some information about the current role that these are playing on the cooling processes on the ground. **RST and road conditions** data are typically collected as well, in order to provide an empirical and actual picture of the targeted situation to the winter road maintainers and operators. This data is also particularly important because it is typically used to validate and calibrate the road weather models which are executed in the back-end.

A road weather monitoring system is typically characterized by a network of **fixed RWIS stations**, installed at the roadside. Novel approaches take in consideration the possibility to collect RST spatially distributed data as well by mounting proper sensor on **mobile probes** (e.g. maintenance vehicles) and organize periodic thermal mapping operations during different meteorological conditions. The technological progress of the different components of these measurement systems are a fundamental and enabling element which directly determines the accuracy and the reliability of an entire RWIS, and therefore needs to be properly investigated before any design and implementation action.

The typical high-level architecture of a static RWIS station is presented in

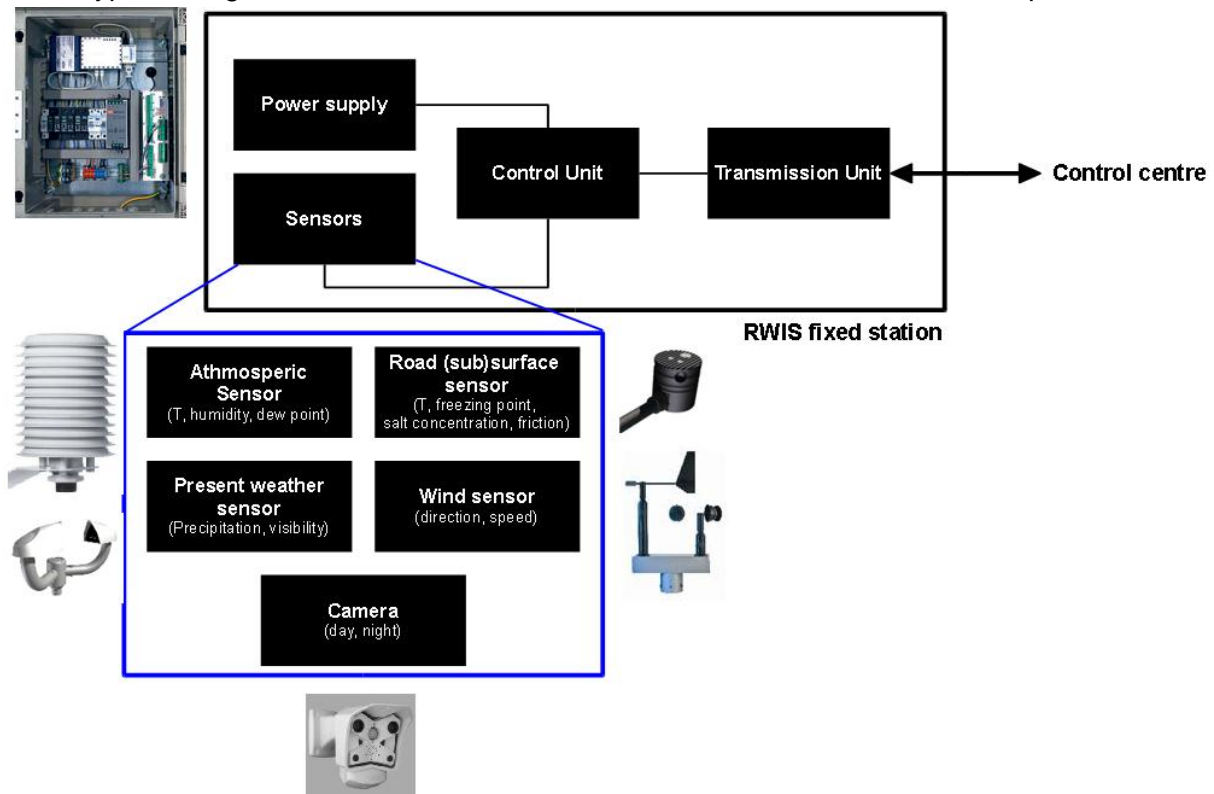


Figure 28. The main components that build it are:

- a set of sensors capable to monitor the **road conditions**, and namely the following parameters:
 - the **road surface temperature**;
 - the **road subsurface temperature**;

- the **road conditions** (typically labeled with reference the “standard” thematic classes “dry”, “wet”, “ice” and “snow”);
- the concentration of **residual de-icing chemicals**;

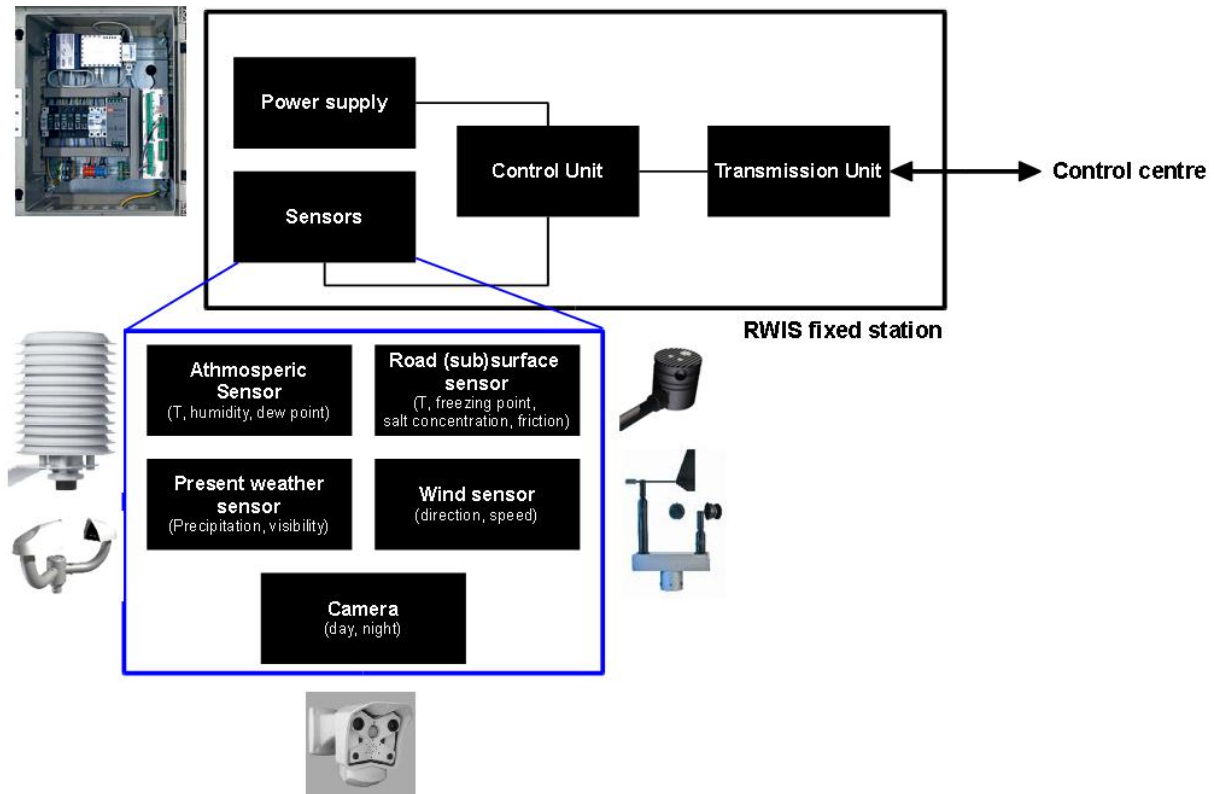


Figure 28: High-level architecture of a static RWIS station.

- the actual **freezing point** (modified as a function of the applied treatments);
- the **water film layer thickness**;
- the **friction coefficient**;
- a set of sensors that collect data on different meteorological parameters, e.g.:
 - the **air temperature**;
 - the **relative humidity**;
 - the **dew point**;
 - the **wind speed and direction**;
 - the **precipitation type and intensity**;
 - the **visibility level**;
 - the **barometric pressure**;
 - the **incoming solar radiation**;
- a traffic detection and counting system, which is able to automatically count the number of passing vehicles and classify them as a function of their membership class (e.g. heavy / light vehicles);

- a **power supply system**, which can be directly connected to the electric grid or implemented through batteries and autonomous energy productions systems, possibly using renewable sources (e.g. solar panels, wind power systems);
- a **remote control unit**, which is responsible for the local storage of the collected raw data and eventually for a first set of pre-processing computation on them;
- a **communication unit**, which allows to deliver the sensor data to a back-end system and to perform remote diagnostics controls of the correct functioning of the different components of the RWIS station;
- a **video monitoring system** which allows a remote visual control of the environmental conditions near the RWIS station.

2.2.1 Power supply

One of the most important aspects for a static RWIS station is the power supply. The energy demand of all different sensors and sub-systems is not exactly negligible, since it's typically in the order of 300-1200 [WH/day]. The availability of a direct connection to the public electric grid is often a key element when choosing the location of an installation, which may not fit with the specific monitoring needs of the road maintainers. The typical conservative approach for this is to position the stations in the coldest points of the network, thus having the possibility to anticipate phenomena which may appear also in other warmer parts of it. However, not always these opposite needs can be properly addressed, and expanding the public electric grid for such a requirement may often be unpractical from a time and economic perspective. Autonomous power generation and conservation systems are thus becoming an interesting option for this and similar road monitoring application fields.



Figure 29: The fuel cell based power supply system installed within the ASFINAG highway network [48].

An available solution in this direction, which was recently installed within the ASFINAG highway network in Austria at ten different locations, is to use **fuel cells** eventually combined with solar panels [48]. The advantage of fuel cells with respect to conventional batteries is that energy is stored separately and in a much more efficient way thanks to its conversion in hydrogen, and can lead to significant reduction in the overall power consumption. In the empirical experience mentioned above, it has been possible to guarantee a continuous power supply to the 50 [W] static RWIS stations for about 50 days. On the other side, such systems are typically much more expensive and require a certain maintenance overhead, in particular as far the hydrogen tanks is concerned.

Very innovative solutions, in some cases still far from being commercialized on the market, are starting to appear in this application domain. An interesting example in this direction is the MotionPower™ technology patented by the US company New Energy Technologies Inc., which is based on the principle to convert the **kinematic energy** of the transit vehicles electric energy [49]. In detail, the idea is to use artificial bumps that oblige vehicles to decelerate and thus to release part of their kinematic energy which may be accumulated in a proper energy storage system (Figure 30). From a mathematical point of view, the “ideal” accumulated energy E associated to a specific vehicle (the “effective” one is actually a fraction of it, because of heat dissipation losses) can be expressed as:

$$E = E_{kin}^{(1)} - E_{kin}^{(2)} = \frac{1}{2}m(v_1^2 - v_2^2)$$

[18]

where m is the total vehicle mass and v_1 and v_2 are the initial and final speeds, respectively.

In conclusion, the power supply system of a static RWIS station must be carefully designed as a function of different and in some cases conflicting requirements, namely (i) the entire power consumption of all different devices; (ii) the space and maintenance constraints determined by a specific roadside location; and (iii) the costs associated to the different power supply options. In some cases, one may also take in consideration security risks, i.e. the probability that at a certain location expensive energy generation and storage systems could be stolen by third spiteful people.



Figure 30: The MotionPower™ energy production system based on the accumulation of the kinematics energy released by the transit vehicles [49].

2.2.2 Remote control and communication unit

Remote control and communication functions are typically covered by standard and technology-consolidated equipment such as a datalogger, which is a flexible and modular device, having the ability to interface with sensors of different nature and produced by different suppliers. Different standardized protocols are available for the data transmission; the most famous and widespread are probably (i) **SDI-12** (*Serial Data Interface at 1200 Baud*), a serial asynchronous protocol based on ASCII format; and (ii) **MODBUS**, a serial protocol mostly used in industrial application for the data communication between electronic devices. Data can be typically downloaded also to an external system (e.g. a PC) thanks to a standard serial connection (e.g. RS232).

A datalogger avails of a modem as well for the transmission of the raw data to a back-end server. Different wired / wireless high bandwidth technologies are today available for accomplishing this task, the most used are (i) the **cellular network** (i.e. through 2G / 3G / 4G technology); (ii) **wireless local area networks** (e.g. Wi-Fi); (iii) dedicated **radio links**; and (iv) **optical fibre networks**.

2.2.3 Road conditions measurement technologies

Road conditions can be monitored by a static RWIS station through two different techniques: (i) a more traditional one, which avails of **invasive sensors** which are placed directly on the road; and (ii) a novel one, which is based on **non-invasive sensors** installed at the roadside. The two techniques are not exclusive, but complementary: in fact, the non-invasive approach is in the condition to determine only the road conditions at the surface layer, and the invasive approach is therefore required in case there is a specific necessity to take measurements of parameters referring to the subsoil, e.g. the subsurface temperature. Table 3 provides a comprehensive overview of all specific enabling technologies which are used to measure the different road conditions parameters through both methodologies; it is worth noting that the measurement of the **friction coefficient**, which is an important parameter especially in North Europe, where it is widely accepted the possibility of not always having “black” ideal roads, is typically done with mobile probes, and therefore is analysed in more detail in the next paragraph.

Parameter	Invasive techniques	Non-invasive techniques
Surface temperature	Negative (Positive) Temperature Coefficient (NTC / PTC)	Pyrometry
Subsurface temperature	Negative (Positive) Temperature Coefficient (NTC / PTC)	-
Road conditions	Wet / dry detector; snow detector	Active (e.g. LIDAR) / passive (e.g. optical) remote sensing system
Freezing point	Indirectly calculated as a function of other measures / active cooling system	Active (e.g. LIDAR) / passive (e.g. optical) remote sensing system
Residual salt concentration	Four-electrodes principle	Active (e.g. LIDAR) / passive (e.g. optical) remote sensing system
Water film layer thickness	RADAR	Active (e.g. LIDAR) / passive (e.g. optical) remote sensing system
Friction	-	Indirectly calculated as a function of other measures

Table 3: Comprehensive overview of the invasive and non-invasive technologies for the measurement of road conditions parameters.

As far as **surface temperature** is concerned, it can be measured through a direct contact with the road by means of a *Negative Temperature Coefficient (NTC) sensor*. The basic idea at the base of this technology is to measure temperature variations as a direct function of electric resistance variations which may be directly observed through thermistors, i.e. specific semiconductor sensing elements. Other devices could be considered for this task, e.g. thermoresistances, which are made up of metallic conductor materials, but the advantage of considering semiconductors is the possibility to reach a much higher sensitivity, typically with an improvement of an order ten.

From a mathematical point of view, the relationship between resistance R and temperature T is the following:

$$R(T) = \rho(T) \frac{L}{S} = \frac{1}{\sigma(T)} \frac{L}{S}$$

[19]

where L and S are the length and the section area of the semiconductor element, and ρ is its electrical resistivity. The reciprocal value of the latter one, i.e. the electrical conductivity ($\sigma = 1/\rho$), is the parameter which is directly influenced by temperature variations. This relationship is typically modelled through a negative exponential relationship, i.e.:

$$\sigma(T) = \sigma_1 e^{-\frac{T_1}{T}}$$

[20]

In case of NTC thermistors, the relationship between temperature and resistance can be directly expressed through the Steinhart-Hart equation [50]:

$$\frac{1}{T} = \frac{1}{T_0} + \frac{1}{B} \ln\left(\frac{R}{R_0}\right)$$

[21]

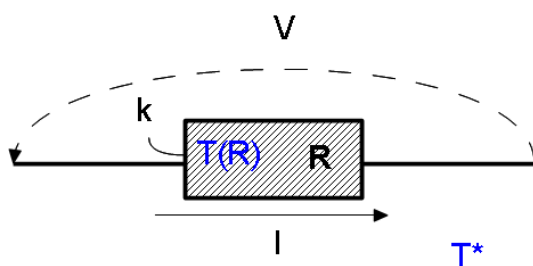


Figure 31: NTC temperature sensor measurement principle.

where B is a constant value, and T_0 is the reference temperature when $R = R_0$.

The measurement of the “target” temperature T^* is finally taken by considering the “temperature potential” between this temperature value ($T = T(R)$) and the heat power loss:

$$T^* = T(R) - \frac{1}{k} \frac{V^2}{R}$$

[22]

where k is a dissipation constant, expressed in $[mW/^\circ C]$. As far as the non-invasive measurement of the surface temperature is concerned, the state-of-art technique is **pyrometry**. A pyrometer is a device made up of a detector and an optical system, which is able to focus the incoming thermal radiation on it (Figure 32). The physical principle at the basis of this measurement system is the Stefan-Boltzmann law:

$$j^* = \varepsilon \sigma T^4$$

[23]

where ε is the emissivity of the road surface, $\sigma = 5.67 \cdot 10^{-12} [W/cm^2 \cdot ^\circ K^4]$ is the second Boltzmann constant, T is the target RST to be measured, and finally j^* is the measured thermal radiation (expressed in $[W/m^2]$).

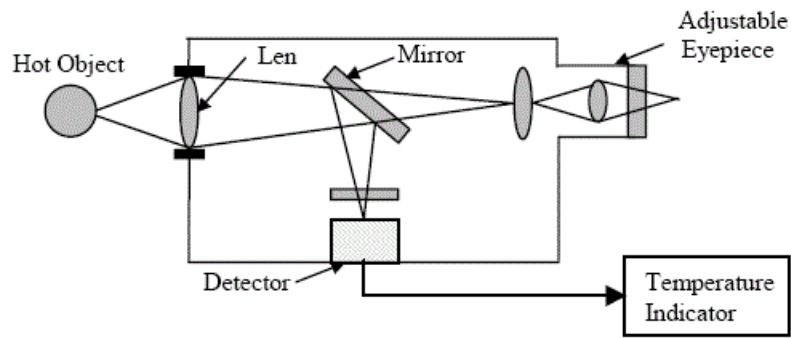


Figure 32: Reference high-level architecture of a pyrometer (Source: globalspec.com).

This measurement system is typically designed to work in the infrared bandwidth domain, in order to filter the undesired radiation components and minimize the noise that the environment is in the condition to introduce in the system.

The reference state-of-art performances of available commercial invasive and non-invasive RST measurement systems are summarized in Table 4. Accuracy is slightly better with invasive instruments, but in general both technologies guarantee a comparable detail level. Non-invasive techniques are typically much more flexible and cheaper (if installation and maintenance costs are taken in consideration), but could suffer of higher external interferences (e.g. caused by transit vehicles in the line of sight of the system), and thus the post-processing of the data could be more complex.

Performance indicator	Invasive techniques	Non-invasive techniques
Measurement range	(-40; +70) [°C]	(-40; +70) [°C]
Accuracy	± 0.2 [°C] (between (-10; +10) [°C])	± 0.8 [°C]
Resolution	± 0.1 [°C]	± 0.1 [°C]

Table 4: Performances of invasive and non-invasive RST measurement techniques.

A significant limitation of both systems is the reduced capability in the space domain, since they are in the condition of providing a measurement of RST which is linked to a very small area of the road (typically in the order of some centimetres), that could be more or less significant of the whole local RST patterns in the surrounding spatial domain. A possible solution in this direction could be the use of **infrared pyrometer cameras**, which are able to gather thermal images of a wider portion of road network, and give an assessment of the spatial variations of RST. Limited deployments of these systems are however available in the RWIS domain, in part motivated by their actual high costs, and in part justified by the lack of availability of efficient and high-accuracy 3D RST elaboration and forecasted models.



Figure 33: Infrared pyrometer camera (Source: testolimited.com).

Road conditions can be determined and classified through different approaches. In the case of invasive techniques, the common approach is to use a **couple of detectors**: one is used to distinguish between dry and wet conditions through an electrode that gives in output a voltage which is proportional with respect to the current values of surface humidity; one is used to determine the presence of snow by detecting the intensity of light transmitted by two LEDs (in case of snow, transmitted light is reflected to the detector). This technique is typically combined with certain methods for the measurement of the **residual salt concentration** and the **freezing point**, the most adopted are:

- the **four electrode principle**, which is based on the idea of taking salinity measurements by letting a constant alternating current flowing the two outer electrodes and measure the voltage in correspondence of the two inner electrodes (Figure 34). If water is present, the voltage is proportional to the concentration of salt, and an estimation of the freezing point can be thus calculated;
- an **active cooling system**, which is based on the idea to heat and cool repeatedly and in a controlled way the surface of a sensor, and to measure the temperature in correspondence of which a freezing condition is detected.

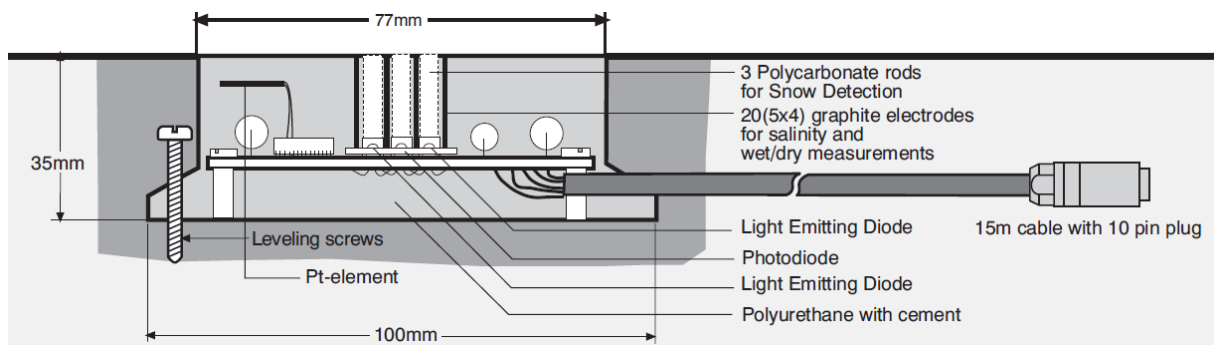


Figure 34: Possible design of an invasive road conditions sensor [51].

Radar systems are furthermore used in case of invasive measurements of the **water film layer**. In this case, the principle is to determine this parameter as a function of the time of arrival of the echoes of the transmitted signals and/or by automatically evaluating the backscatter coefficient. Research works such as [52] - [53] have moreover demonstrated the potentiality of considering polarimetric radar systems operating at millimetre-wave frequencies to further characterize the film layer which may be present on the road surface.

This idea to use **passive / active remote sensing** for the characterization of the road conditions have led in the last years to the introduction of a significant set of **commercial non-invasive road measurement** products. Pattern recognition algorithms and techniques applied to either passive long wave radiation emitted by a selected location on the road surface (passive case), or the backscattered signal which is produced by reflection of a transmitted infrared light beam (active case – LIDAR-based system), can provide a plenty of useful information concerning the road, e.g. not only a classification of its condition, but also information such as residual salt concentration (consequent estimation of freezing point),

water film layer characteristics (e.g. thickness and consistency), and estimation of the friction value (Figure 35).

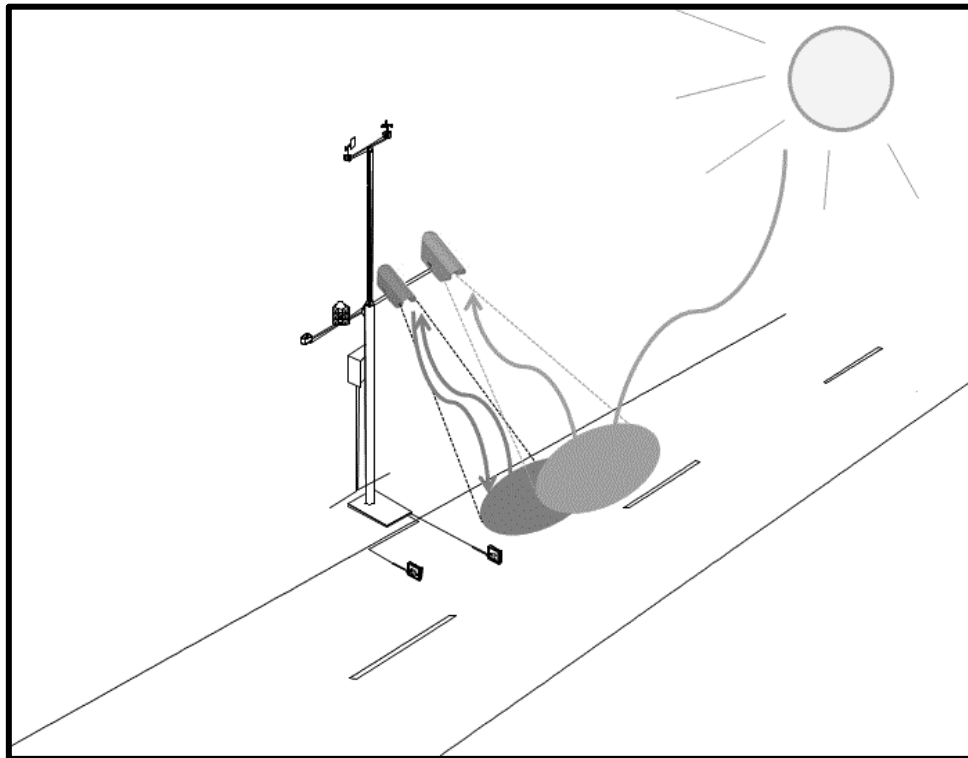


Figure 35: Remote sensing techniques applied in the road weather application domain for non-invasive road conditions measurements.

Table 5 provides an overview of the typical performances which can be achieved through both measurement approaches; the comparison is made for referencing purposes on the water film layer thickness only. The considerations made concerning the performance of the RST measurement techniques can be applied even in this case; non-invasive technologies have the potential to take more precise measurements, but in a limited range only.

Performance indicator	Invasive techniques	Non-invasive techniques
Measurement range	(0;4) [mm]	(0;2) [mm] (up to 10 [mm] in case of snow)
Accuracy	± 0.1 [mm]	n.a.
Resolution	± 0.1 [mm]	± 0.01 [°C]

Table 5: Performances of invasive and non-invasive water film layer measurement techniques.

2.2.4 Roadside weather conditions measurement technologies

Roadside weather conditions are typically measured with the same sensors and devices which are widespread in the meteorological community. Different technologies and techniques are commonly used in order to collect data about different meteorological parameters which may have an impact on road safety.

As far as **air temperature** is concerned, the reference technology is even in this case based on **NTC sensors**, with the only difference that these are placed at a typical height of 2 [m] and not within the road surface (or subsurface).

Relative humidity (RH), which is defined as the ratio between the pressure of water vapour with respect to the saturated vapour pressure of water at a specific temperature, is typically measured through a **capacitive element**, by taking advantage of the direct relationship between the dielectric constant k and the relative humidity:

$$C(RH) = \frac{k(RH)\epsilon_0 A}{d}$$

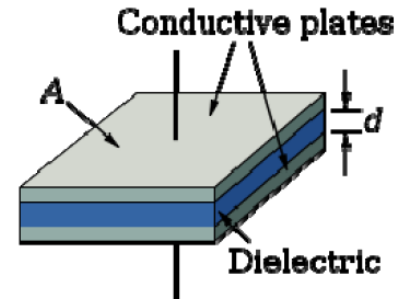


Figure 36: The reference geometry of a capacitor.

[24]

where $C = C(RH)$ is the capacity, $\epsilon_0 \cong 8.85 \cdot 10^{-12}$ [F/m] is the vacuum permittivity, and A and d are the geometrical properties of the capacitor (Figure 36).

It is possible to demonstrate [54] that the comprehensive relationship $C = C(RH)$ is in first approximation linear, in particular within the interval $5\% < RH < 95\%$. The variations of capacity are transformed in an electrical signal which is then post-processed in order to obtain the final measurement of relative humidity. At present, research is investigating alternative dielectrics which are able to increase the performance of this type of sensors and reduced the power consumption. A possible solution in this direction is represented by **Multi-Wallet Carbon Nanotubes (MWCNTs)**, which have already demonstrated a significantly higher sensitivity [55] (Figure 37).

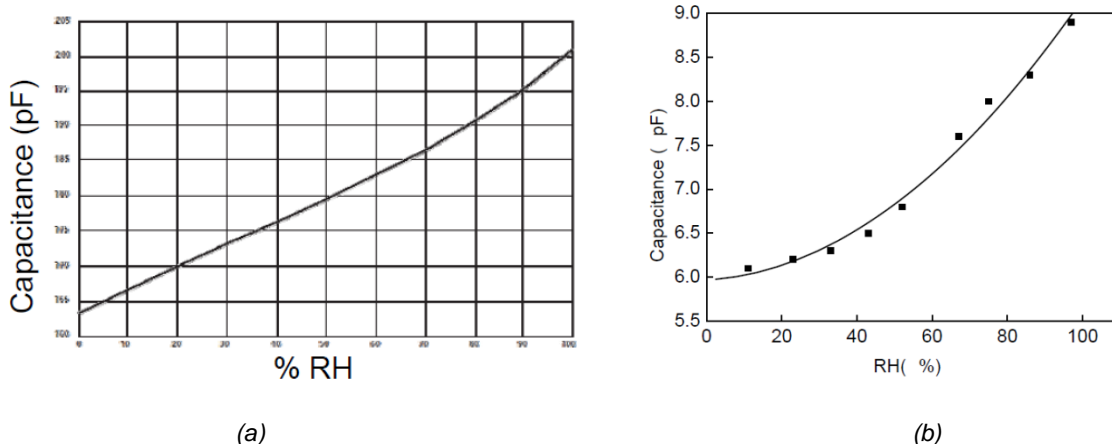


Figure 37: Empirical relationships between capacity and relative humidity in different dielectric sensing elements: (a) standard capacitive element [56]; (b) MWCNTs [55].

Air pressure is typically measured through with **Micro Electro Mechanical Systems (MEMSs)**, in particular through two different transducing principles:

- **piezoresistive**, i.e. through a transformation of mechanical quantity in an electric voltage signal (Figure 38);
- **capacitive**, i.e. through a transformation of a capacity variation in an electric voltage signal, as in the relative humidity case (Figure 40).

Both sensor technologies use a siliceous pressure sensitive diaphragm, and thanks to their efficient sensitivity with respect to low temperatures and high pressure values, as well as their low power consumption, they are today quite widespread in the market.

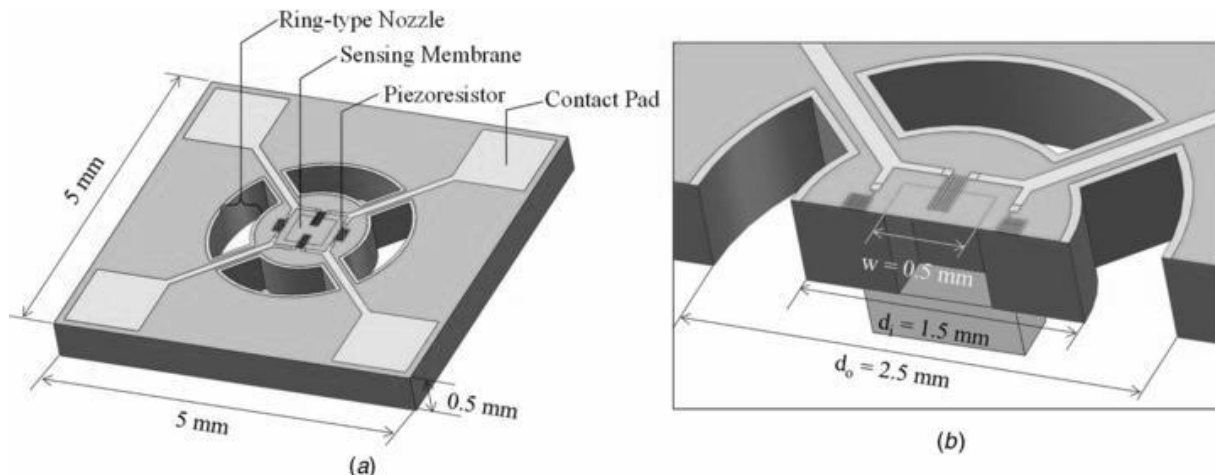


Figure 38: Typical layout of a piezoresistive air pressure sensor [57].

These sensors are able to measure air pressure as a function of a reference pressure level, through a measurement approach which can be:

- **absolute**, i.e. in case the measurement refers to a closed space with artificial vacuum inside it, which is the typical method followed in road weather applications (Figure 39);
- **relative**, i.e. in case the measurement refers to the environmental pressure value (equal to 1 [atm]);
- **differential**, i.e. in case the measurement refers to an arbitrary air pressure value.

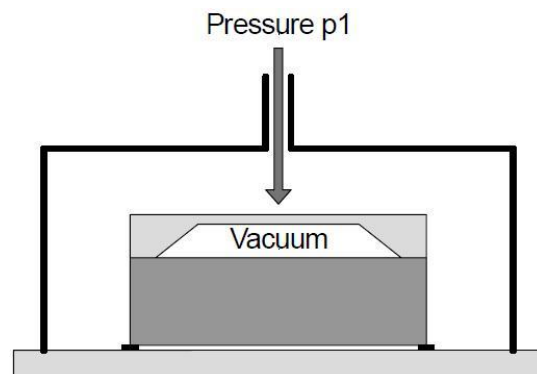


Figure 39: Absolute air pressure level measurement approach.

Present weather sensors have as objective to take measurements of the precipitation rate and type. Traditionally, this kind of parameters have been measured for years through **pluviometers** (or rain gauges), which are in the conditions of collecting precipitation through different detection techniques (the most common include graduated cylinders, weighing gauges, tipping bucket gauges and simple buried pit collectors). These containers are connected to a recording device system typically consisting of a pen mounted on an arm attached to a geared wheel that moves as a function of the precipitation level accumulated.

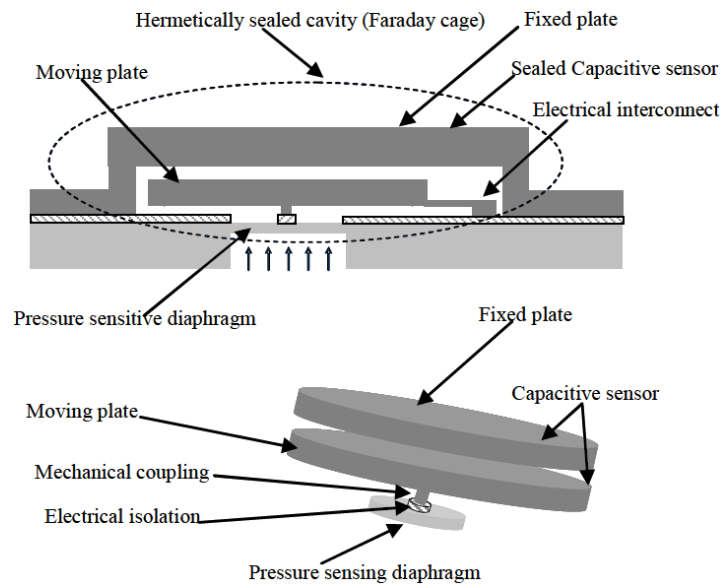


Figure 40: Typical layout of a capacitive air pressure sensor [58]

The main limitation concerning the use of pluviometers in road weather applications is related to the impossibility to immediately realize that a precipitation event has just started, since a certain precipitation quantity must be accumulated before a signal is triggered; moreover it is not possible to classify the type of precipitation. For this reason, new measurement techniques known as **disdrometers** were introduced, with the purpose to also characterize further parameters such as the *Drop Size Distribution* (DSD), i.e. the distribution of the water droplets dimension, and their correspondent falling rate, which can univocally identify the type of precipitation. One of the first instruments proposed in the scientific literature was the **Joss-Waldvogel disdrometer**, which is based on the idea of generating a voltage pulse of amplitude U_L as function of each water droplet of diameter D , based on the following relationship:

$$U_L = kD^n$$

[25]

where k is simply a proportionality constant.

Disdrometers can rely on different measurement principle; they can be **acoustic**, in case acoustic signals are generated in output, or even be **camera-based**, i.e. which create an optical image for each fallen water droplet. In road-weather applications, however, two classes of disdrometers have managed to reach a certain market:

- **optical disdrometers**, which are based on the idea to measure the effects produced by water droplets passing a beam light between a lighting source and an optical receiver (Figure 41);
- **radar disdrometers**, which analyse the echoes produced by the water droplets as a consequence of transmitted microwave electro-magnetic pulses.

As far as optical disdrometers are concerned, an optical transmitter creates a laser infrared beam, which is pulsed in the time domain and is characterized by a certain power. In case of

absence of precipitation, the optical receiver, which focalizes the beam to a detector through a complex optical system, generates an electrical signal which is proportional to the power of the received light signal. When a precipitation event takes place, droplets have a double impact on the output signal, i.e. they produce a reduction in the signal amplitude, which is directly linkable to their dimension, and a certain duration of this signal reduction, which is proportional to the transit time of the droplet within the laser beam and therefore directly linkable to the precipitation rate. By properly processing these signal reductions one can precisely estimate type and amount of precipitation fallen on the ground.



Figure 41: Principle of functioning of an optical disdrometer (source: thiesclima.com)

Radar disdrometers are based on a different functioning principle, i.e. to post-process the echoes which are produced by reflection of the transmitted pulses with the water droplets. From a mathematical point of view, it is possible to directly express the received power P_{RX} as a function of the radar reflectivity η :

$$P_{RX} = \beta \frac{\eta V_R}{R^4}$$

[26]

where β is a constant which depends of the design choices of the entire radar system, V_R is the resolution volume and R is the distance between the target (the water droplets) and the radar system itself. The radar reflectivity is the most important parameter in this equation, since it contains the information related to the actual precipitation event, and can be expressed in turn as a function of the reflectivity factor Z :

$$\eta = \frac{\pi^5 \alpha}{\lambda^4} Z$$

[27]

where α is the dielectric constant of the target material, and λ is the wavelength of the system. Typically, similar radar systems work at the frequency of 24 [GHz], which corresponds to a wavelength of 12.5 [cm], which is comparable to the dimension of the water

droplets. The reflectivity factor Z is directly linked to the dimension of the elementary scattering objects and can be modelled through a discrete or continuous model, respectively:

$$Z = \sum_{i=1}^N D_i^6 \quad [28]$$

$$Z = \int_0^{+\infty} N(D)D^6 dD \quad [29]$$

where D_i is the diameter of the i -th elementary scattering objects, and N is their total number within the resolution volume; $N(D)$ is the *Drop Size Distribution* (DSD) of the randomized variable D , which is typically modelled through a Gamma distribution in which the precipitation rate R_f is directly expressed:

$$N(D) = N_o e^{-kR_f^{\beta''} D} \quad [30]$$

where N_o , k and β'' are the parameters of the probability density function. A radar disdrometer is thus natively in the condition to statistically evaluate the distribution of the water droplets dimension; in order to determine the precipitation speed and more generally their falling precipitation motion as well, it is however necessary to evaluate the power spectrum in the Doppler frequencies domain.

Wind speed and direction are meteorological parameters measured through **anemometers**. Different anemometers classes are available at the state of art, and are based on different physical principles, as illustrated in Table 6.

Anemometer class	Description
Anemometers based on mechanical principles	Based on the mechanical motion generated by wind
Electronic anemometers	Based on the thermal field variations determined by wind
Sonic anemometers	Based on the influence of wind on the time of flight of ultrasonic signals
Laser Doppler anemometers	Rely on the Doppler effect induced by wind on a couple of controlled laser signals

Table 6: Overview of the physical principles at the base of state-of-art anemometer classes.

Mechanical anemometers are the most traditional wind measurement systems, and have their origin already in the nineteenth century. The principle is to generate mechanical energy thanks to the wind intensity, and to use it to put in motion a mechanical rotating device, which can be for example a skyvane or a system of hemispherical cups. In the latter case, the cups are typically coupled with a vane in order to take measurements of the wind direction as well.

The vane is connected to a circular system of relays, which are commuted instantaneously as a function of the wind direction variations. The intensity of the wind speed can be measured on the base of two different techniques, namely:

- **electromagnetic induction**, which is able to create a time-variant magnetic field as a function of the mechanical energy produced by the wind (based on the Faraday-Neumann-Lenz law), and thus to create a correspondent electric voltage;
- **optoelectronics**, in which an optoelectronic transducer generates an electric voltage signal whose intensity is directly proportional to the rotation speed of the mechanical device.

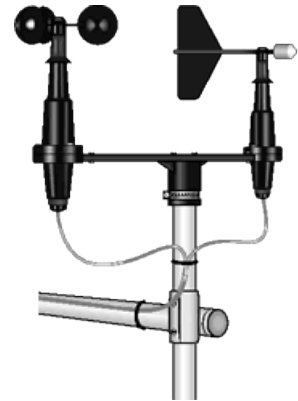


Figure 42: Mechanical anemometer example.

Electronic anemometers are a new generation of wind measurement instruments, and are based on bi-dimensional thermal flow sensors (Figure 43). These sensors consist of a silicon chip which integrate a certain number of resistive radiating elements (heaters) and temperature sensors, organized according to a specific symmetric organization. They work in *Constant Average Temperature Difference (CATD)* mode, i.e. the temperature of the central diode is kept constant through the system of surrounding heaters. When an air flow enters in contact with the anemometer, a temperature gradient is revealed by the temperature sensors system, and this can be put direct in relationship with the speed and direction of the wind. The orthogonal components of this temperature gradient are then finally amplified and processed outside the chip. The main problem with this solution

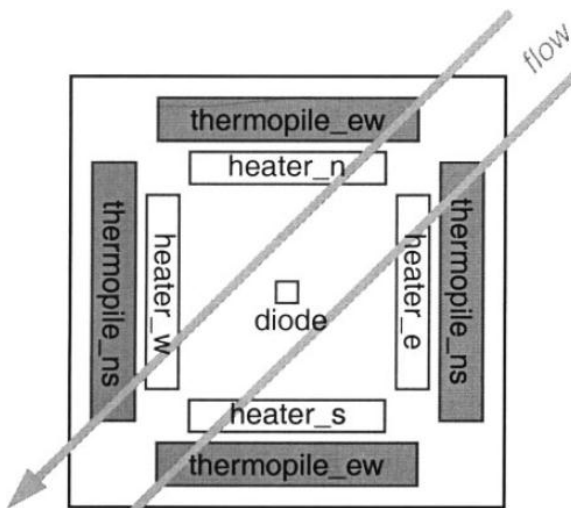


Figure 43: Reference architecture of an electronic anemometer based on a 2D thermal flow sensor [60].

is that output signal have a very low amplitude (typically in the order of $[\mu V]$), and are characterized by a low signal-to-noise ratio.

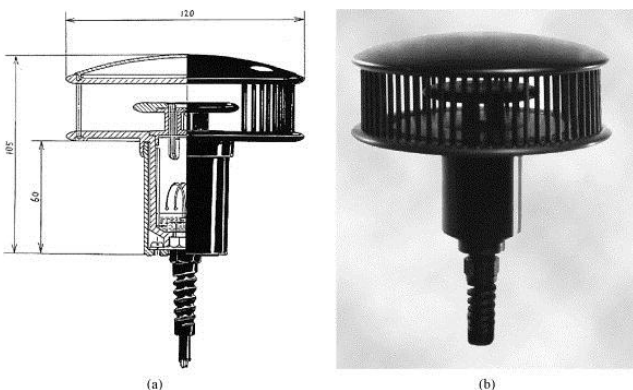


Figure 44: Layout of an electronic anemometer based on ZDT approach [59].

An alternative solution, known as *Zero Differential Temperature (ZDT)* approach, is to keep a constant temperature not just in correspondence of the central diode, but within the entire chip. In this case, the wind is characterized by taking in consideration the thermal power dissipated by the heaters in order to maintain this reference temperature condition; the temperature sensors are only

used to evaluate the sign of the equivalent temperature gradient.

Sonic anemometers are based on a further different principle, i.e. to measure the *Time Of Flight* (TOF) of a sonic signal at a typical frequency of 100 – 300 [kHz] which is transmitted among a couple of transducers, which is directly related to the wind speed v_w according to this simple relationship:

$$TOF = \frac{L}{v_s + v_w}$$

[31]

where L is the distance between the two transducers and v_s is the speed of sound in air.

By measuring TOF in both transmitting directions, it is possible to have to estimate v_w as a direct function of L and the observed TOF values. In practice, a sonic anemometer is implemented as shown in Figure 45. Three transducers are put at the vertexes of an equilateral triangle, with the possibility to measure wind components in different points. In every measurement cycle, each transducer sends N impulses to the other two transducers. In this way, it is possible to collect $6N$ TOF measurements, which are then statistically post-processed in order to extract robust wind speed and direction values. This approach has proved to be particularly reliable, even in case of particular turbulent air flows conditions.



Figure 45: Sonic anemometer.

An evolution of sonic anemometers is represented by the **acoustic-resonance anemometer** patented by FT Technologies (Figure 46). The basic idea is to generate ultrasonic resonant acoustic signal as a function of the entering air flow, and to take wind measurements as a function of the generated stationary wave peculiarities. The advantage of the system is that it can automatically compensate variations caused by changes in temperature, humidity and pressure, but the complexity is always maintain the sensor in resonance conditions.

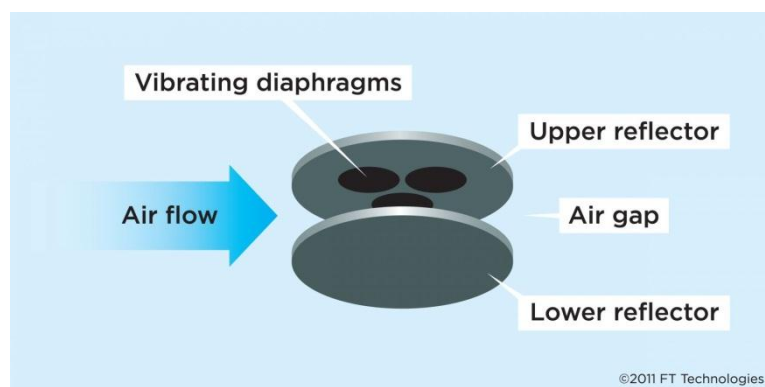


Figure 46: Principle of functioning of an acoustic-resonance anemometer (Source: FT Technologies)

One of the most interesting solutions from a technological point of view, but unfortunately not widely spread in the market because of its high cost (in particular in terms of calibration and complexity terms), is represented by **Laser Doppler Anemometers** (LDA) [59]. Two incident laser signals, separated by an angular distance equal to θ , radiate a certain measurement volume. Inside it, a flow with seeding particles enters in collision with these signals, and a backscatter phenomenon is produced in direction of the receiving / transmitting system. The backscattered signal is received by a light detector (typically implemented by a *Photo Multiplier Tube*), which generates an electric current whose amplitude is proportional to the received energy (Figure 47). At the reception side, it is possible to isolate an aggregated Doppler frequency f_d , defined as the medium Doppler frequency experienced by both laser signals, which is equal to:

$$f_d = \frac{v}{\lambda} \sin(\theta/2)$$

[32]

where λ is the signals' wavelength and v is the wind speed. Further post-processing operations are then necessary in order to properly manage the ambiguities of the Doppler phenomena and estimate the wind direction as well.

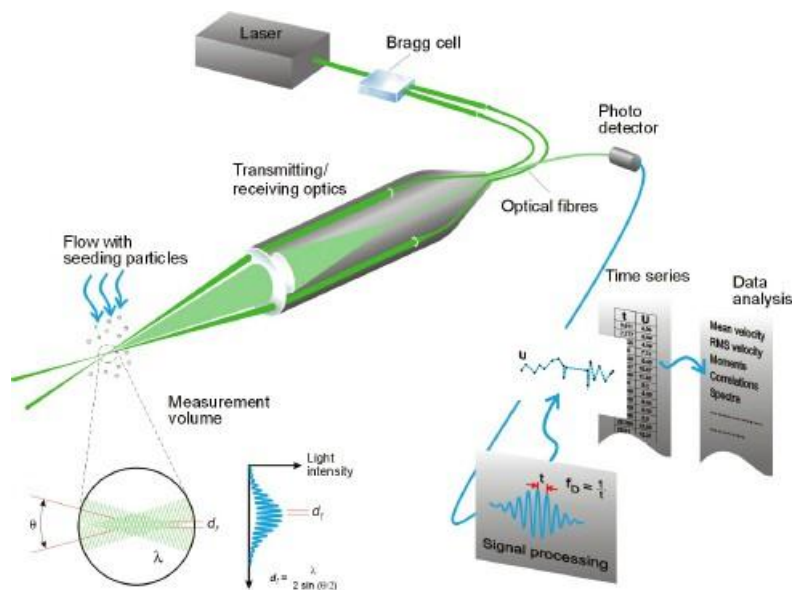


Figure 47: Principle of functioning of a Laser Doppler Anemometer (Source: dantecdynamics.com)

The last class of measurement instruments which are used in road weather applications and which is worth to be analysed within this overview section is those related to **visibility**. This is a topic which is a little bit outside the scope of the project, since fog is a meteorological phenomenon which is not exactly related to the winter road maintenance and is not particularly common in the alpine region of interest. Despite this, it is worth providing some brief insights about the recent technological enhancements that have been proposed for this kind of measurement applications. Fog is a very complex phenomenon, since it is typically very irregular in space. Different parameters and indicators are available in order to

determine the actual level of visibility, for example the *atmosphere Extinction Coefficient* (EXCO), or the meteorological visibility. In road weather applications, however, the *Meteorological Optical Range* (MOR) is commonly considered. This range is defined as the line-of-sight distance which is necessary to weaken by 95% a luminous flux which is generated by a source operating at a reference temperature of 2700 [°K].

The common fog measurement instrument is illustrated in Figure 48. A light emitter transmits a signal towards a near measurement volume. Light is backscattered as a function of the water droplets which are present in the atmosphere and is detected by a receiver put at an angular distance equal to ϑ with respect to the transmitter. The luminous intensity I can be expressed in direct relationship with the geometry of the measurement system, i.e.:

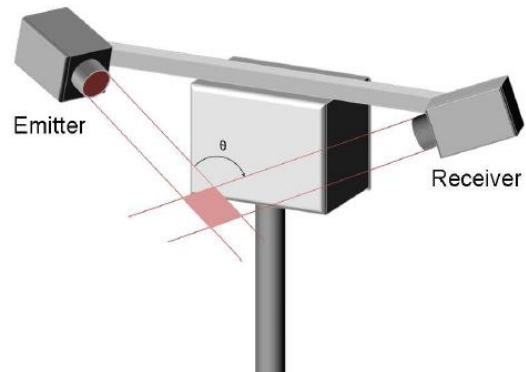


Figure 48: Principle of functioning of a common visibility meter [60].

$$I = AI_0Vf(\vartheta)e^{-kd}$$

[33]

where A is a constant which depends on the power and optical system used at the transmitter side, I_0 is the luminous intensity of the transmitting light signal, V is the measurement volume, k is the EXCO parameter and d is the total distance between transmitter and receiver. By measuring I , it is possible to estimate the EXCO parameter and indirectly the MOR.

An alternative to this technology is the use of cameras. EXCO and MOR can be measured by evaluating the luminous intensity of the acquired image stream (Figure 49). The resolution of the system is in this case strongly dependent on the optical resolution of the camera and its geometry.

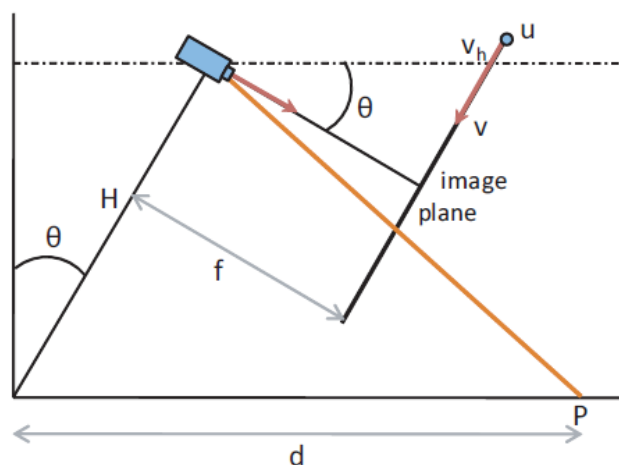


Figure 49: Principle of functioning of a camera-based visibility meter [60]

As a conclusion of this overview of the reference measurement technologies of road weather phenomena through static RWIS stations, Table 7 illustrates the typical measurement ranges and accuracy for all major meteorological parameters of interest, based on technical sheets of commercially viable products.

Parameter	Measurement range	Accuracy
Air temperature	[-50; + 60] [°C]	±0.01 [°C] for T < 10 [°C]
Relative humidity	[0;100] %	±0.1% for T < 10 [°C]
Air pressure	[300; 1200] [hPa] (capacitive)	±1.5 [hPa]
	[600; 1100] [hPa] (piezoresistive)	
Present weather	[0.3; 5] [mm] (water droplets dimension through Doppler Radar)	±0.01 [mm]
Wind	[0; 50] [m/s] (mechanical)	±0.3 [m/s]
	[0; 60] [m/s] (electronic)	±0.3 ± 3% measured value [m/s]
	[0.1; 85] [m/s] (sonic)	±0.5 ± 5% measured value [m/s]
Visibility	[3; 30] [km/h]	±5% between 0-16 [km] (in homogeneous conditions)

Table 7: Reference measurement ranges and accuracies for different meteorological parameters.

2.2.5 Traffic conditions measurement technologies

Despite it is not a direct objective to provide a detailed report on all available traffic monitoring technologies, it is useful to provide a comprehensive glance about what is today technologically viable in the traffic detection domain. The recent evolution of the *Intelligent Transportation System* (ITS) sector has brought on the market several possibilities to gather data concerning the traffic conditions on the road. Two different approaches may be considered for static traffic detection [61]:

- **intrusive**, i.e. in case the traffic detectors need to be placed inside the roadway;
- **non-intrusive**, i.e. in case the detectors can be installed above roadway or side-fire.

A third approach has recently emerged, namely the use of **off-roadway technologies** such as remote sensing and in particular probe vehicles. This aspect will be specifically addressed in the following paragraph and in Chapter 5.

Intrusive technologies are in use already since a couple of decades. Despite their massive presence on the market, they present several operational problems and limitations, e.g. traffic flows disruptions in case of installation and maintenance, high failure rates under certain monitoring conditions, and above all inflexibility, with the possibility to change monitoring location after an installation has taken place.

Various intrusive technologies are available on the market, more specifically:

- inductive loops**, which are based on the idea to detect the variations of the inductance of magnetic loop as a consequence of a vehicular transit, which are converted in frequency variations of a detector oscillator (Figure 50). The inductance variations are measured through a loop arranged in one or more insulated tires put in a shallow slot sawed in or across the road pavement. Different loop detectors exist (i.e. saw-cut, trenched-in and preformed), and determine the way the loop needs to be installed (and maintained) in the road pavement. Inductive loops can not only determine volume, presence and occupancy of the vehicles, but also their speed and their type, determined as a function of post-processing operations based on fundamental traffic variables relationships and automatic pattern recognition of the inductance variation signal, respectively. This method has been to be accurate and reliable, but however suffers of significant installation and maintenance costs as well as high failure rates;

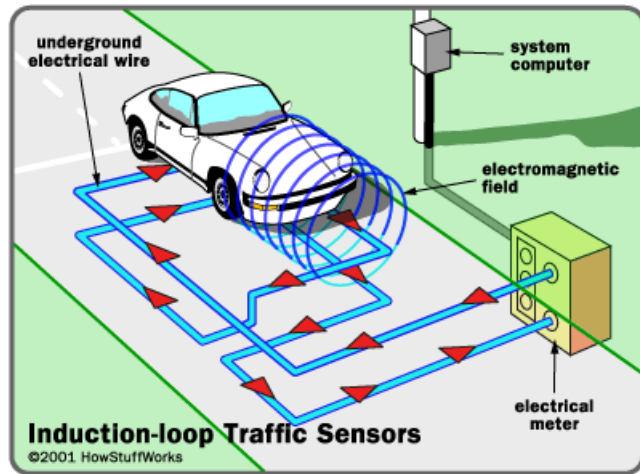


Figure 50: Principle of an inductive loop (source: auto.howstuffworks.com)

- magnetic detectors**, which measure the effects of the metallic components of vehicles on the Earth's magnetic field through magnetic detectors (e.g. induction or dual-axis fluxgate magnetometers). The advantages of this traffic detection solution is that the installation requires fewer disruptions to traffic flows, have typically an increased service life;

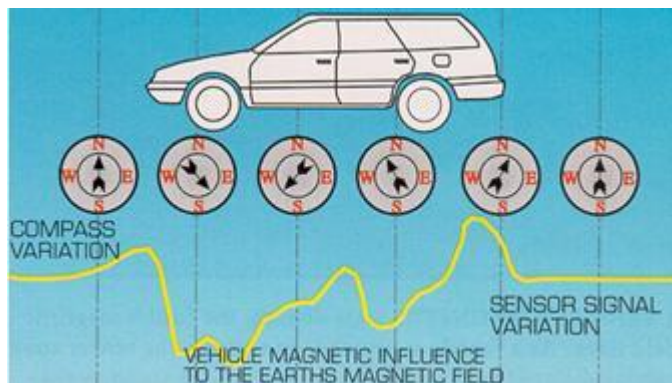


Figure 51: Principle of a magnetic traffic detector (source: fhwa.dot.gov)

- pneumatic rod tubes**, the first traffic detector technology ever invented, already introduced in the 1920s, and which is based on the idea to sense vehicle pressure and convert it in air pressure bursts which are sent through a rubber tube and then converted in an electronic signal. Post-processing operations can also lead to vehicular classifications. This approach is simple and low-cost, and typically applied for short-term counting operations;
- piezoelectric detectors**, which transform the kinetic energy of transit vehicles in electrical energy. Since the kinetic energy is directly associated to the force or weight

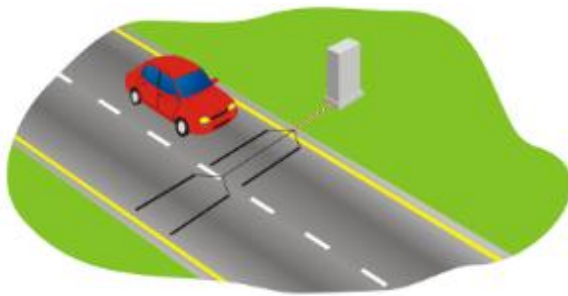


Figure 52: Principle of a piezoelectric traffic detector
(source: metrocount.com)

of the vehicles, these sensors can also detect distinguish this parameter, which may be of particular importance in certain traffic control operations (i.e. Weigh-In-Motion (WIM) applications). Speed can be also measured but in this case multiple detectors are required.

Non-intrusive technologies represent in some way the new generation of traffic detectors technology, since it has the potential to solve (or at least improve) many of the limitations of the intrusive detectors. In fact, since they can be installed over the road or at its side, they are capable to minimize traffic disruptions caused by installation and maintenance activities. During their first launch on the market, non-intrusive technologies were typically more expensive and less mature than intrusive ones, and this initially limited their diffusion. The improvement of these technologies and the reduction of costs have gradually allowed them to improve their market share. Different principles can be used for making non-intrusive traffic measurements; the most traditional are:

- **active and passive infrared detectors**, which are based on the idea to detect the presence of a vehicle by analysing either (i) the variations in the time of flight of a backscattered signal which is generated as a consequence of an artificially generated infrared signal (*active detectors*), or (ii) the thermal radiation changes which are proportional to the emissivity differences (*passive detectors*). These detectors operated in the infrared frequency range (100-105 [GHz]) and can produce in output either a 1D signal or an image. Active detectors can be implemented with both low-energy LEDs as well high-energy lasers can be used, depending on the particular installation requirements, and are more capable in the sense that they can also classify traffic;
- **microwave radars**, which can be implemented by taking advantage of either (i) the Doppler effect or (ii) the processing of frequency-modulated continuous wave (FMCW) signals. In the first case, a transit vehicle is detected when a variation of the Doppler frequency occurs as a function of the relative motion of the system detector-vehicle; in the second case the range from the detector is considered to measure presence and speed of the vehicles. The advantage of the latter ones is that it is possible to recognize the presence of very slow vehicles as well;

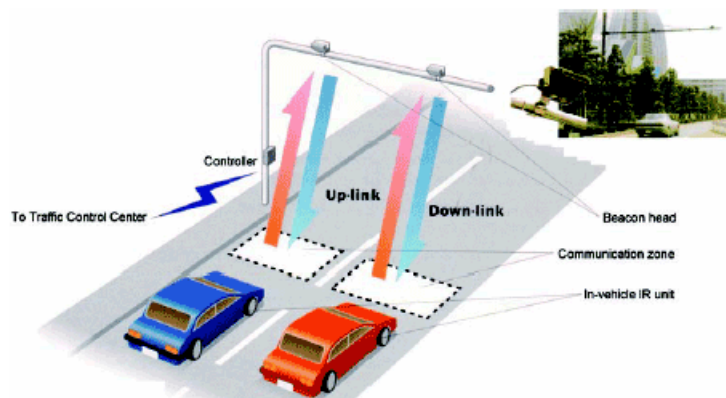


Figure 53: Principle of an active infrared traffic detector
(source: fhwa.dot.gov)

- **ultrasonic and passive acoustic detectors**, which rely on passive or active remote sensing principles but applied in the acoustic domain. Ultrasonic detectors are active systems which typically work in the frequency range [2-300] [KHz], and can use as “investigating” signals both pulse trains as well as FMCW signals. On the contrary, passive detectors measure the acoustic energy produced by the variety of sources which are present in the environment, and try to detect the presence of passing vehicles;



Figure 54: Ultrasonic vehicle detector (source: global-sei.com).

- **video image processing techniques**, which automatically extract traffic information from images related to a certain detection area. These systems are typically characterized by one or several cameras, designed in order to efficiently work in this application domain, a microprocessor-based equipment for the storage and pre-processing of the successive video frames, and dedicated software algorithms which are run with the aim to detect the presence of vehicles in them. Different approaches can be followed for the latter scope, i.e. variations in the pixel intensity, or object tracking recognition methods based on gradients and morphology metrics. The advantage of these advanced but expensive techniques is the capability to gather a variety of different traffic data, which can also include natively fundamental traffic parameters such as density, travel time, queue lengths, headway, and others.

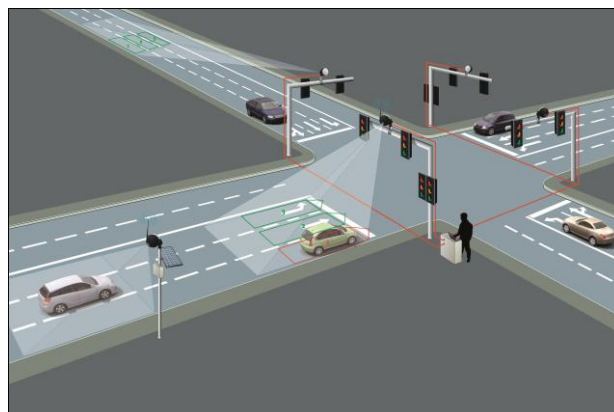


Figure 55: Video image processing techniques applied to traffic detection domain (source: aldridgetrafficcontrollers.com.au)

2.3 Mobile probes

Static RWIS stations give the possibility to detect road weather conditions in real-time at specific points of the road network, typically selected as a function of their relevancy in it or because they anticipate certain phenomena that then propagate in the rest of the network. But what does it happen in the unmonitored areas of it? The main limitations of these technologies is that they are fixed, and despite their typical high accuracy they can natively not be representative of the whole road conditions situation.

Probe vehicles have the potential to overcome this problem. In the last decade, the tremendous development in communication and on-board technologies has opened the door to a next generation of use case scenarios in the road weather community. Data collected by vehicles, which are acquired in a spatially distributed way along their trip, can be now easily shared on a real-time basis with central systems, with the possibility to feed elaboration and forecasting modules.

The first application of this new concepts has been developed in the traffic conditions domain (i.e. off-roadway technologies) [62]. By just considering the motion of a certain critical mass of vehicles within a road network (e.g. GPS position, speed, acceleration), the so-called **Floating Car Data** (FCD) and eventually fusing this information with conventional traffic detectors measurements, it is possible to have a distributed picture of traffic conditions and average travel times, and early detect the presence of sudden traffic jams (Figure 56).

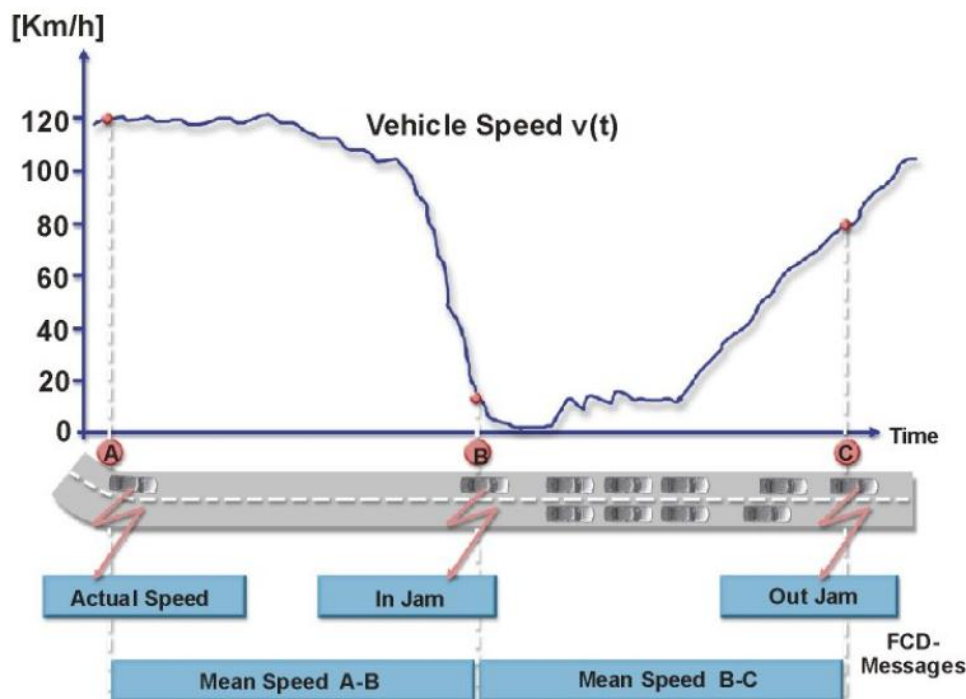


Figure 56: Traffic jams detection through FCD messages [62].

A direct application in the RWIS application domain is possible if **eXtended FCD** are considered, namely data available on the vehicle CAN bus coming from different on-board systems such as (Figure 57):

- the windscreen wipers or rain sensors;
- the external thermometer and the air-conditioning system;
- the vehicle's light system (e.g. eventual activation of fog lights);
- the hazard warning flashers;
- the vehicle dynamics control system;
- other *Advanced Driver Assistance Systems (ADAS)*.

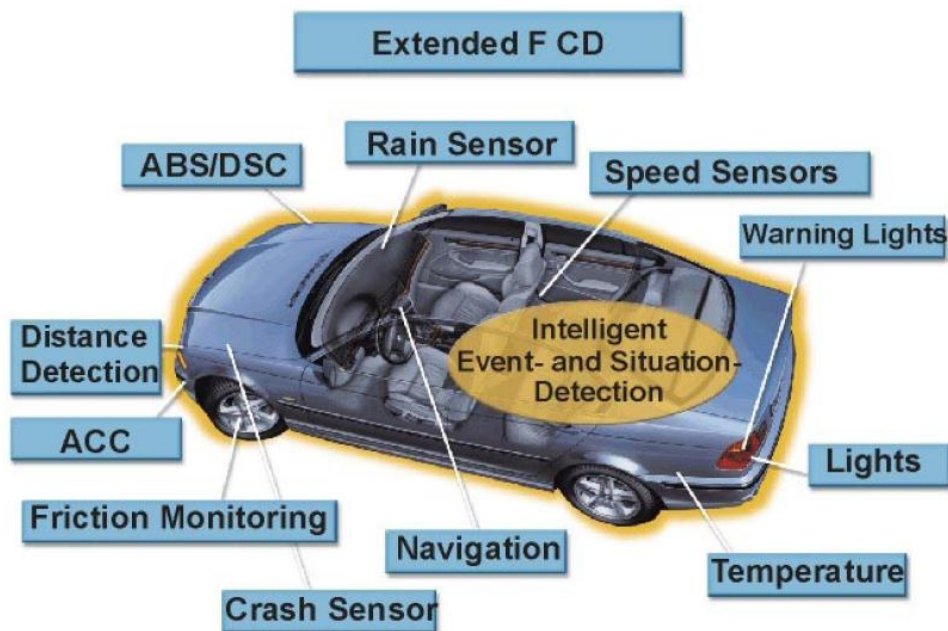


Figure 57: On-board systems which can provide XFCF that can be potentially used in RWIS [62].

An interesting vision of what will be possible in the next years thanks to this continuously maturing technology, fused with the advent of cooperative ITS (C-ITS), is provided, among the others, in a recent research work done by the Information Department of the Engineering Faculty at the University of Trento, in partnership with Fiat Research Centre [63]. However, at present it is not actually clear how to properly integrate and fuse all this enormous (but less accurate) data stream within road weather models; a lot of research and development is actually in place, as demonstrated by the high attention given to this topic in international conferences such as SIRWEC. A more extensive perspective of the various initiatives linked to this topic in the reference literature will be available in Chapter 4 and 5.

Probe vehicles open the doors not only in terms of spatial / temporal integration of data concerning road weather conditions, but also in terms of completeness of available information which may be considered in road weather models. In particular, two parameters are worth to be mentioned:

- **friction.** Friction measurements are particularly important in areas like in the north of Europe (e.g. Finland, Sweden and Norway), in which the road maintenance service is organized in a way, such that the main road need not be bare in all conditions, but must only guarantee certain friction conditions. Friction measurements are particularly suited to be carried out with mobile probes, and different technical approaches are today available, the most widespread are [64]:
 - **traditional friction meters**, i.e. very accurate and low costs in-car devices to be connected to the on-board unit of the vehicle which are able to determine friction through specific heavy breaking tests;
 - **acceleration sensors meters**, which are based on a similar principle but do not need of complex preliminary on-board installations;
 - **mobile optical friction meters**, which are based on the remote monitoring techniques described in the non-invasive road conditions paragraph of this chapter (road surface reflectivity evaluation);
 - **mechanical friction meters**, which have one more measuring wheels with a slip or toe, and estimate friction as a function of the measured forces which are needed to keep this component in place (Figure 58).



Figure 58: Different friction measurement devices mounted on a probe vehicles [64].

From different points of view, optical meters seem the most promising technology in a future perspective of road weather conditions monitoring, but at present it is not sufficiently reliable to be considered for winter maintenance quality control use scenarios [64];

- **road construction discontinuities.** For route-based forecasting systems based on geographical parameters databases, a major source of error is represented by spatial

discontinuities in the road construction peculiarities. In [65], Chapman et al. propose the idea to use Ground Penetrating Radars (GPRs) to detect these discontinuities and thus enhance the outputs of this model.



Figure 59: Road construction discontinuities detection through GPR [65].

Despite first empirical results show little accuracy improvements, this idea is clearly representative of the still latent potential of probe vehicles applications in this domain. “Third party” off-board sensors connected (wirelessly through short-range communications such as Bluetooth) to the vehicular on-board unit, which has the capability as well to integrate (X)FCD is the inevitable scenario which, if integrated in fully connected environments, where vehicles will not only be able to send probe data but also receive processed information by the other transport system components (e.g. roadside units, other vehicles, central systems, etc.) will open the doors to next-generation RWIS. For example, maintenance vehicles will be in the condition from one side to provide real-time salting operations data, and on the other side to optimize these treatments on the base of information shared by the surrounding environment.

3. Road-weather models

The previous Chapter has put in evidence all the different enabling technologies that are available today for collecting data from different roadside sources, which are today not only static stations installed nearby the roads anymore but also probe vehicles which have the capability at reasonable costs to gather information along all the road stretch under control. But how can all this data be properly processed automatically in order to get a comprehensive glance of the road surface conditions? And moreover, how can weather nowcast/forecast information be efficiently considered in modelling tools in order to make prediction of how this state will evolve in the near future?

The aim of this Chapter is to provide a comprehensive overview of the different techniques available at the state-of-art which have been suggested in order to accomplish these tasks, which are typically carried out at a “central” monitoring level where the decision-making process takes place. In fact the output of these models, conventionally known as “road-weather models” are the main information handled by *Maintenance Decision Support Systems* (MDSS), i.e. software tools at disposal of the road maintainers and operators that are used to efficiently plan the maintenance operations, which are going to be discussed in the following Chapter.

The reference elaboration chain is macroscopically a two-step process, as illustrated in Figure 60, in which it is clearly evidenced the approach to fuse data coming from the (static) RWIS stations with the outputs of properly downscaled meteorological models, that are produced on their part by properly evaluating data coming from different data sources, i.e. meteorological observations of different types and nature and land coverage information.

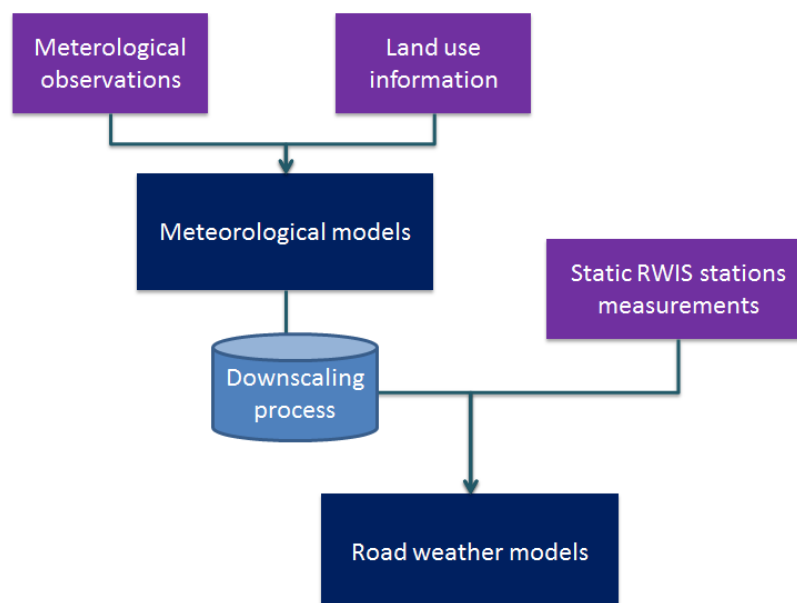


Figure 60: Road weather models reference elaboration chain.

3.1 Numerical prediction of weather forecasts

Numerical Weather Predictions (NWP) are based on very complex mathematical models describing the structure and the phenomena of the atmosphere and oceans to predict the meteorological conditions for the following days (Figure 61). More specifically, differential equations systems based on the laws of physics, fluid motion and chemistry are numerically solved in order to calculate winds, heat transfer, solar radiation, relative humidity and surface hydrology in each 3D voxel in which the planet could be divided.

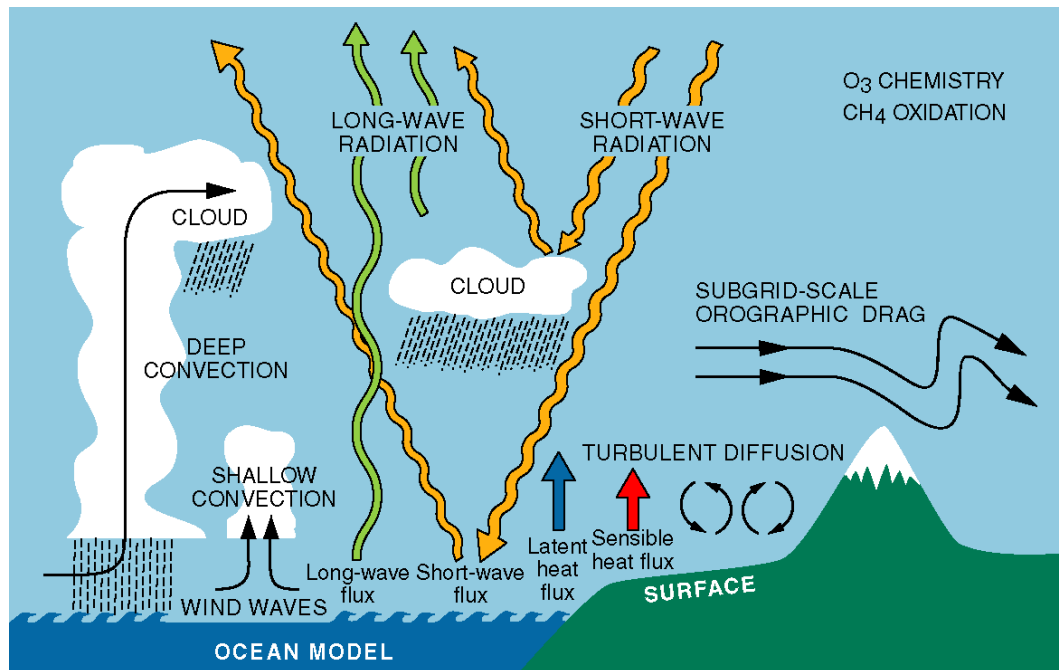


Figure 61: An overall perspective of the atmosphere phenomena which determine the weather conditions [66].

The spatial resolution of the model is the linear distance between these points, in correspondence of which the equations are evaluated and solved. Horizontal and vertical resolution, i.e. the spatial resolution in the two orthogonal directions of the plan, can be in general different, depending on how the grid is organized. Models are also characterized in terms of temporal resolution, since the results of the elaboration processes are available only at certain discrete times. Very-high performance calculators are necessary to run such models and generate similar predictions. Only few of the international weather centers have the economical capability to buy and maintain similar equipment, and despite the exponential increase in the processing power of computers, the forecast skill of numerical weather models can extend only to about six days with an acceptable accuracy. Several factors are still affecting their precision, in particular the density and quality of observations used in input or other simplifications introduced in order to speed up the elaboration process. In Figure 62 it is possible to observe the increasing trend in the forecast skill during the years with reference different time horizons after the run of the model; the benchmark parameter is the 500 [hpa] geopotential height. Improved models and data-assimilation systems, large number of satellite observations and increased computer power contributed to forecast improvements, and a reduction of the gap between the north and south hemisphere scores.

3.1.1 Forecast models classification

Although atmospheric models deal with the same basic physical equations, it's possible to categorize them depending on their structure and purpose. A first macroscopic subdivision can be the following [67]:

- **weather forecast models:** they are used to predict short-term and detailed behaviour of the atmosphere;

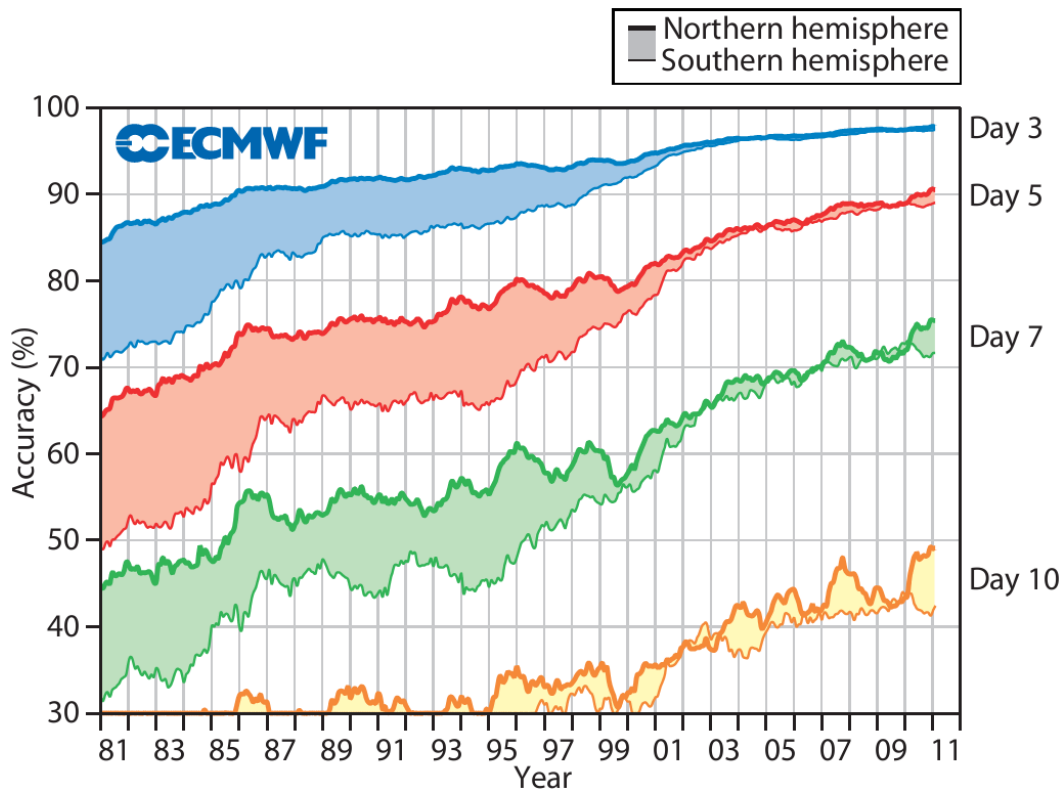


Figure 62: The improvements of ECMWF weather forecasts in the two hemispheres among years (Source: ECMWF).

- **climatic models:** they address the average behaviour of the atmosphere over much longer time span, typically hundreds of years;
- **“specific-purpose” models:** there are a wide range of possible fields in which forecast models can be implemented as for instance for the air quality, for the modelling of the ocean surface, for the forecast of tropical cyclones, for wildfire modelling, etc.

While the chaotic behaviour of the atmosphere complicates the production of accurate short-term forecasts, this factor is not such a limiting factor for climatic models, since that are mostly interests in longer time averages. Weather forecast models can be further divided into two main types:

- **Limited Area Models (LAM)**, which deal with a small part of atmosphere and so they can achieve better local accuracy and resolution zooming only into the regions of interest. These models typically need of the output of synoptic model to set the initial status at their boundaries;
- **global models**, which require a very expansive computing power, because they deal with the whole atmosphere on the entire planet, and provide the boundaries for LAM models.

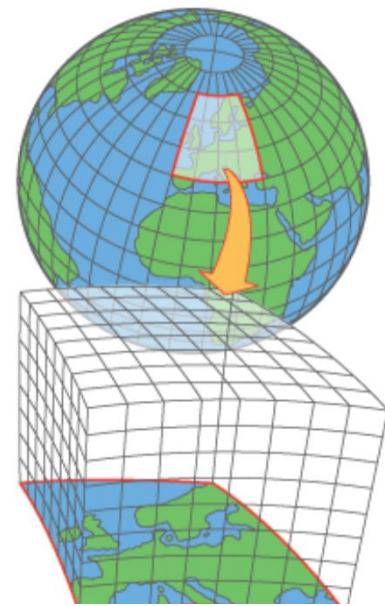


Figure 63: LAM and global models (source: FMI)

The forecast starts from a known initial state. Using the tendencies obtained from the physical atmospheric equations, the evolution of the atmospheric state, during a finite length of time (time step) at each point, is then calculated. This new state is then used as the initial state for the next time step and so on, until the desired forecast length has been covered.

Based on the forecast length, weather models can be further classified as **very short** (i.e. with a time horizon of less than one day), **short** (up to 3 days), **medium** (up to 15 days) and **long** (over 15 days). The spatial resolution is usually coarser in long range forecast than the short-term, due to the computer capacity limitations; usually, the better is the resolution of the model, the more accurately the real atmospheric behaviour can be simulated.

3.1.2 Data assimilation and parameterization processes

A fundamental prerequisite for a weather forecast is to know the initial state of the atmosphere at the beginning of the forecast as accurately as possible. For this purpose, in addition to the information coming from models, several ways to include surface observations obtained from international networks (SYNOP), balloon soundings, data from ships, drifting buoys, aircrafts and recently also information from weather radar and satellite have been designed. Due to the diverse nature and type of the data and their different spatial location, all these data are processed by an objective analysis method, which perform quality control and obtain values at locations usable by the models mathematical algorithms: this process is called **data assimilation**. This data, more reliable and in great number in the north hemisphere, make possible a better forecast for this area.

Some meteorological processes are at a too small or complex scale to be explicitly included in numerical weather prediction models. For this reason it's necessary to represent these phenomena by relating them, also statistically, to other variables at a different scale that the model can resolve. This procedure of expressing the effect of sub-grid processes is called **parameterization**. A typical example of sub grid process is the convective precipitation, as illustrated in Figure 65.

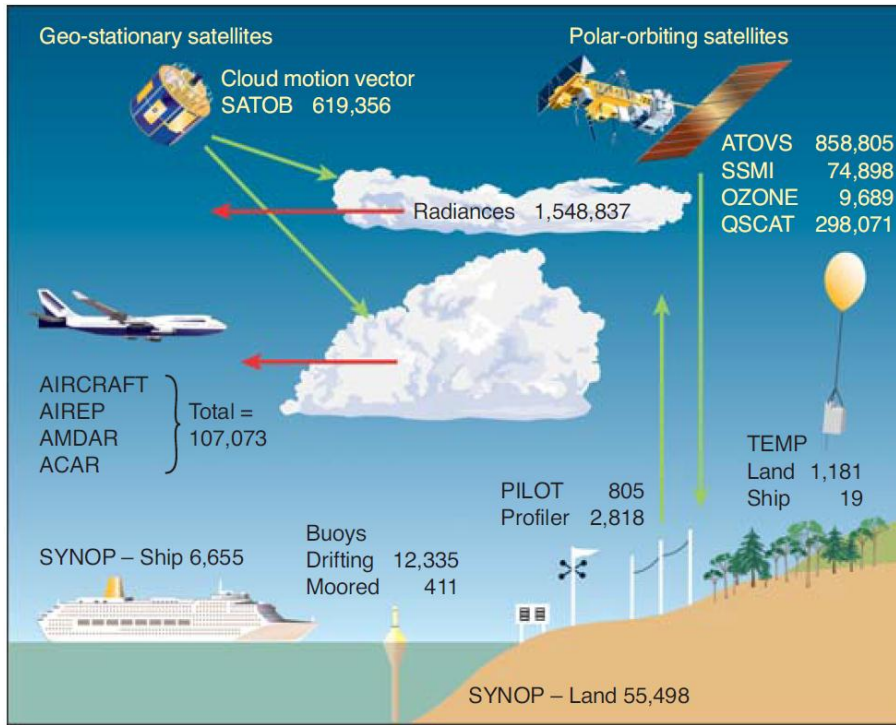


Figure 64: A complete perspective of different data sources of weather data (source: Met Office).

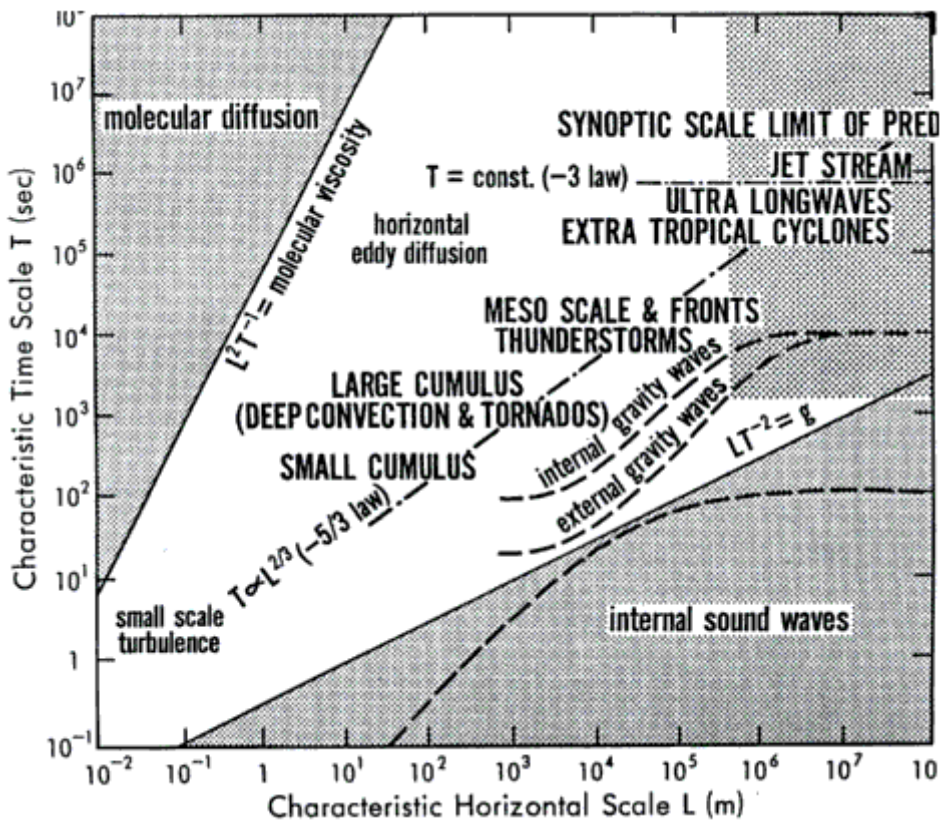


Figure 65: Space and time scales for convective precipitation phenomena (source: ECMWF).

3.1.3 Ensemble forecasts and nowcasting

As presented above, a forecast is an estimate of the future state of the atmosphere created by estimating the present state, and then calculating how this state will evolve in time using a numerical weather prediction computer model. Being the atmosphere a chaotic system, and not being able to observe every detail of the atmosphere, very small errors in its initial state can lead to large errors in the forecast. An ensemble system can be used to test how these small differences in the initial conditions may affect the outcome of the forecast.

Instead of running just a single forecast, the computer model is run a number of times from slightly different starting conditions that are consistent with the uncertainties in the observations; the complete set of forecasts is referred to as the **ensemble forecast** (Figure 66). In this way an estimate of the forecast uncertainty and an indication of which weather events may occur can be produced.

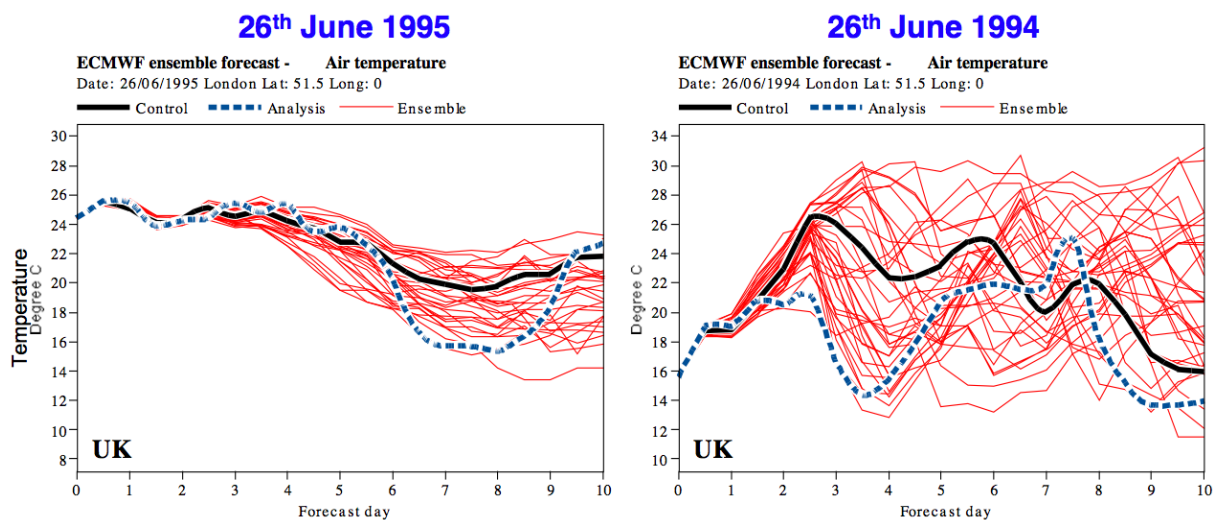


Figure 66: Example of ensemble forecast output (source: easterbrook.ca)

The weather forecasting within the next few hours is often referred to as **nowcasting**; it permits a detailed guidance on the location, extent and timing of imminent, high impact weather events. Usually these models work with a gridbox of high resolution (e.g. 1 -3 [km]) and with a rapid update cycle, also exploiting weather radar and satellite data for the analyses.

3.1.4 Weather forecasts limitations in mountainous areas

The simulation of the atmosphere behavior in mountainous areas is difficult, and accordingly, also their weather forecast. The goodness of predictions are as good as the understanding of the underlying physics/thermodynamics processes (and to a lesser extent, chemistry). To make accurate forecasts, it is fundamental to know the meteorological phenomena taking place at a small-scale resolution, and understand how they interact with others parameters. Models on appropriate gridbox scales are then needed to properly describe all this mathematically or parametrically, in order to simulate the possible effects of these

phenomena based on field measurements initializations. There is a dynamic scientific community that is specifically making research in this field, supported by the continuous increase in computing power that facilitates the possibility of simulation. Despite this, the sudden weather changes and the chaotic behavior of the atmosphere are today still far away to be well understood, characterized and simulated.

The weather forecast models utilize a simplified orography to perform their elaboration [68]. In Figure 67 it is possible to appreciate the reference orography which is used in the COSMO model (which has a spatial resolution of 2,8 [km]) to represent the Autonomous Province of Trento [69]. For people knowing well the geographical peculiarities of this region, it is immediately recognizable how the main and larger valleys are only sketched, while the narrow ones aren't represented at all. Even altitudes are only indicative, and in some cases can be very different from reality. Similar considerations can be applied for the orography considered within the two different models running at ECMWF (Figure 68), which have a horizontal resolution of 32 and 16 [km], respectively [70].

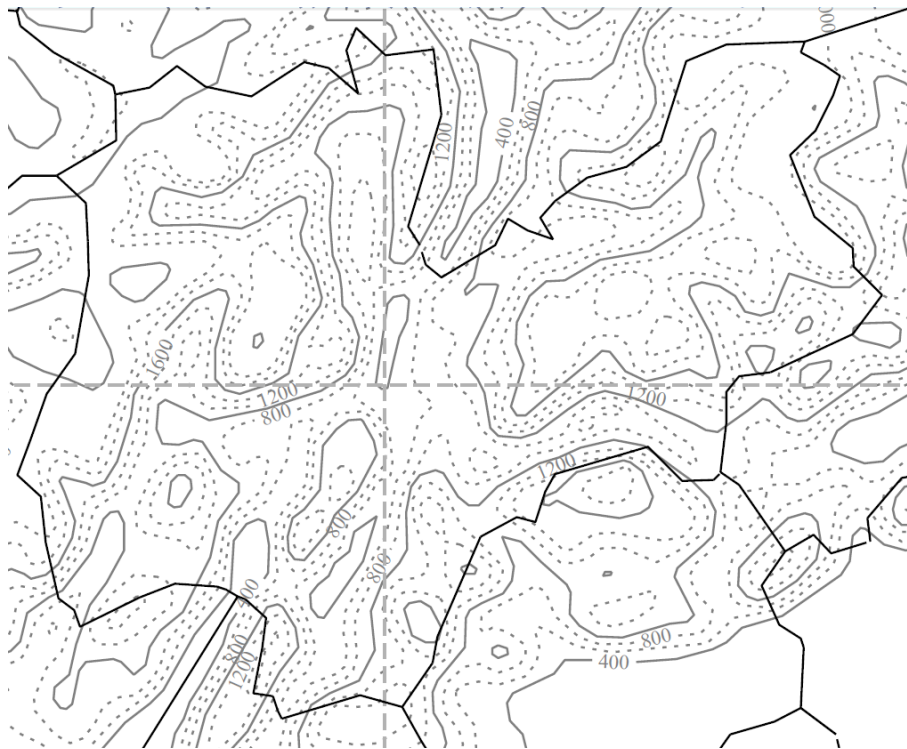


Figure 67: The orography of the Autonomous Province of Trento in the COSMO NWP model.

Because of the aforementioned reasons, the manual interpretation of professional meteorologists, especially in mountainous regions, who know in depth the territory and have at disposal different real time data set at different spatial and time resolution, is of fundamental importance to optimally understand the variety of output information generated by NWP and properly relate them to the land orography.

Model grids for ENS (32 km) and HRES(16 km)

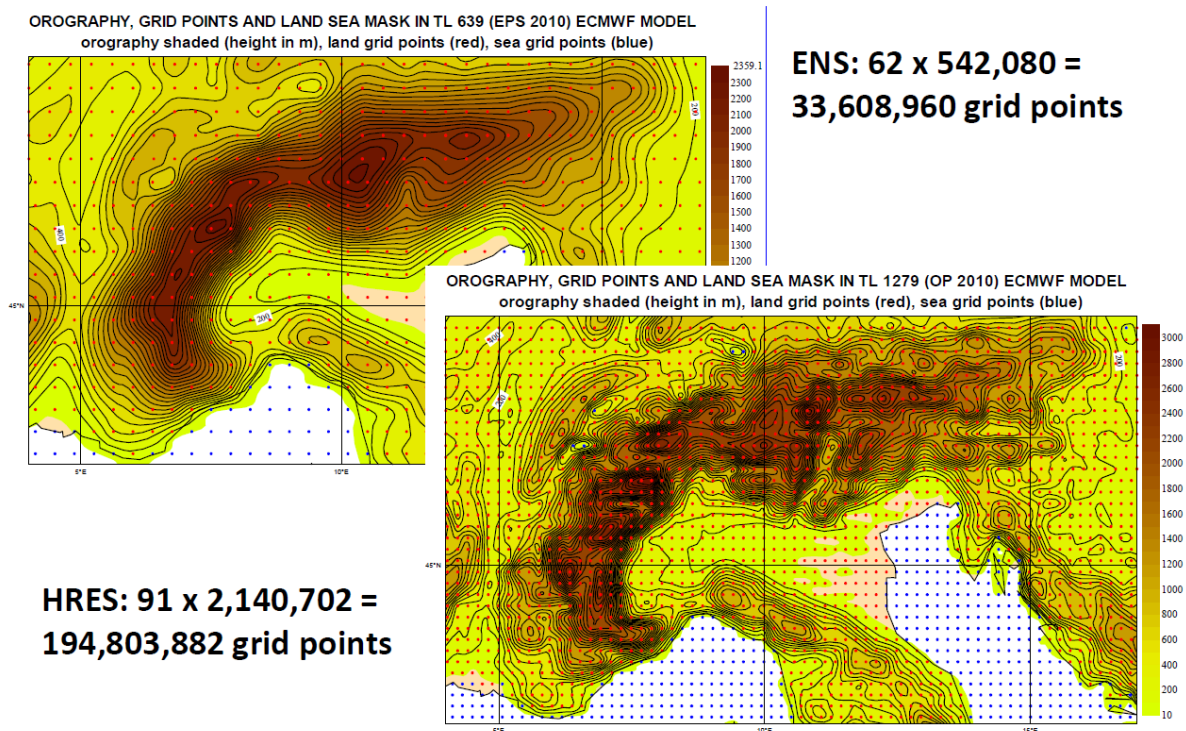


Figure 68: The orography of the north of Italy in the ECMWF NWP models.

3.2 Weather forecasts reference models

As already mentioned, the generated results of NWPs are the one of the basic input source for an RWIS elaboration and prediction system, which has the ability to include this information in order to properly predict several road parameters including the road surface temperature. For the purpose of the CLEAN-ROADS project, three different NWP models (in part already cited) are considered particularly interesting for this kind of application, namely:

- **WRF** (*Weather Research and Forecasting Model*) whose data are provided by a third-party provider (i.e. the local company CISMA) [71];
- **COSMO N2 RUC** (*Rapidly Updating Cycle*), whose data are provided by ARPA Emilia-Romagna [72];
- **ECMWF**, whose data are directly provided by the *European Centre for Medium-Range Weather Forecasts*.

In Table 8 the different meteorological parameters considered in the NWPs are listed. It is worth noting that relative humidity in COSMO is indirectly estimated on the base of the values of other variables.

FORECAST			
VARIABLE	SOURCE		
	WRF	COSMO	ECMWF
Air temperature (2m)	X	X	X
Dew point	X	X	X
Rain precipitation quantity since the beginning of the forecast	X	X	X
Snow precipitation quantity since the beginning of the forecast	X	X	X
Wind speed (10 m)	X	X	X
Surface pressure (at the station height)	X	X	X
Cloud coverage	X	X	X
High cloud cover	X	X	
Medium cloud cover	X	X	
Low cloud cover	X	X	
Relative humidity	X	X	X
Wind direction (10m)	X	X	X
Short wave incident radiation	X		
Long wave incident radiation	X		
Precipitation rate	X	X	X

Table 8: NWP models of interest for CLEAN-ROADS – forecasted meteorological parameters.

The scheduled runs of the different NWPs are presented in Table 9; the hours are expressed in UTC time (Coordinated Universal Time) and the outcome is available only several hours later. It is immediately to underline the fact that for the purpose of the project, the values provided by ECMWF have to be interpolated in time in order to get an equivalent temporal resolution which is acceptable for the application domain under study.

RUNS OF THE MODELS									
ECMWF	0:00	12:00							
WRF	0:00	6:00	12:00	18:00					
COSMO	0:00	3:00	6:00	9:00	12:00	15:00	18:00	21:00	

Table 9: Details of the temporal runs of ECMWF, WRF and COSMO NWP models.

3.2.1 ECMWF model

The *European Center for Medium Range Weather Forecasts* (ECMWF) is an independent intergovernmental organization supported by 34 Member States of the European Union that cooperate together with a series of international organizations and other non-European states. It has a wide-ranging programme of research and development directed at improving the quality and variety of forecast products for the medium-range and beyond. The main products elaborated from the organization space from medium range forecasts, deterministic forecasts, ensemble prediction system, epsgrams, ocean analyses, monthly and seasonal forecasts, atmospheric composition forecast and other.

The product which is considered in CLEAN-ROADS is in particular the deterministic forecast (**Atmospheric Model high resolution 10-day forecast (HRES)**), whose main features are summarized in Table 10.

Feature	Description
Type of model	Synoptic and hydrostatic
Horizontal resolution	about 16 [km]
Vertical resolution	91 layers
Runs / day	2 (0:00, 12:00 UTC)
Forecast validity	up to 240 [hours]
Forecast time step	6 [hours]
Data availability	6 [hours] delay

Table 10: Overview of the main features of the ECMWF HRES model.

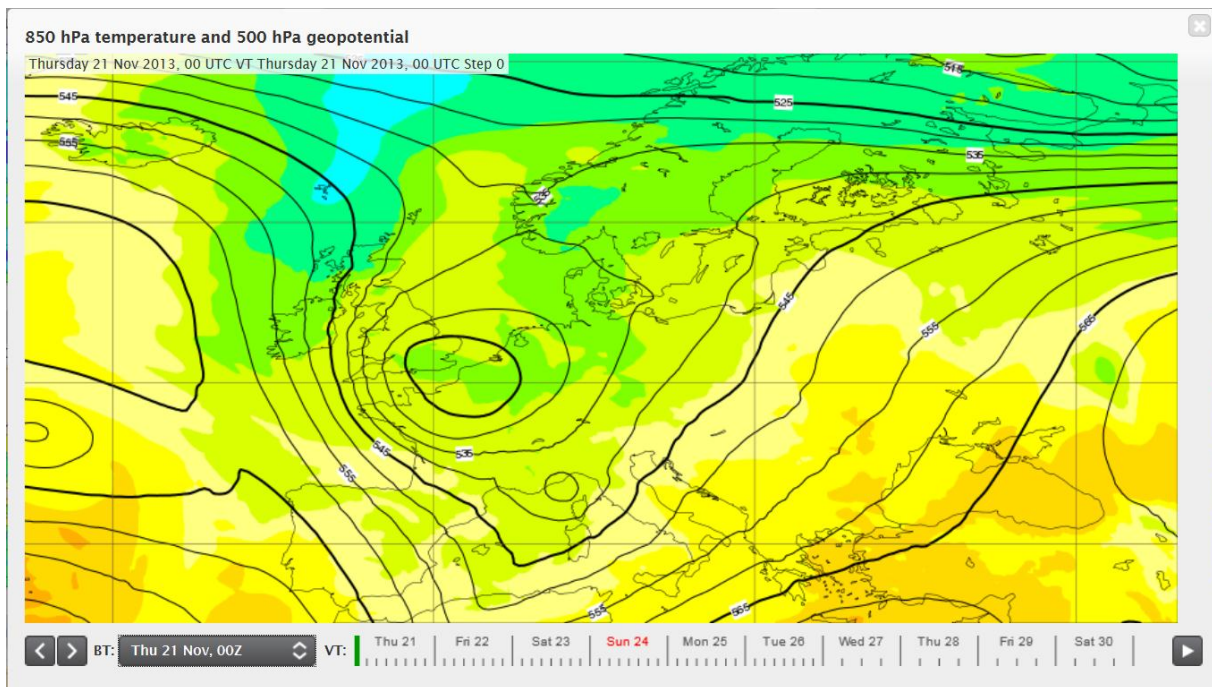


Figure 69: An example of output of the ECMWF NWP model [70].

3.2.1 COSMO N2 RUC model

The Consortium for Small-scale Modeling (COSMO) develop, improve and maintain a non-hydrostatic limited-area atmospheric model, to be used both for operational and for research applications by the members of an international consortium (Germany, Switzerland, Italy, Greece, Poland). With a license agreement, the model, may be used for operational and research applications by other national (hydro-) meteorological services, universities and research institutes. **COSMO LAMI** (*Limited Area Model Italy*) is one of the five *limited area models* (LAM) taken as reference in the **SRNWP** program (*Short Range Numerical Weather Prediction*) of EUMETNET [73]. The IdroMeteoClima Service of ARPA Emilia-Romagna has developed a model, originated from COSMO I2, defined as **COSMO N2 RUC** (*Rapidly Updating Cycle*) with the intention to produce, with a reasonably small delay, a very short range numerical weather forecast giving an idea of the possible local evolutions of the meteorological situation. This model takes advantage of radar data and other additional observations that are locally available (e.g. aircraft reports, surface station networks). This

modeling suite is currently under testing and validation phase, and its main features can be summarized as indicated in Table 11.

Feature	Description
Type of model	Limited area and non hydrostatic (LAM)
Horizontal resolution	2,8 [km]
Vertical resolution	40 layers
Boundary condition	From COSMO I7 model
Runs / day	8 (0:00, 3:00, 6:00, 9:00, 12:00, 15:00, 18:00, 21:00 UTC)
Forecast validity	up to 18 [hours]
Forecast time step	1 [hours]
Data availability	about 4 [hours] delay

Table 11: Overview of the main features of the COSMO N2 RUC model.

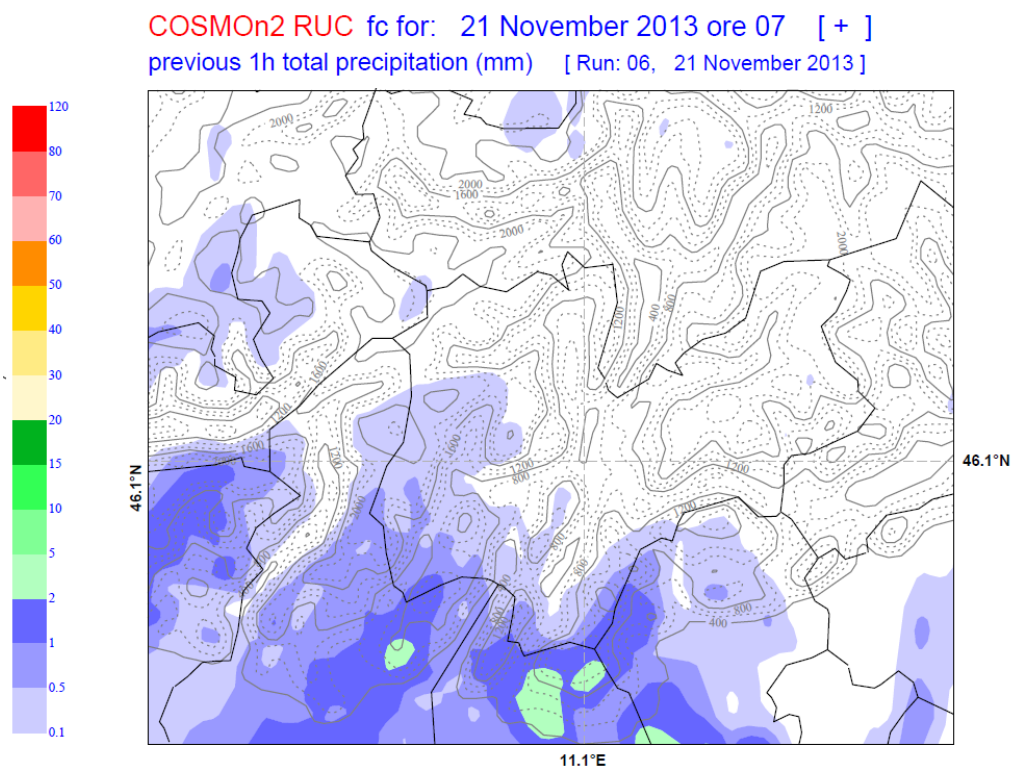


Figure 70: An example of output of the COSMO N2 RUC model.

3.2.2 WRF model

The development of the *Weather Research and Forecasting* (WRF) modelling system is a multiagency effort intended to provide a next-generation mesoscale forecast model and data assimilation system that will advance both the understanding and prediction of mesoscale weather and accelerate the transfer of research advances into operations. The model is being developed as a collaborative effort among several American institutions working in the field of meteorology, environmental, oceanic and atmospheric modelling, defense, aviation, prediction of storms and with the participation of a number of university and scientists. WRF

is continually developed by working groups with the aim of improving different aspect of the model and supporting the worldwide community of users coming from more than 130 countries. CISMA, a local company dealing with environmental issues, runs this model, customized for the complex alpine orography, with three different set of spatial boundaries in order to compute the weather forecasts over different geographic areas. The main features of the model are summarized in Table 12.

Feature	Description
Type of model	Limited area and non hydrostatic (LAM)
Horizontal resolution	2 [km]
Vertical resolution	40 layers
Boundary condition	From GFS model
Runs / day	4 (0:00, 6:00, 12:00, 18:00, UTC)
Forecast validity	up to 42 [hours]
Forecast time step	1 [hours]
Data availability	about 3-4 [hours] delay

Table 12: Overview of the main features of the WRF model run by the local company CISMA.

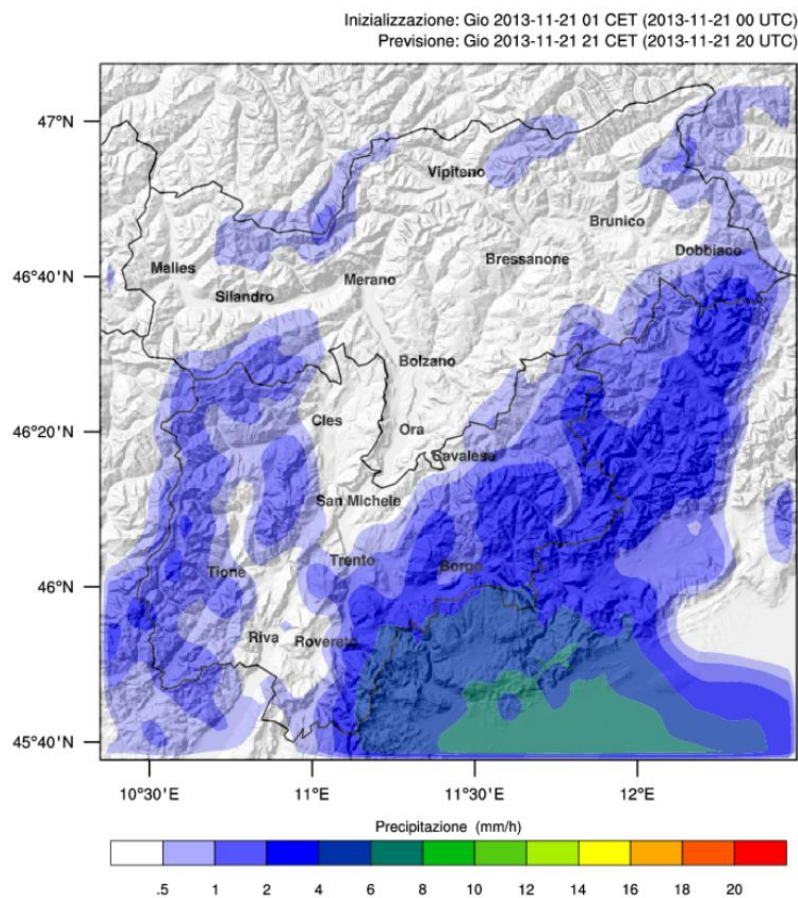


Figure 71: An example of output of the WRF model run by local company CISMA.

3.3 Road-weather reference models

A classical approach for the real-time determination of the road conditions evolution is to refer to mathematical models based on physical principles, which try to describe, in a more or less accurate way, the different relationships between the different meteorological parameters which have a certain influence on the variables of interest in the target problem, namely (i) the road surface temperature (RST) and (ii) the possible presence (and nature) of a water film on the road surface.

These models can be classified as a function of their order of spatial dimensionality, namely (Figure 72):

- **zero-dimensional models (0D)**, also known as “energy-balance” models, which try to estimate the heat fluxes balance in correspondence of the road surface and thus to determine its current conditions;
- **mono-dimensional models (1D)**, also known as “heat conduction” models, which try to characterize the entire vertical profile of temperature $T(z, t)$;
- **bi (three)-dimensional models (2/3D)**, which try to extend heat conduction models on the longitudinal axis (i.e. in the direction of the road infrastructure) and eventually on the orthogonal one ($T(\underline{r}, t)$ where $\underline{r} = [x, z]^T$ or $r = [x, y, z]^T$).

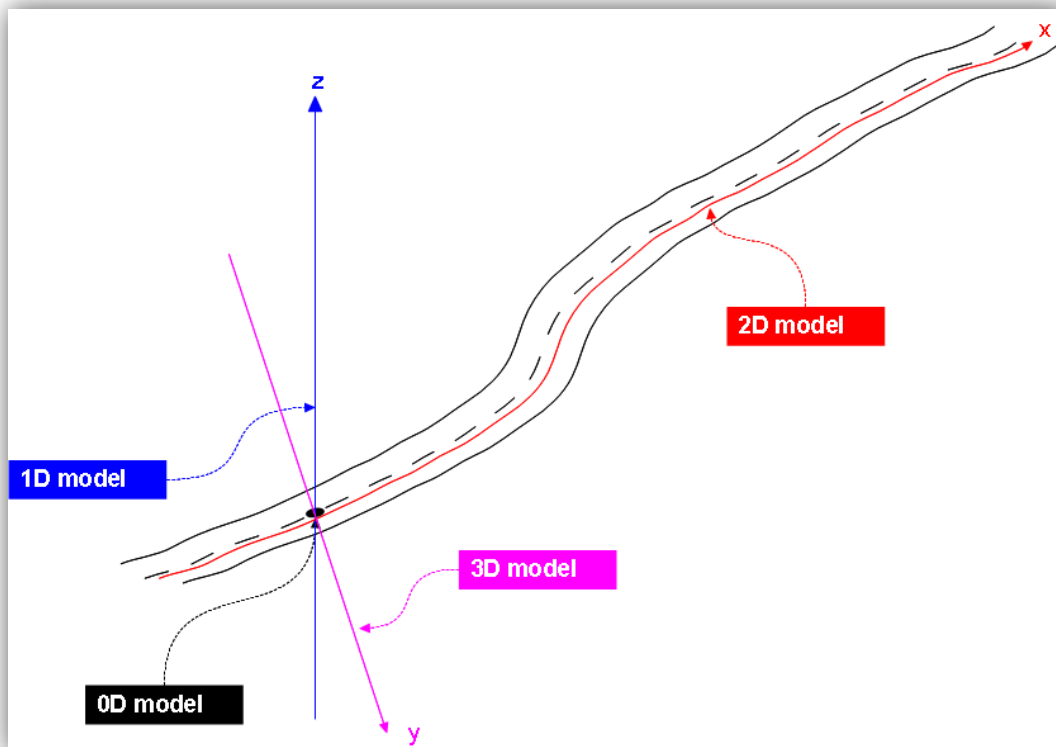


Figure 72: A graphical representation of different dimensional road weather models.

Zero- and mono-dimensional models are at the basis of the first **Road Weather Information Systems (RWIS)**, whose aim is specifically to determine the evolution of RST at specifically points where static RWIS stations are located. Thanks to the data gathered by the available

set of road weather sensors, typically installed in correspondence of certain cold hotspots where road treatments typically take place first, it is possible to continuously feed the model and thus to properly represent and above all foresee the road surface conditions and thus properly organize the maintenance activities.

A significant advancement of RWIS was introduced at the beginning of year 2000 through the development of the first **extended RWIS** (XRWIS) concepts, i.e. models designed with the idea to spatially extend 1D models and in order to provide road maintainers with *route-based forecasts*. A relevant step forward in the scientific community was achieved through the very well-known work of Chapman et al. in 2001 [1]- [6], in which instead of first XRWIS proposals based on (at the time) very expensive thermal mapping operations, the second dimension was introduced by integrating a geographical parameters database (GPD), which have shown to be the dominant factors for explaining very localized variations of RST.



Figure 74: A possible output of Salting Routing Optimization algorithms [74].

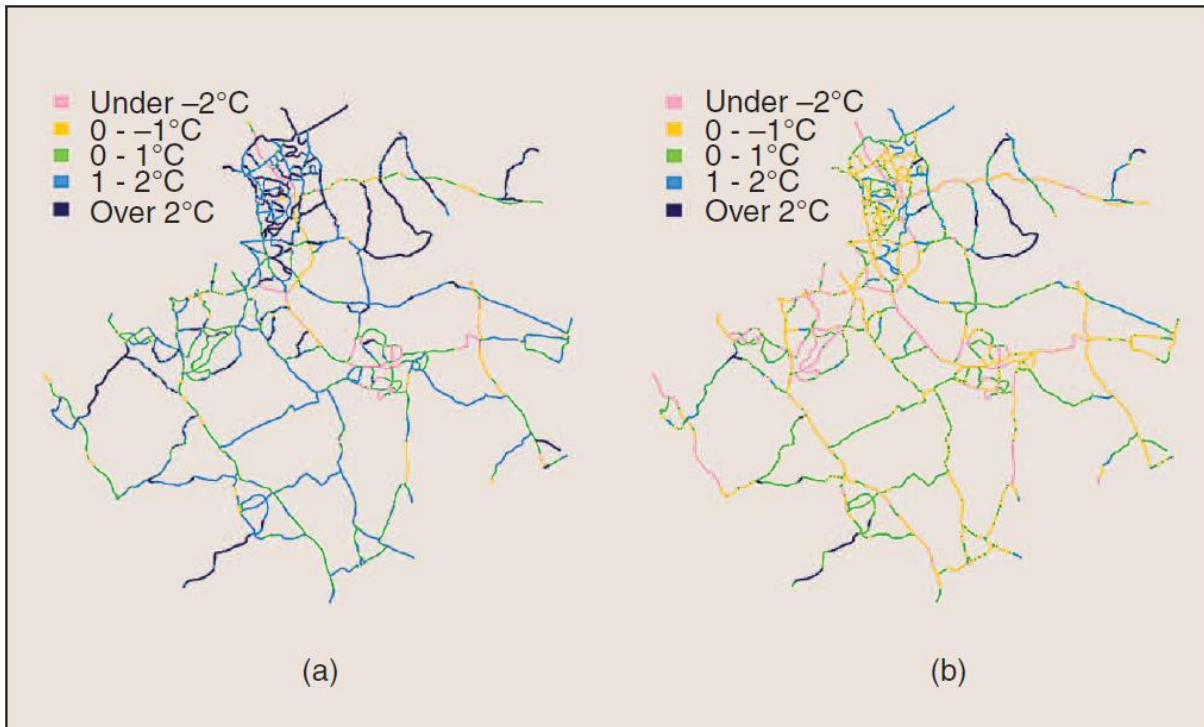


Figure 73: An example of the route-based forecast output which can be obtained through a XRWIS [74].

XRWIS represent today the state-of-art in this application domain, and most of the commercial solutions available have the capability to model road conditions within the whole

road network. Research is now moving on a further improvement of XRWIS, namely the idea to integrate them with **salting routing optimization** (SRO) algorithms able to provide road maintainers with exact indications about the specific amount of de-icing chemicals that must be applied in order to avoid the formation of ice on the roads. An example of these new future capabilities is provided in [74], where a SRO system that includes evolutionary algorithms within a XRWIS is introduced, The possible output of such a system could be a route-based GUI for the road maintainers, with a qualitative / quantitative indication of chemicals to be applied (Figure 73).

3.3.1 Zero-dimensional models

The physical zero-dimensional energy-balance models are nothing more than a single equation, in which the variable to estimate (the RST) is expressed in terms of different factors which represent more or less accurately the energy transfers that take place in correspondence of the route surface. The model is of course solved by a unique equilibrium point, which can vary in time as a function of the boundary conditions described in the model. As a matter of example, the zero-dimensional energy-balance model proposed by Thornes in 1984 is presented in details [75]. This model is particularly relevant in the RWIS community since it is at the base of many current state-of-art solutions.

$$RST = \sqrt[4]{\frac{1-\alpha}{\sigma} (Q + q) - \frac{LE+H+S}{\sigma} + T_{sky}^4}$$

[34]

where α is the surface albedo, Q is the direct beam solar radiation, q is the diffuse radiation, σ is the second Boltzmann constant ($\sigma \cong 5.67 \cdot 10^{-12} [\text{W}/\text{cm}^2 \cdot \text{K}^4]$), T_{sky} is the radiation temperature of the sky hemisphere, H and LE are the sensible and latent heat fluxes, respectively, and S is the heat flux to the road construction.

This model was continuously improved in the following years, with the objective to build a specific model for each of the input parameters of the system with a direct correspondence with the measureable meteorological variables (e.g. precipitation rate, wind speed and direction, relative humidity, etc.). For instance, Thornes itself proposed in 1986 an additional coefficient for better approximate the impact of precipitation on the latent heat flux [76].

3.3.2 One-dimensional models

Mono-dimensional heat conduction models have the ability to model in time the entire vertical temperature profile $T(z, t)$, under the hypothesis that boundary conditions in the orthogonal plan are ideally homogeneous (i.e. by neglecting lateral heat fluxes transfers). The reference equation for this class of models is the following:

$$C_m \frac{\partial T(z, t)}{\partial t} = \frac{\partial}{\partial z} \left(k \frac{\partial T}{\partial z} \right)$$

[35]



where C_m is the heat capacity and k is the thermal conductivity.

In order to solve this differential equation with respect to $T(z, t)$, it is necessary to identify a set of conditions in order to fix the problem at its boundaries. The typical constraints that are introduced are the following:

- **condition at starting time** $T(z, t = 0) \forall z \in \mathbb{R}$, which is initialized by a set of empirical values provided by measurement systems, eventually interpolated together;
- **lower-bound condition** $T(z = z_{min}, t) \forall t \in \mathbb{R}$, which sets a fixed constraint in time of the temperature at the minimum depth $z_{min} < 0$ considered by the model. This value is typically the time average of the empirical values measured at this altitude;
- **upper-bound condition** $T(z = 0, t) \forall t \in \mathbb{R}$, which solves an energy-balance model as described in the previous paragraph.

Mono-dimensional models are at the base of some of most widespread road weather models, for example Ice Break, developed by J. Shao at the beginning of the '90s [43].

3.3.3 Two/three-dimensional models

Two/three-dimensional models, at the base of XRWIS, are a quite recent evolution of zero- or mono-dimensional models, which try to model the current (and forecasted) road conditions in the different point of the surrounding space, and in particular on the road network.

As already mentioned, the first XRWIS attempts were based on the idea to efficiently integrate the data collected by site- specific forecasts around the road network through thermal mapping campaigns, which when initially suggested were expensive to organize and manage, and therefore difficultly repeatable with a certain frequency in time. In order to solve this main practical limitation, Chapman et al. proposed an alternative solution based on a **GPD** in order to get route-based forecasts (called "ENTICE"), which includes:

- latitude, longitude and altitude;
- a cold-air pooling index (CAPI);
- the sky-view factor;
- the road type and land use.

These parameters are initially determined through specific surveys carried out with mobile probes; sky-view factors are in particular determined thanks to fish-eye images. This approach has empirically demonstrated how RST variations can be well explained through meteorological factors at a macroscopic (i.e. regional) level, and through geographical parameters at a microscopic one (i.e. road stretch level). In particular, specific statistical-regressive analysis have put in evidence how the inclusion of a GPD in the model has been able to explain up to the 75% of residual variations of RST.

An alternative approach, which significantly simplifies the complexity of the **ENTICE** model (in particular the non-negligible effort to initialize the GPD) and probably offers more immediate possibilities to use it within real-world applications, was recently introduced by

Shao during the last edition of the SIRWEC conference as a spatial extension of the **IceBreak** model [43]- [77]. In particular, the extension is performed through a 2-D **inverse distance weighting** (IDW) algorithm, which tries to optimally weight the RST measurements collected by an existing network of static RWIS stations in order to estimate RST at a specific point of the road network. The weighting process is mainly governed by the distance with the different static RWIS stations, as indicated in the following relationship:

$$z_j = \frac{\sum_{i=1}^n \frac{z_i}{(d_{ij} + \delta)^\beta}}{\sum_{i=1}^n \frac{1}{(d_{ij} + \delta)^\beta}} \quad [36]$$

where z_j is the interpolated measurement computed for the point x_j , z_i is the empirical measurement provided by the static RWIS station installed in the point x_i , d_{ij} is the distance between the point x_i and x_j , and β and δ are two degrees of freedom that must be properly defined.

From an operative point of view, the XRWIS is run through this set of steps:

- subdivision of the road network in elementary route stretches of uniform length (e.g. 200 [m]);
- model calibration based on a comprehensive set of geographical parameters and land use information;
- execution of the 1D model for each point x_i ;
- execution of the IDW algorithm and computation of the road conditions for each elementary route stretch;
- updating of z_j and z_i once the new measurements of the static RWIS stations are available.

The advantage of this approach is not only to the possibility to have a high resolution of RST in space in a simple way, but also to easily extend this approach in the third dimension as well, and thus characterize even the area nearby the road network.

3.4 State-of-art models

In the literature different road weather models, based on the theoretical fundamentals described in the previous paragraph, have been proposed with the aim to estimate the current RST and above all to predict it in the short-term period. In the following pages, the details of the most widespread and/or interesting ones are described. The background information collected in this paragraph is presented in particular with the intention to provide a consolidated initial overview for the future design process of the central CLEAN-ROADS elaboration and forecast engine.

3.4.1 METRo

METRo (*Model of Environment and Temperature of Roads*) is a 1D road forecast software created and distributed by the Canadian Meteorological Centre since 1999 as free and open source software (FOSS) [78]- [79]. This road weather model is capable to provide forecasts of both (i) the road surface temperature (RST) and (ii) the road surface conditions, and was designed with two main requirements in mind, i.e. the abilities to:

- closely work together with a NWP model already in use by this centre, i.e. the **Global Environmental Multiscale** (GEM) model;
- automatically adapt to the field measurement of static RWIS stations.

Being released as FOSS, this software has been continuously improved during the years thanks to a wide community of organizations, including governmental institutions. METRo, is nowadays used not only in Canada but in several countries worldwide, and is *de facto* the state-of-art reference road weather model in the RWIS community.

The software is a combination of three different models, namely:

- a zero-dimensional **energy balance model** of the road surface;
- an one-dimensional **heat conduction model** for the determination of the entire vertical temperature profile;
- an additional model able to take into account the **situation of water/ice accumulation on the road**.

Energy balance model

The energy balance model considered in METRo is based on the following equation:

$$R = (1 - \alpha)S + \varepsilon I - \varepsilon \sigma T_S^4 - H - L_a E \pm L_f P + A \quad [37]$$

where R is the residual radiation flux (i.e. the input for the other two modules of METRo) calculated as the sum of (i) the **net solar radiation flux** (where S is the incoming flux and α is the albedo), (ii) the difference between the **absorbed incoming infrared radiation flux** εI (where ε is the emissivity) and **emitted flux** $\varepsilon \sigma T_S^4$ (where σ is the second Boltzmann constant, $\sigma \cong 5.67 \cdot 10^{-12} [W/cm^2 \cdot ^\circ K^4]$, and T_S is the road surface temperature), (iii) the **sensible turbulent heat flux** H , (iv) the **latent heat flux** $L_a E$ (where L_a is the vaporization or sublimation heat and E is the water vapour flux), (v) the **flux associated with phase changes of precipitating water** $L_f P$ (where P is the precipitation rate, L_f is the heat of fusion water and \pm indicates a freezing or thawing state, respectively), and (vi) the anthropogenic flux A , which takes in consideration the additional “human-generated” heat source caused by vehicular transits (i.e. the effect of friction from the tires and the heat released by the engines).

Some of the parameters of the model were estimated during the first calibration runs of METRo. For instance, the road surface albedo varies linearly from a snow-free value of 0.1 to a snow-covered value of 0.5 in case of snow accumulation between 1-6 [kg/m²]; the emissivity has been set to the value $\varepsilon = 0.92$. Different approximations are considered in this energy balance model, the most important being:

- **shading effects**, which are not taken in consideration at all. Static RWIS stations providing the data for the forecast should therefore be placed in open areas where this aspect is irrelevant. In any case, shading effects can be easily included in METRo by properly generalizing the net solar radiation flux term;
- **sensible turbulent heat flux** and the **water vapour flux**, which probably represent the most relevant approximation in the model and are associated to the most complex heat transfer processes which take place on the road. More specifically, METRo uses the Monin- Obukhov similarity theory even if the basic hypothesis for its application are not exactly fulfilled at the road level (steady conditions of flow over a homogeneous surface) [80];
- the **measurement of input meteorological parameters**, which are used for the calculation of the heat fluxes components, are performed in suboptimal conditions. In particular, METRo takes in consideration air temperature and relative humidity measurements taken at a height of 1.5 [m], and wind speed and direction measurements taken at a height of 10 [m]. This is due to practical limitations, since the measurement height should be in reality large enough in order to eliminate the influence of the underlying road;
- the **flux associated with phase changes of precipitating water** takes into account the release of energy when rain freezes on a road under 0 [°C] or the expense of energy when snow melts on a road above 0 [°C]; the simplification in the model is related to the assumption that the precipitation is considered to have completely melted or frozen during one model time step (which is set at 30 [s]);
- the **anthropogenic flux** is an arbitrary value, typically set at 15 [W/m²]; however this value has demonstrated to be inefficient at certain location, and responsible for the appearance of biases. For this reason, a compensating mechanism has been introduced for determining the right value of A as a function of the performance of METRo during the previous days, and more specifically of the mean errors in night time road temperatures only, when this term has revealed more influent. In particular, A is modified once per day by 1.0 [W/m²] for each Celsius degree of bias.

An added value of METRo is that it contains a mechanism to take into account the increased turbulence generated by vehicular transits. More specifically, a minimum value for the wind v_c at different times of the day can be set as a direct function of the traffic levels. The turbulent heat fluxes are expressed as:

$$H = -\rho c_p C_m \max(v, v_c) C_h (T_a - T_s) \quad [38]$$

$$E = -\rho C_m \max(v, v_c) C_h (q_a - q_s) \quad [39]$$

where ρ is the air density, c_p is the specific heat of air at constant pressure (fixed at 1005,46 [J/kg · °K]), v is the wind speed, T_a is the air temperature, and q_a is the specific humidity. The value of specific humidity at the surface q_s is estimated through this relationship:

$$q_s = \begin{cases} \min[q_a, q_{sat}(T_s)] & \text{if } W_l + W_s = 0 \\ q_{sat}(T_s) & \text{if } W_l + W_s \geq W_c \end{cases}$$

[40]

where $q_{sat}(T_s)$ is the saturated value of specific humidity, W_l and W_s is the water accumulation on the surface in liquid and solid (snow/ice) form, respectively, and W_c is a threshold value fixed at 0.5 [kg/m²]. For values of $W_l + W_s$ in the range [0; W_c] a linear interpolation between these two values is considered. Finally, C_m and C_h are two dimensionless transfer coefficients, for momentum and heat and moisture, respectively, which are initialized based on the results of previous research studies.

Heat conduction model

The road heat conduction model computes the temperature profile $T(z, t)$ inside the road material using an one dimensional heat diffusion equation:

$$C(z) \frac{\partial T(z, t)}{\partial t} = - \frac{\partial G(z, t)}{\partial z}$$

[41]

where $C(z)$ is the heat capacity and $G(z, t)$ is the ground heat flux, which is directly related to the temperature profile through the following differential relationship:

$$G(z, t) = -k(z) \frac{\partial T(z, t)}{\partial z}$$

[42]

where $k(z)$ is the heat conductivity. Heat capacity and conductivity profiles are directly related to the properties of the road material, and thus are known a priori and fixed in the model based on typical reference values.

The model is solved at two different numerical grids, depending on the type of road: for normal roads, a variable-resolution grid is used, while a uniform-resolution grid is employed for bridges and overpasses. This difference is introduced because of the completely different conditions at the bottom layers (soil for normal roads and air for bridge and overpasses); for normal roads, it is useful to significantly improve the resolution of the model in correspondence of the road surface.

From an operational point of view, the variable resolution grid is directly obtained from the uniform one by considering a simple coordinate transformation $z \rightarrow \zeta$:

$$\zeta = a \cdot \ln(1 + bz) \quad [43]$$

The resolution of the uniform grid is 0.01 [m]; the degrees of freedom a and b are set in order to have a maximum resolution of 0.01 [m] at the road surface and a resolution of about 0.05 [m] at a depth of 0.5 [m]. The bottom of the grid is set at a depth of 1.4 [m].

The heat conduction model is controlled by the following set of conditions:

- the **initial value of ground heat flux** is set equal to the residual radiation flux calculated by the energy balance model, i.e. $G(0,0) = G_0 = R$; in alternative, a temperature value of 0 [°C] is imposed in case a melting or freezing process is ongoing, if “signalled” by the water/ice accumulation model;
- the **bottom boundary condition** is of no flux in case of normal road (or of air temperature for bridges).

Water/ice accumulation model

The surface water/ice accumulation model simulates the evolution of the amount of water (W_l) and snow (W_s) on the road surface, which is governed by the following couple of equations:

$$\frac{dW_l}{dt} = P - E + \frac{R - G_1}{L_f} - r \quad [44]$$

$$\frac{dW_s}{dt} = P - E - \frac{R - G_1}{L_f} - r \quad [45]$$

where G_1 is the downward heat between the first and second model layers in the road and r is the runoff; the other variables are a direct input of the energy-balance model. The third term $(R - G_1)/L_f$ contributes to the equation only at 0 [°C]. The runoff is modeled through the following function:

$$r = \begin{cases} c(W_l - W_r) & \text{if } W_l > W_r \\ 0 & \text{if } W_l \leq W_r \end{cases} \quad [46]$$

where $c = 0.003 [s^{-1}]$ and $W_r = 1.0 [kg/m^2]$. It is worth noting that in [45] water runoff actually represents snow removal operations (which can be caused by either traffic or maintenance operations), which are modelled as described in [46] but substituting W_l with W_s .

Forecast process

The preliminary stage of the METRo forecast process is the **atmospheric forcing**, in which weather forecasts are included in input either by completely automated means or by manual interventions of the meteorologists. In both cases, the first Canadian release of the model was directly related to the three-hourly forecasts of the aforementioned GEM model, eventually editable by meteorologists through a proper GUI. In particular, METRo includes every 12 [hours] only the weather forecasts of specific locations where static RWIS stations are located. During this phase, all meteorological input parameters such as air temperature and humidity, wind and precipitation are linearly interpolated to the METRo time steps. It is worth noting that in case of manual modifications by meteorologists on the cloud cover variable, radiation fluxes are not directly taken from GEM (since they are not reliable anymore because of this modification) but through parameterizations developed from a statistical analysis of the GEM radiative fluxes.

In Figure 75 the three main core stages of the METRo forecast process are presented. The first stage takes principally into account the station observations; in the coupling stage, both station observations and meteorological forecast are used to determine a correction coefficient for radiative fluxes in order to minimize the forecast error; and finally in the third stage, the road surface temperature (RST) and road conditions are forecasted for a number of hours in accordance with the length of the weather forecast input file.

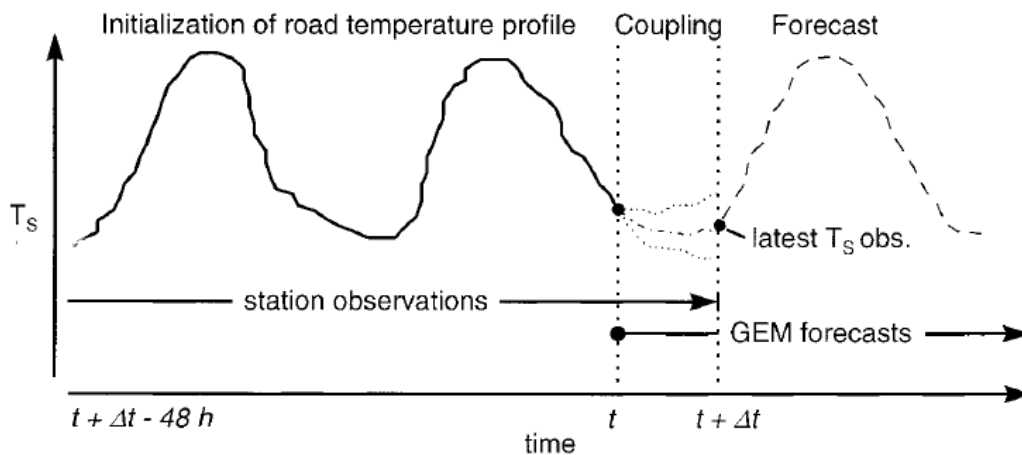


Figure 75: The three stages of the METRo forecast process [79].

To **produce an initial road temperature profile**, METRo uses the road temperature observation at the surface and subsurface from the last two days to force the heat-conduction model. The subsurface temperature is taken at a depth of 0.4 [m]. In case surface observations are missing for a period exceeding 4 [hours], the heat conduction equation is initialized through an analytical solution which assumes a sinusoidal RST diurnal pattern. It is worth noting that both initialization approaches (i.e. with or without empirical static RWIS data) have demonstrated to produce similar forecasts accuracies, as a demonstration of the robustness of this road weather even in case of data scarcity.

The second phase of the forecast process is known as **coupling**; in this phase METRo adjusts the available atmospheric forecasts gathered during the atmospheric forcing period



to the actual station observations. The delay between the time in which atmospheric forecasts are available and METRo forecasts are computed is equal to about 8 [hours]; during this period, the model makes suitable adjustments to the initial energy balance. More specifically, the parameters of this equations are initialized with the surface observations (except RST), while the radiation fluxes (which are not observed variables) are calculated through an iterative process in order to obtain a computed forecast RST which is only 0.1 [°K] far from the observed one. One of the limitations of METRo is that at least 3 hours of observations are needed to produce results which are representative of the temporal resolution of the atmospheric forecast.

At the end of this process, the **forecasts** are computed. The model is initialized with the most recent observed values and then forced, at subsequent times, with a combination of the initial values and of the original forecast values. The weights pass exponentially from the initial to the forecast values over a period of 6 hours. In its actual configuration, METRo forecasts are generated two times a day (at 3:00 and 15:00) with a time horizon of 24 [hours].

Operational details on the input parameters

In order to run METRo, three different type of information are operationally needed: (i) the configuration of the static RWIS stations; (ii) the related surface observations and (iii) the atmospheric forecasts. The file of the station configurations contains general information about the geographic location, the grid resolution layers and other metadata. Figure 76 presents an example of this configuration file, in which the information concerning the first static RWIS station of CLEAN-ROADS have been inserted.

Figure 77 shows a list of parameters accepted by METRo as input for its elaborations; only the road surface temperature and road subsurface temperature are mandatory fields, as well as the date. The observation file reported in Figure 78 reports shows all the measurements taken by the first static RWIS station of the CLEAN ROADS project that are provided every 10 [minutes] as input to the software.

```

<?xml version="1.0" encoding="UTF-8"?>
- <station>
  - <header>
    <filetype>rwis-configuration</filetype>
    <version>1.0</version>
    <time-zone>EST1EDT</time-zone>
    <production-date>2013-12-03T01:39:01.8547346Z</production-date>
    <station-type>road</station-type>
    <sst-sensor-depth-type>0</sst-sensor-depth-type>
  - <coordinate>
    <latitude>46.21</latitude>
    <longitude>11.151</longitude>
  </coordinate>
</header>
- <roadlayer-list>
  - <roadlayer>
    <position>1</position>
    <type>asphalt</type>
    <thickness>0.18</thickness>
  </roadlayer>
  - <roadlayer>
    <position>2</position>
    <type>crushed rock</type>
    <thickness>0.3</thickness>
  </roadlayer>
  - <roadlayer>
    <position>3</position>
    <type>sand</type>
    <thickness>1.12</thickness>
  </roadlayer>
</roadlayer-list>
</station>

```

Figure 76: METRo input files – static RWIS station configuration file.

Field description	Element name	Unit
Date and time of observation	observation-time	ISO 8601
Air temperature	at	Celsius
Dew point	td	Celsius
Presence of precipitation	pi	0: No -- 1: Yes
Wind speed	ws	km/h
Road condition	sc	SSI code
Road surface temperature	st	Celsius
Road subsurface temperature (40 cm)	sst	Celsius

Figure 77: METRo input files – list of surface observation parameters required.

```

<?xml version="1.0" encoding="UTF-8"?>
- <observation>
  - <header>
    <filetype>rwis-observation</filetype>
    <version>1.0</version>
    <road-station>Stazione - 1</road-station>
  </header>
  - <measure-list>
    - <measure>
      <observation-time>2013-12-01T12:10:00</observation-time>
      <at>8.61</at>
      <td>-9.77</td>
      <pi>0</pi>
      <ws>0</ws>
      <sc>-999</sc>
      <st>9.51</st>
      <sst>3.54</sst>
    </measure>
    - <measure>
      <observation-time>2013-12-01T12:20:00</observation-time>
      <at>8.67</at>
      <td>-9.79</td>
      <pi>0</pi>
      <ws>0</ws>
      <sc>-999</sc>
      <st>9.78</st>
      <sst>3.76</sst>
    </measure>
  </measure-list>
</observation>

```

Figure 78: METRo input files – static RWIS station measurements file.

The forecast file contains the data utilized from METRo to foresee the behaviour of road in the next future. Figure 79 gives an overview of the different forecast parameters required from the software and their element name; an example of input forecast file is presented in Figure 80.

Field description	Element name	Unit
Date and time of forecasted elements	forecast-time	ISO 8601
Air temperature (1.5 m)	at	Celsius
Dew point (1.5 m)	td	Celsius
Rain precipitation quantity since the beginning of the forecast	ra	mm
Snow precipitation quantity since the beginning of the forecast	sn	cm
Wind speed (10 m)	ws	km/h
Surface pressure (at the station height)	ap	mb
Octal cloud coverage (0-8)	cc	octal

Figure 79: METRo input files – list of forecast parameters required.

```
<?xml version="1.0" encoding="UTF-8"?>
- <forecast>
  - <header>
    <filetype>forecast</filetype>
    <version>1.1</version>
    <station-id>1</station-id>
    <production-date>2013-12-02T00:00:00Z</production-date>
  </header>
  - <prediction-list>
    - <prediction>
      <forecast-time>2013-12-02T00:00:00Z</forecast-time>
      <at>-0.1</at>
      <td>-6.8</td>
      <ra>0</ra>
      <sn>0</sn>
      <ws>0.9</ws>
      <ap>925</ap>
      <cc>0</cc>
      <wd>38</wd>
    </prediction>
    - <prediction>
      <forecast-time>2013-12-02T01:00:00Z</forecast-time>
      <at>-0.5</at>
      <td>-7.4</td>
      <ra>0</ra>
      <sn>0</sn>
      <ws>1</ws>
      <ap>925</ap>
      <cc>0</cc>
      <wd>34</wd>
    </prediction>
  </prediction-list>
</forecast>
```

Figure 80: METRo input files – forecasts file.

The forecast input file is given to METRo with an hourly timestamp; in addition to these parameters, it's possible to add other forecast information such as the anthropogenic flux, the solar flux and the infrared flux. All input files must be in XML format and have to follow some temporal constraints and formal conventions to be correctly managed from the model.

3.4.2 FASST

FASST (*Fast All-season Soil STrength*) is a complex physically based dynamic state-of-the-ground 1D model developed by researchers at the Engineer Research and Development Center's Cold Regions Research and Engineering Laboratory (ERDC-CRREL) as part of the Army's Battlespace Terrain Reasoning and Awareness research program. The main objective of FASST is the evaluation of an energy and water budget that quantifies both the flow of heat and moisture at the interfaces ground/air, ground/snow and snow/air using both meteorological and terrain data. FASST is in the conditions to accurately estimate the ground moisture and/or ice content, temperature, and freeze/thaw profiles, as well as soil strength and surface ice and snow accumulation/depletion. It is not the purpose of this deliverable to provide a very detailed evaluation of FASST as carried out for METRo, since the reference theory is much more wide and complex. For any in-depth analysis, a comprehensive description of the physical relationships and assumptions of FASST is given in [81]; in [82] a

lot of practical documentation is available for properly using the software. To predict soil temperature, moisture profile and the thickness of any frozen and/or thawed soil layers, FASST uses up to nine modules according to data available; it needs to be run for each area with similar attributes (slope, aspect, soil, and land cover). In Figure 81 a graphical overview of the covered phenomena in FASST, as well as their interaction on the different ground layers, is given.

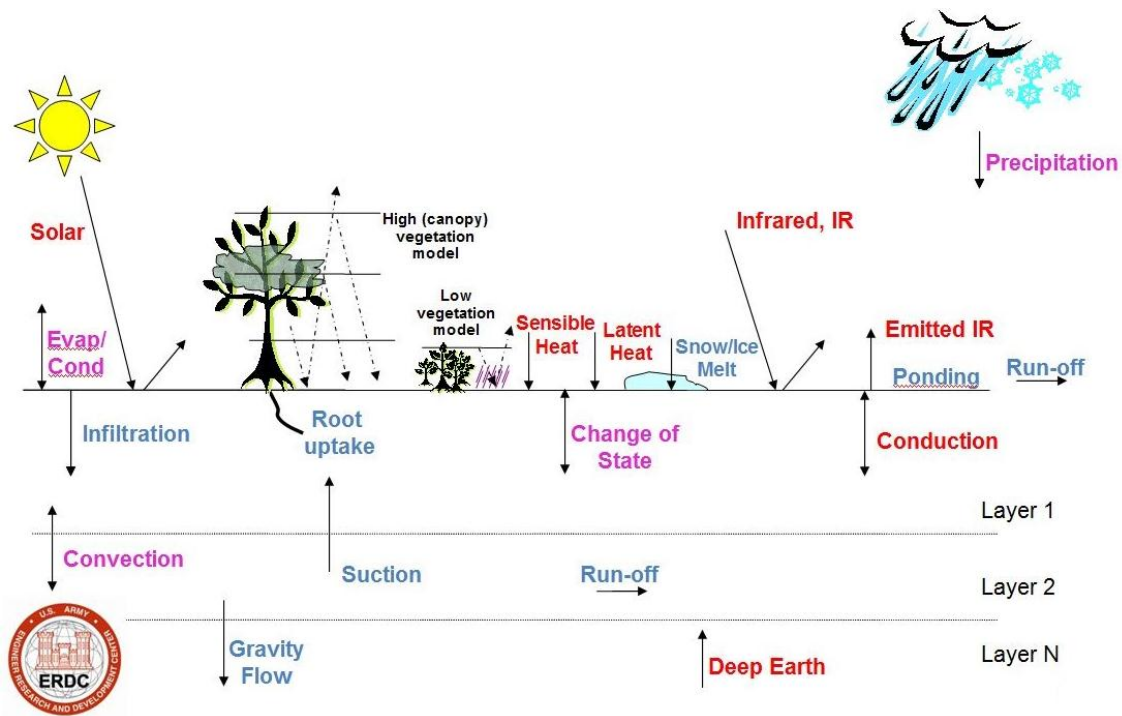


Figure 81: The application domain of FASST model.

The nine modules of FASST are able in particular to accomplish the following tasks:

- read the information related to meteorological data and make any necessary unit conversions and assumptions;
- generate the appropriate values of solar infrared information (if missing) based on cloud amount and type;
- read the information related to initial conditions, soil profile and meteorological data from the input control file;
- initialize the soil profile and the state of the ground;
- calculate the emitted and net IR fluxes;
- calculate the soil temperature and the volumetric moisture content profiles;
- check for freezing and/or thawing processes and calculate the soil strength;
- detect the presence of accumulation or melting processes of snow/ice on ground and the relative runoff;
- making proper time updates if necessary;
- output the result.

A graphical representation of all these tasks as well as the relationships between the different modules is given in Figure 82.

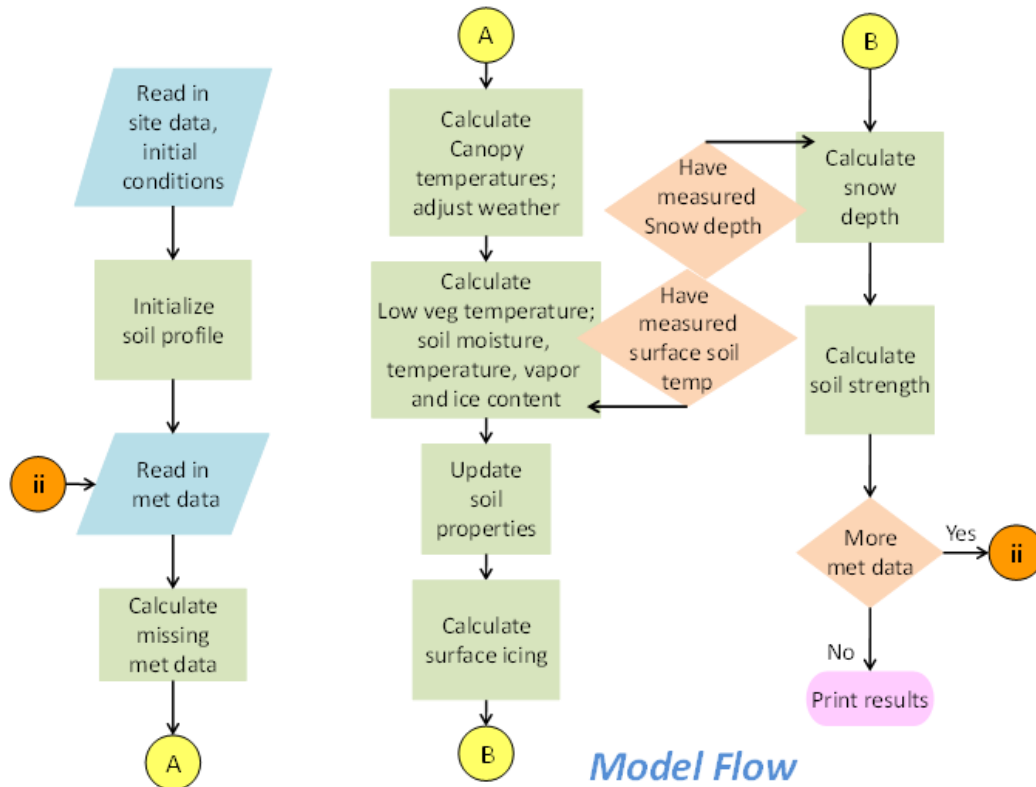


Figure 82: An overview of the interaction between of the flow of FASST model.

FASST requires four types of inputs: **meteorological data**, **soil properties**, **initial conditions** and **site information**. The data format is the standard ASCII; file structure, time step and input transmission mode have to follow a codified structures and rules.

Meteorological data

The only mandatory parameter that FASST needs is the *observed air temperature* coupled with time and date. The reference data frequency is between 1-3 [hours] but the program accepts also data ranging from 1 [minute] to 24 [hours]. The complete meteorological data set that is possible to give in input to FASST is given below; if not all parameters are supplied the software assumes standard values.

- date and hour;
- air pressure [mbar];
- air temperature [°K] and relative humidity [%];
- wind speed [m/s] and direction [degrees from N, + = clockwise];
- precipitation rate [mm/hour] and type [SEDRIS enumeration];
- low cloud amount [0 – 1], height [km] and type [SEDRIS enumeration];
- middle cloud amount [0 – 1], height [km] and type [SEDRIS enumeration];

- high cloud amount [0 – 1], height [km] and type [SEDRIS enumeration];
- total, direct and diffuse incoming solar radiation [W/m²];
- incoming and emitted Infrared radiation [W/m²];
- solar zenith and azimuth angle [degrees];
- snow depth [m];
- soil surface temperature [°K].

The translation of the raw input meteorological file is called by a software component called **Met Reader**. It requires three different files (meteorological data, information about the station and other metadata) to produce the input file that is effectively used in order to produce the FASST elaborations (Figure 83).

979	34	44.700	-84.640	351.800	0	1	4.00	1.00	9999.00	2.000												
Year	JD	Hr	M	APres	ATemp	RH	WnSp	WDir	Prec	PT	Prec2	PT2	LCamt	LCHT	LCT	MCamt	MCHT	MCT	HCamt	HCHT	HCT	STO
				mbar	C	%	m/s	m/s	mm/stp		mm/stp		km	km		km	km		km	km		W/m ²
1992	259	0	0	976.00	18.30	98.00	3.30	268.00	0.000	1	0.000	1	1.00	0.72	2	0.00	0.00	0	0.00	0.00	0	0.0
1992	259	1	0	976.00	17.80	99.00	3.00	255.00	0.000	1	0.000	1	1.00	0.72	2	0.00	0.00	0	0.00	0.00	0	0.0
1992	259	2	0	976.10	16.50	100.00	0.80	258.00	0.000	1	0.000	1	0.40	0.72	1	0.00	0.00	0	0.00	0.00	0	0.0
1992	259	3	0	976.40	16.00	100.00	1.10	256.00	0.000	1	0.000	1	1.00	0.72	1	0.00	0.00	0	0.00	0.00	0	0.0
1992	259	4	0	976.60	15.70	100.00	1.60	219.00	0.000	1	0.000	1	0.70	0.72	1	0.00	0.00	0	0.00	0.00	0	0.0
1992	259	5	0	977.00	15.70	100.00	0.90	284.00	0.000	1	0.000	1	1.00	0.72	1	0.00	0.00	0	0.00	0.00	0	0.0
1992	259	6	0	977.50	15.60	100.00	2.10	213.00	0.000	1	0.000	1	1.00	0.72	1	0.00	0.00	0	0.00	0.00	0	0.0
1992	259	7	0	977.90	15.70	99.00	3.50	201.00	0.000	1	0.000	1	1.00	0.72	1	0.00	0.00	0	0.00	0.00	0	0.0
1992	259	8	0	978.40	16.00	99.00	1.50	211.00	0.000	1	0.000	1	1.00	0.72	1	0.00	0.00	0	0.00	0.00	0	30.0
1992	259	9	0	978.80	16.40	99.00	0.30	134.00	0.000	1	0.000	1	0.90	0.72	2	0.10	4.20	4	0.00	0.00	0	123.9
1992	259	10	0	979.10	17.60	99.00	0.40	263.00	0.000	1	0.000	1	1.00	0.72	2	0.00	0.00	0	0.00	0.00	0	227.4
1992	259	11	0	979.60	18.40	94.00	2.50	274.00	0.000	1	0.000	1	1.00	0.72	1	0.00	0.00	0	0.00	0.00	0	157.3
1992	259	12	0	979.90	19.20	88.00	5.00	252.00	0.000	1	0.000	1	1.00	0.72	1	0.00	0.00	0	0.00	0.00	0	263.1
1992	259	13	0	979.90	20.10	83.00	6.40	258.00	0.000	1	0.000	1	1.00	0.72	2	0.00	0.00	0	0.00	0.00	0	275.4
1992	259	14	0	979.10	20.70	78.00	2.90	245.00	0.000	1	0.000	1	0.20	0.72	2	0.70	4.20	4	0.00	0.00	0	339.6
1992	259	15	0	979.00	21.50	76.00	5.40	231.00	0.000	1	0.000	1	0.20	0.72	2	0.60	4.20	4	0.20	6.99	6	384.0
1992	259	16	0	978.70	22.80	72.00	4.10	219.00	0.000	1	0.000	1	0.20	0.72	2	0.40	4.20	4	0.40	6.99	6	453.3
1992	259	17	0	978.80	22.50	74.00	5.60	186.00	0.000	1	0.000	1	0.70	0.72	2	0.30	4.20	4	0.00	0.00	0	209.0

Figure 83: An example of the FASST input file generated by Met Reader.

Soil properties

The soil parameters, besides the meteorological data, have significant effect on FASST ability to accurately predict the state of the ground. The soil data, required from the software, investigate a wide range of soil properties; fortunately FASST, besides the possibility to set these parameters manually, provide a standard set of parameters related to specific type of terrain. The 23 different terrain types range from gravel to clay, between well and poorly graded materials, from bedrock to asphalt and so on to cover a wide range of choices. In Figure 84 a list of the values associated to the different soil types is reported.

Initial conditions and site information

The set of metadata describing the reference initial conditions and the site which FASST tries to model includes (Figure 85):

- location of the setting files;
- site geographical information;
- time and date information;
- number and type of layers;
- vegetation information (type, canopy);
- ground water level and other specifications.

Soil Type	Bulk Dry Density γ_d (g/cm ³)	Porosity n	Emissivity ¹ ϵ	Albedo ¹ α	Quartz Content ² q	Organic Fraction θ_{of}	Fine/Coarse*	Specific Heat ³ C_s (J/kg·K)
GW	1.95	0.296	0.92	0.40	0.65	0.00	1	820.0
GP	2.16	0.203	0.92	0.40	0.65	0.00	1	820.0
GM	1.91	0.324	0.95	0.40	0.65	0.00	1	820.0
GC	1.87	0.34 ⁴	0.92	0.40	0.65	0.00	1	820.0
SW	1.876	0.320 ⁵	0.92	0.40	0.80	0.00	1	830.0
SP	1.594	0.415 ⁵	0.92	0.35	0.80	0.00	1	816.4
SM	1.474	0.526 ⁵	0.92	0.35	0.80	0.05	1	850.6
SC	1.88	0.400 ⁵	0.92	0.35	0.80	0.05	1	830.0
ML	1.457	0.464 ⁵	0.94	0.40	0.35	0.10	2	845.7
CL	1.589	0.422	0.97	0.23	0.05	0.10	2	854.1
OL	1.165	0.533	0.955	0.265	0.20	0.25	2	837.4
CH	1.517	0.457	0.98	0.30	0.05	0.10	2	845.7
MH	1.060 ¹	0.547	0.94	0.30	0.35	0.10	2	830.0
OH	0.841 ¹	0.892	0.955	0.265	0.20	0.25	2	866.7
PT	0.25	0.70	0.92	0.40	0.05	0.50	2	830.0
SMSC (MC)	1.60 ¹	0.396	0.92	0.40	0.80	0.05	1	830.0
CLML (CM)	1.617	0.397	0.96	0.30	0.20	0.10	2	830.0
EV	1.876	0.320	0.92	0.40	0.80	0.00	1	830.0
CO	2.185	0.020	0.90 ⁶	0.40 ⁶		0.00		850.0
AS	2.500	0.020	0.94 ⁶	0.125 ⁶		0.00		880.0
RO	2.700	0.020	0.89	0.40		0.00		800.0
SN	0.920	0.020	0.90	0.70		0.00		

Figure 84: Reference soil types details defined by FASST.

```

c:\fasst_support\weather\zipfile_data\singleCellExample_met.out      !met data file
0 0 2.0 -1                  !first time through test; single vs multi (0 = single); gap (days) between files; # lines to print
-1.0 60.0 1 1 1 5 0      !gwl; vegint; print profile; print fluxes; print snow info; define frozen
0                          !met id
fasst.out                 !output met and surface info file name
ground.out               !output of soil temperature, moisture, strength profiles
fluxes.out              !output of surface fluxes
veg_temp.out            !output of vegetation temperatures
snow_info.out          !output of snow information
10.0 70.0               !surface slope (degrees from horizontal), surface aspect angle (degrees from N, + = clockwise)
-999.0                  !surface roughness length (m)
0                        !no open water
0.0 0.0                 !initial snow depth (m)
0.0                     !initial ice thickness (m)
2                        !type of low vegetation
0.05
999.0
999.0
10.0
5                          !type of high vegetation
13.0 0.96
6,4.75,1.0,5.0,0.3,0.1,0.225,0.98
6,3.25,1.0,5.0,0.3,0.1,0.046,0.98
6,1.10,1.0,3.0,0.2,0.5,0.038,0.98
1                          !number of soil layers
-1 1.0                  !layer soil type, layer thickness (m) [grsp]
g2nw
c:\fasst\inp_files\gr1_soil.inp  !user soil data file
n
2                          !type of low vegetation
0.05
999.0
999.0
10.0
5                          !type of high vegetation
13.0 0.96
6,4.75,1.0,5.0,0.3,0.1,0.225,0.98
6,3.25,1.0,5.0,0.3,0.1,0.046,0.98
6,1.10,1.0,3.0,0.2,0.5,0.038,0.98
g2nw
c:\fasst\inp_files\gr1_soil.inp  !user soil data file

```

Figure 85: An example of FASST input file with the initial conditions and site information.



Outputs

FASST generates 10 different output files; some of them are effectively useful for the users while other are used for the subsequent analysis of the software only (i.e. elaboration outputs telling the user e.g. how the output variables were generated, if specific error were produced, etc.). The output files containing user-relevant information are generated at the same frequency with which the input file are given to the model, and can be categorized as follow:

- meteorological data with information concerning the surface conditions;
- soil profile data;
- surface heat fluxes;
- vegetation temperatures;
- snow profile (if snow is present during the simulation);
- mobility specific data.

3.4.3 GeoTop

RWIS typically rely on 1D road weather models such as METRo, eventually spatially extended through a Geographical Parameters Database (GPD) as described in [1]- [6]. In the literature, however, complex 3D models typically used in the hydrogeological sector are available as well. One of the most interesting for CLEAN-ROADS, in particular because of its geographical origins and the local expertise on it within the scientific and industrial community, is GEOtop, a distributed hydrological model with coupled water and energy balance developed by a research team at the University of Trento at the beginning of the '90s and released as FOSS [83]. The purpose of GEOtop is to estimate in a spatial/temporal continuum way the rainfall-runoff and the energy fluxes, with particular attention to evapotranspiration in small mountain catchments (Figure 86). The reference application domain is the water resources and hydrogeological risk management, but theoretically is applicable in RWIS application as well, since, given in input meteorological data and soil parameters, it is in the condition to return in output, among others:

- the radiation and energy fluxes at the Earth surface;
- the temperature and ice content in the soil;
- the height and density of the snow.

Futhermore, the post process software **GEOtopFS** (*GEOtop Factor of Safety*) is in the condition to calculate the dynamic probability of slope instability during a precipitation event. GEOtop is quite known in the environmental engineering community and is wide used by research institutions, universities, public agencies for environment protection and private companies. No information about real-time and /or applications using GEOtop are at present however available.

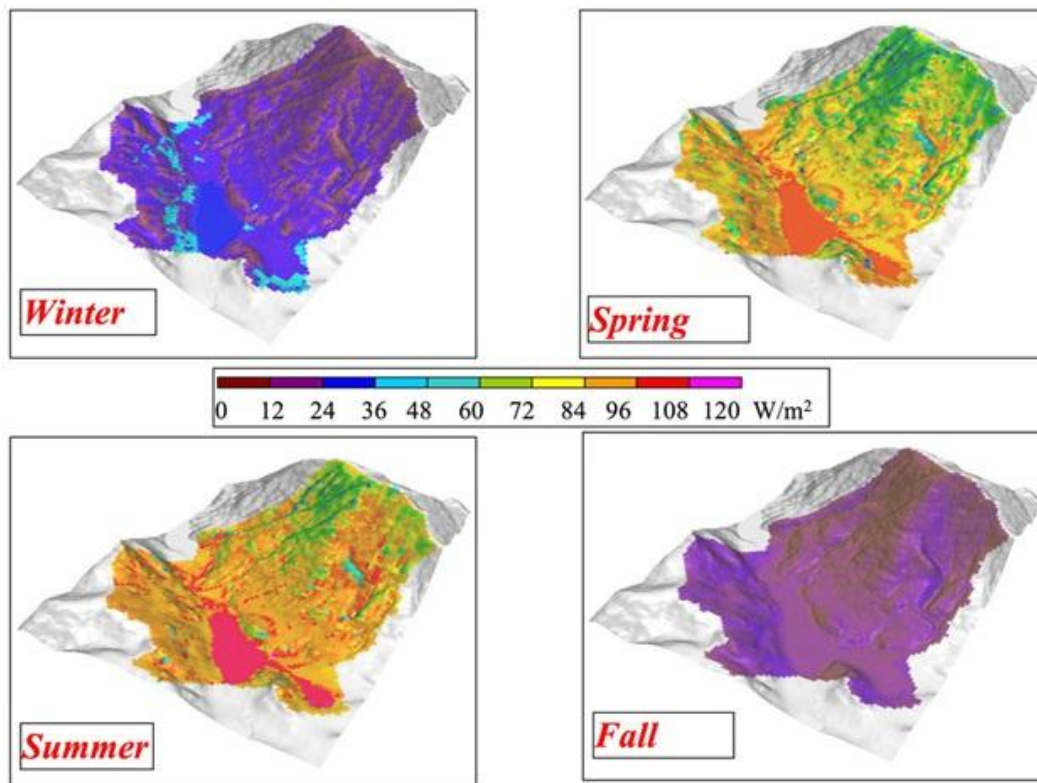


Figure 86: An example of the spatial outputs of GEOtop.

The 3D elaborations are possible thanks to the use of *Digital Elevation Models* (DEMs), which must be given in input to GEOtop as well as meteorological measurements obtained through traditional instruments on the ground but also other distributed data such as radar measurements, satellite terrain sensing or micrometeorological models. GEOtop solves the hydrogeological problem in correspondence of each pixel of the DEM.

The complete input data set can be summarized as follows:

- hourly values of air temperature, relative humidity, wind speed, solar radiation, precipitation data measured by static weather measurement stations, to be installed at a maximum distance of 20 [km] from the target area;
- optionally, hourly values of atmospheric pressure, net solar radiation, snow height and daily values of cloud cover;
- metadata of those weather measurement stations (i.e. geographical coordinates, spatial reference system, other technical specifications);
- DEM;
- land use classification map;
- optionally, other distributed data such as:
 - precipitation levels;
 - results of specific hydrogeological surveys carried out on the soil;
- information concerning the vegetation (type, density, height).

3.4.4 Other road weather models

A plenty of other physical road weather models are available at the state-of-art; the most relevant in the RWIS community, besides METRo, are:

- **IceBreak**, which is a 1D numerical prediction model for RST, road surface state and Friction Index [84]. Unlike many other models that require human intervention (e.g., providing meteorological inputs), IceBreak depends only on sensor measurements and is fully automatic, generating very short nowcasts (3-6 hours). In theory, the model can easily be re-run every time that new observations are available, but typically nowcasts are generated only when the road surface temperature falls below a given threshold. IceBreak has been recently spatially extended in the second dimension as already described in the paragraph 3.3.3;
- **ENTICE**, which is a 2D road weather model in which a previous 0D model was spatially extended through a GPD; improvements and optimizations in the techniques of how properly initialize this database are still under investigation, as described in [85].

An alternative to “physical” road weather forecast models, which has been developed in parallel, is represented by **statistical approaches**, i.e. the idea to estimate the future behavior of road-based variables based on the time series theory [86] and fuzzy logic. An empirical demonstration of the suitability of these modeling techniques was already given in [87], in which the statistical model **HS4Cast** was proposed and validated, with forecast that are comparable in terms of accuracy with those produced by physically-based road weather models (Figure 87). Despite the various studies concerning the application of uni- or multivariable time series models and artificial neural networks (ANNs) in this field, these techniques have had little diffusion in the RWIS community. The main limitation was in fact the necessity to have a huge and complete data set in input in order to properly initialize and/or train the statistical model and thus to have accurate forecasts. This is however difficult to achieve, since meteorological conditions can vary a lot and it’s extremely hard to have one or more reference pattern situations for all of them. Moreover, the computational power was significantly more reduced than today, and the time needed for e.g. continuously train an ANN was incompatible with the typical RWIS requirements. However, thanks to the exponential improvements in the processing capabilities as well as the continuous development of static RWIS stations networks and related data, these technological barriers could be today overtaken and properly proposed again, possibly in combination with reference “physical” road weather forecast models.

3.5 Future perspectives in the road weather modeling

What are the future perspectives of modeling techniques for RWIS? This is a crucial question for CLEAN-ROADS, since the design choice that will be made for its core engine must somehow be aligned with the expected developments that might take place in the international community. An interesting blueprint of the RWIS of the future was given in [88], in which the foundations for future research and development with respect to ice prediction

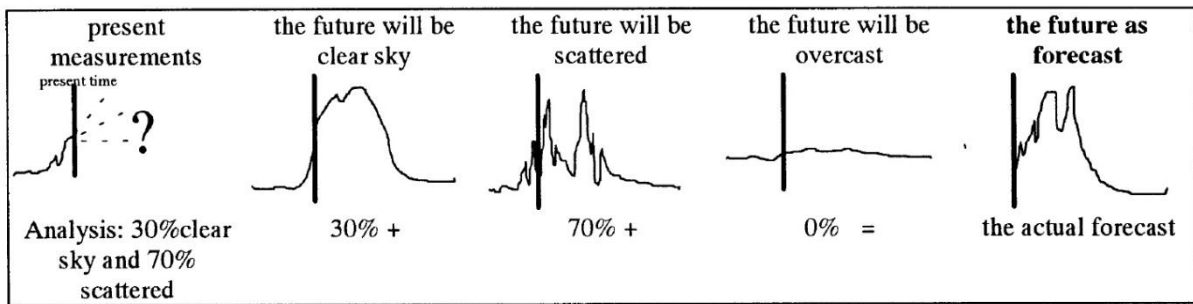


Figure 87: The fuzzy approach of HS4Cast model [87].

was given, in particular by taking in consideration the ENTICE model (Figure 88). Concepts like forecasting minimum temperatures from thermal maps or deterministic stability classes will be abandoned in favor of dynamic GIS-based forecasting tools characterized by the use of:

- **Digital Terrain Models (DTM).** Although accurate altitude datasets can be collected using improved GPS systems (and in the future with Galileo), improved data can be generated from DTM, whose cost has recently fallen to the extent that high resolution models are available for free to the academic community. DTMs can put the basis for the development of enhanced algorithms that can efficiently model e.g. the influence of topography such as katabatic drainage.
- **Mesoscale Modelling.** The zero-dimensional energy balance approach of the model is limiting as there is no simulation of advective processes; meteorological parameters such as wind-speed and in particular, cloud are notoriously hard to forecast being variable both spatially and temporally. This problem is going to be improved by using a mesoscale forecast model, which will forecast the values of these parameters not only for a single outstation.
- **Satellite Landuse Classifications.** The use of satellite imagery can provide a useful source of landuse data to provide parameterisations for models.
- **Road Classifications.** Road type information can be an important input parameter for RWIS; further research is however required to improve road construction parameterisations.
- **Sky-view factors and screening.** The sky-view factor is the dominant control parameter on RST. The actual acquisition of data is difficult as imagery can only be taken in a limited 'surveying window' of homogeneous cloudy conditions. This problem can be eliminated by using near infra-red fish-eye imagery; novel techniques are however needed in order to measure sky-view factors in real time.

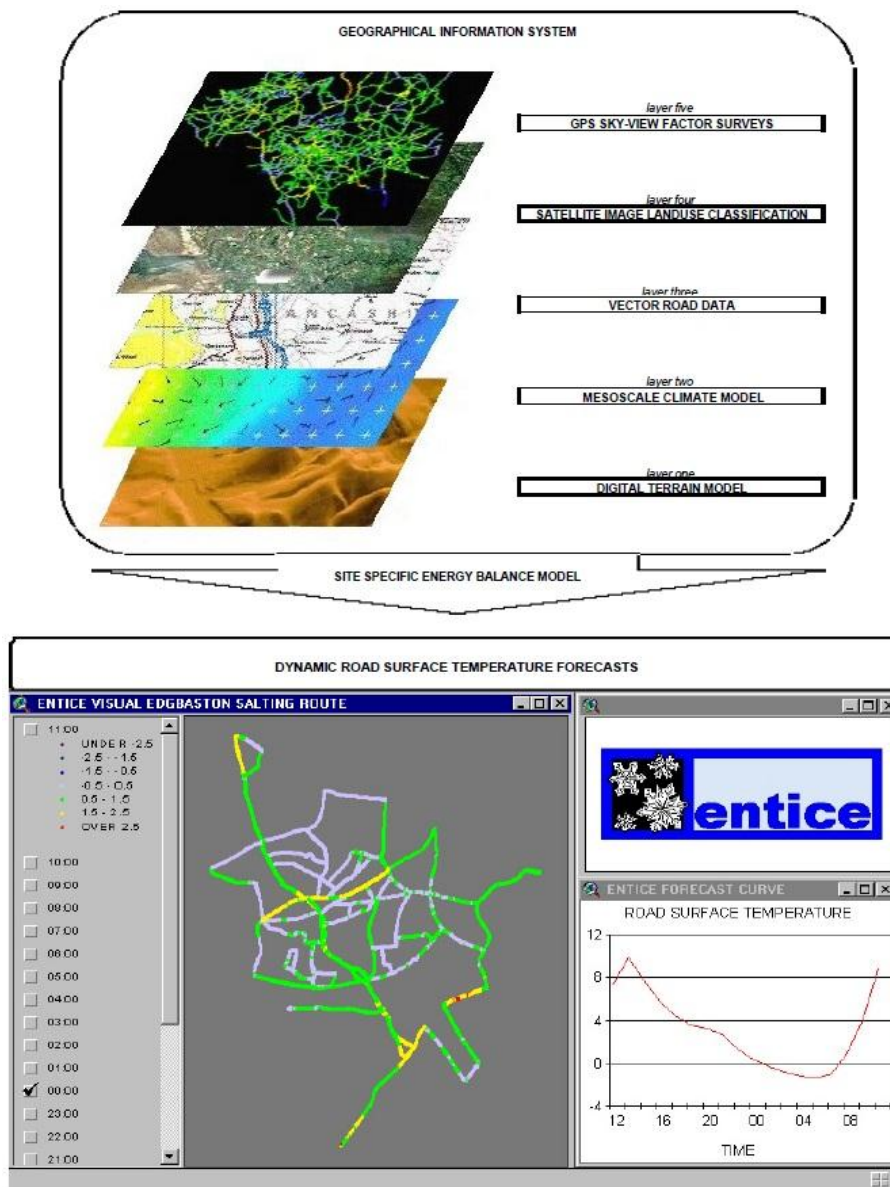


Figure 88: The future evolution of road weather models [88].

An interesting joint study of several road weather models, including METRo and FASST, which is worth mentioning in this preliminary analysis [89]. This study is particularly relevant for CLEAN-ROADS since it offers a comprehensive empirical comparison between the available models, highlighting strengths and weaknesses and thus offering a decision-base on top of which a design choice can be made. Models were compared in terms of forecast performance, code stability, support, efficiency, and ease of use; a synthesis of this analysis is given in Table 13. In terms of overall forecast performance, METRo has shown to return the best forecast for all the cases that were examined, which included a wide range of weather conditions. Moreover, METRo was also very easy to obtain and install, while FASST presented a sharper learning curve before having at disposal a stable version. The main weakness of METRo is the computational time for the forecast process (i.e. 2.0 [s] instead of



0.2 [s] for a 45 [hours] forecast), but is mainly due to the use of XML format (thus optimizable).

Feature	FASST	METRo
Operating System	Windows	Linux
Language	FORTRAN	C++
Code stability	Research (US military)	Operational use (Canada and others)
Installation / documentation	Good	Good
Support / responsiveness	Good	Very good
Model initialization	Easy, well documented	Easy, well documented
Computational speed (48 [h] forecast)	0.2 [s]	2.0 [s]

Table 13: A comparison between FASST and METRo models.

4. Maintenance Decision Support Systems

In the previous chapters the fundamental components of a RWIS have been presented, namely (i) the enabling technologies for the collection of direct / indirect road conditions data and (ii) the reference models for determining accurate estimates for the actual and future period. But how is this information presented to RWIS' users, i.e. road maintenance staff and local travelers, in order to give them an immediate assessment of potential risks on the road? This is not an easy task as one can imagine: users are typically very demanding towards IT systems and have little time and tolerance in finding the information they need. The risk is that if the early user experiences are bad, they will then never use, consider and rely for such decision-support systems. In RWIS, this aspect is particular relevant if **road weather forecasts** are considered. This is a crucial information, in particular for road maintenance staff who is in charge to decide and/or to carry out a salting treatment. The way a forecast is presented is therefore a major issue in the international community, since this has demonstrated to have a very high impact on the effective optimization in the use of winter road maintenance resources.

Traditionally, **RWIS** have been “**deterministic**”, i.e. they have always given to road maintainers only one reference forecast of road conditions. This was typically coupled with 1D systems, strictly linked with the field measurements collected by a static RWIS station installed at a certain cold hotspot point. In reality, early systems were used to provide a couple of forecasts, illustrating the best and worst case scenarios (Figure 89). However, due to little confidence in the system, road maintenance staff was used to base his decisions only on the pessimistic forecast, and thus to produce over-salting treatments. For this reason, RWIS have then rapidly moved to single-forecasts approaches, showing only one reference indication of the expected road conditions behavior. This approach was then maintained even when XRWIS began to be at disposal, typically providing colored route-based map risks (as already shown in Figure 88).

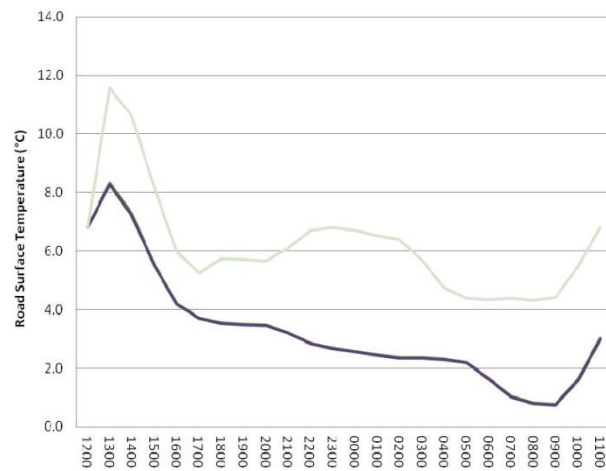


Figure 89: Deterministic road weather forecast [90].

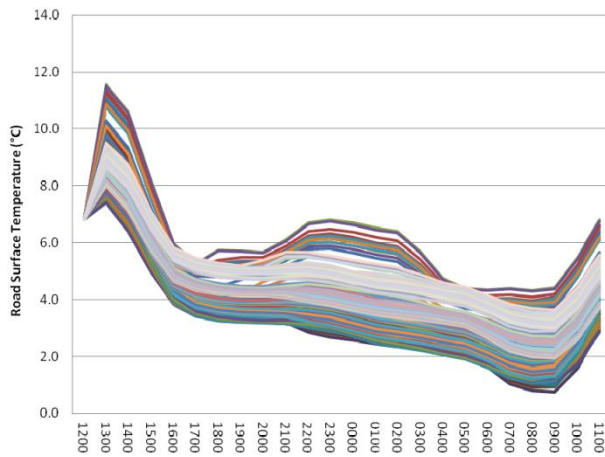


Figure 90: Probabilistic road weather forecast [90].

The RWIS community has however recently started moving in the direction of **probabilistic forecasting**, following a tendency which is clearly observable in a lot of sectors, in particular the meteorological one [90]. As already discussed in this report, the technical concept is to have in output the projections of a model ensemble, which produces a variety of possible output values by perturbing the original conditions across a range of possible values. The new challenge here, which is also strictly linked with the future tendency to have at disposal a plenty of data and output elaborations, is to understand how properly present the

results of these probabilistic forecasts. In fact, road maintenance staff will have a very little acceptance in interpreting a diagram like the one in Figure 90. The trend is to go towards route-based road conditions map, in which a new information is added – i.e. the uncertainty that a specific route stretch will be affected by ice formation phenomena, which could be estimated as the number of such events detected in the ensemble model outputs compared to their totality (Figure 91).

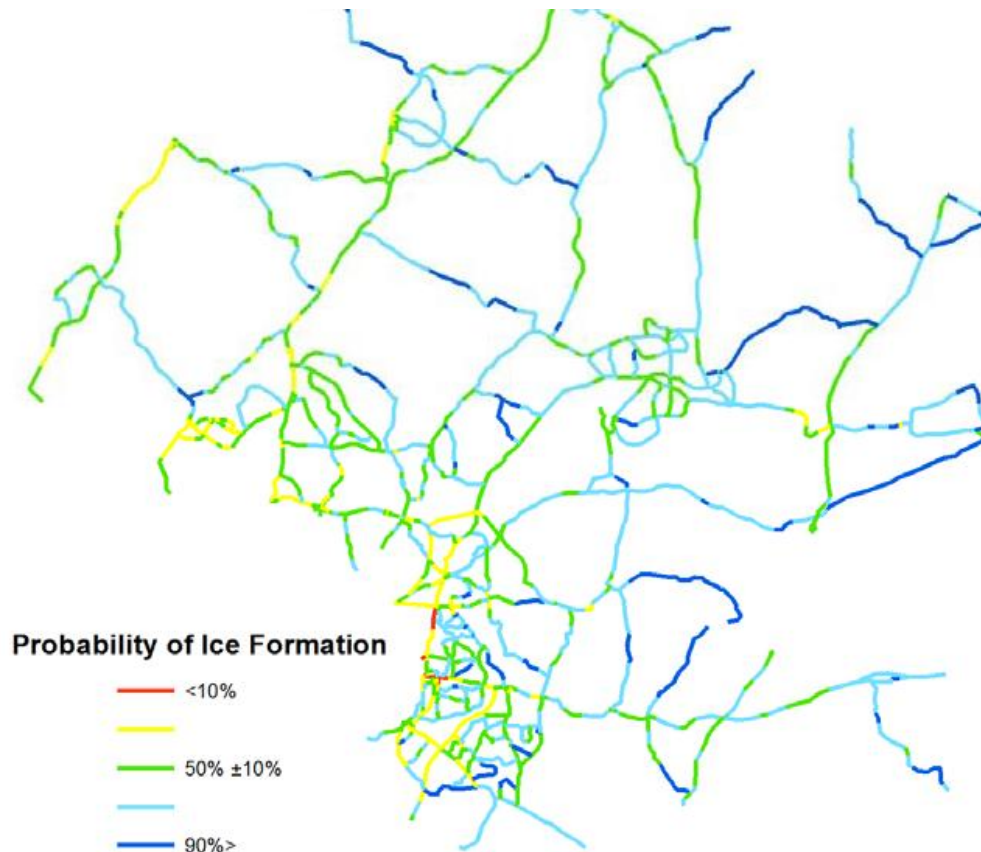


Figure 91: A blueprint of probabilistic RWIS [90].

A pioneer in probabilistic RWIS is the German Nation Weather Service which manages since years a RWIS called SWIS (Straßenzustands- und Wetter-Informations-System), which has decided to follow this new strategy [91]. The impact of probabilistic forecasts is the possibility to (i) increase protective actions and (ii) minimize missed alarms, with the perspective to increase road maintenance costs but reduce significantly costs associated to road weather externalities. The empirical challenge that they have revealed to face is related to the fact that while forecasts are probabilistic in nature, treatments decisions are deterministic; how will a road maintainers react to a probabilistic information? In this perspective, it will have an increased importance an accurate assessment of the cost-benefit analysis, which will drive them in deciding the best overall strategy to follow. By considering this, three different road maintainers user groups can be distinguished:

- **“very advanced” road maintainers**, who know their cost-loss ratio and just ask for uncertainty information;
- **“advanced” road maintainers**, who have little knowledge of uncertainties and prefer to have deterministic information but associated to uncertainties;
- **“basic” road maintainers**, who do not know probability theory and necessitate to have just few and simple information.

Moreover, two typical time ranges use cases must be considered i.e. (i) 1-2 days mid-term work schedule organization and (ii) 1-2 hours short-term road treatments decisions. The introduction of probabilistic RWIS will therefore lead to an increased need to train road maintenance staff (i.e. in order to move “basic” road maintainers to “advanced” or “very advanced”), in particular new employees, and to efficiently incorporate their feedback in the system loop, so that they can increase the feeling that their role is more and more central and crucial in this application domain.

In the following pages of this chapter a comprehensive overview of the most interesting RWIS applications around the world is given. The reference state-of-arte source for this international literature analysis assessment has been mainly the SIRWEC conference, which holds on a two-year basis. While the first paragraph investigates more the different approaches on how a RWIS can support winter road maintenance activities, the second paragraph tries to offer a wide picture of the different RWIS R&D and/or pilot projects.

4.1 RWIS-driven advanced winter maintenance methods

Winter maintenance is essential to provide a high accessibility of regions with extensive snow fall or long winter periods. This is a common requirement for alpine regions, including the Trentino Alto-Adige region. Typical decisions on a strategic level include e.g. choosing between de-icing agents, defining minimum treatment intervals, route quality targets, and specific application rates. In practice, the winter maintenance personal has usually not enough time or information for an optimal consideration of all relevant factors, and being the first responsible if accidents happen they tend to follow “safe approaches” that differs from optimal application rates or timing of treatment. Comparisons of typical winter maintenance situations with practical application rates have shown high potential of savings by preventing

unnecessary salting; therefore the need to define and introduce optimized winter maintenance strategies for all typical reference situations.

4.1.1 Salting treatments recommendations

In order to address this, the federal states of Austria, the Austrian highway operating company (ASFINAG) and the federal ministry of Transport (BMVIT) recently funded a research project at the **Vienna University of Technology**, with the objective to define an advanced winter maintenance model in Austria with practical winter maintenance guides and training coursed for the road maintenance personnel (Figure 92) [92]. In particular, the research analyzed in deep the limited thawing capability of de-icing agents as well as the identified correlations and the salt losses due to drift and discharge caused by road traffic, in order to suggest optimal preventive treatments, based on residual salt availability on the road from previous treatments, that can (i) avoid potentially slippery roads and (ii) ease snow ploughing in the next treatment. The novelty of this research is that a very detailed study of skid resistance based also on road texture data has been included as well [93]. Road textures of flexible or rigid pavements have shown to differ quite significantly, but the most interesting result is that the when the surface area (i.e. the contact area between tires and roads) becomes filled with snow or ice, the skid resistance shows to a have a sudden drop between 60-90%.

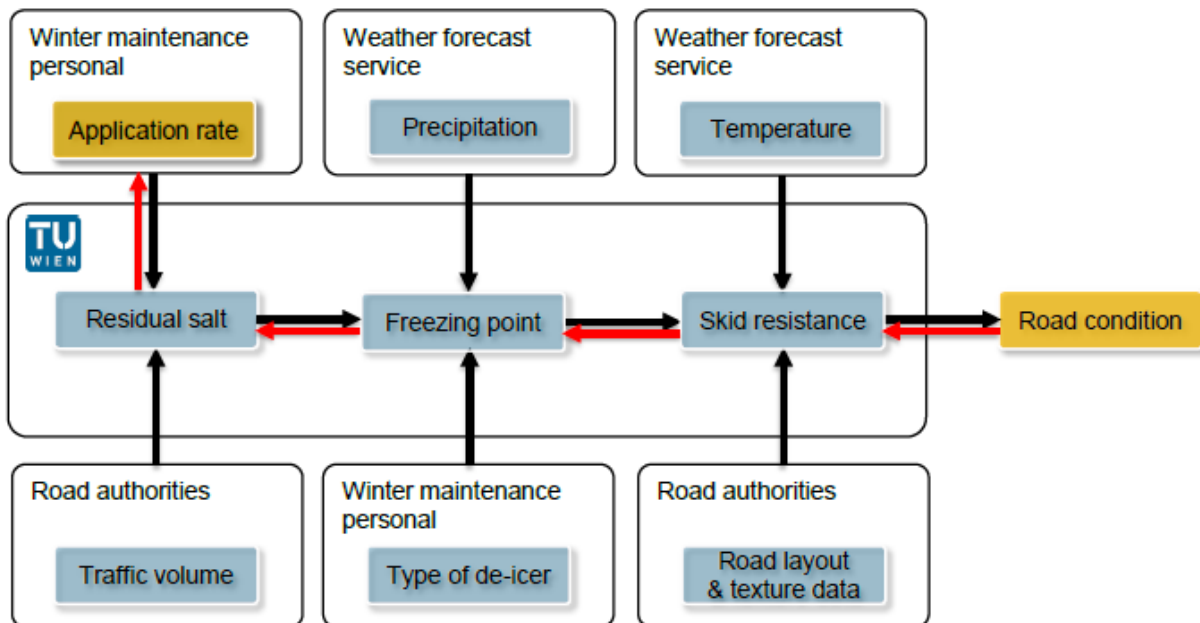


Figure 92: The advanced winter road maintenance model defined by TU Wien [92].

The main results of the initial basic researches revealed the following statements:

- a **preventive treatment** has to be performed prior to each precipitation event unless sufficient residual salt is already available on the road;

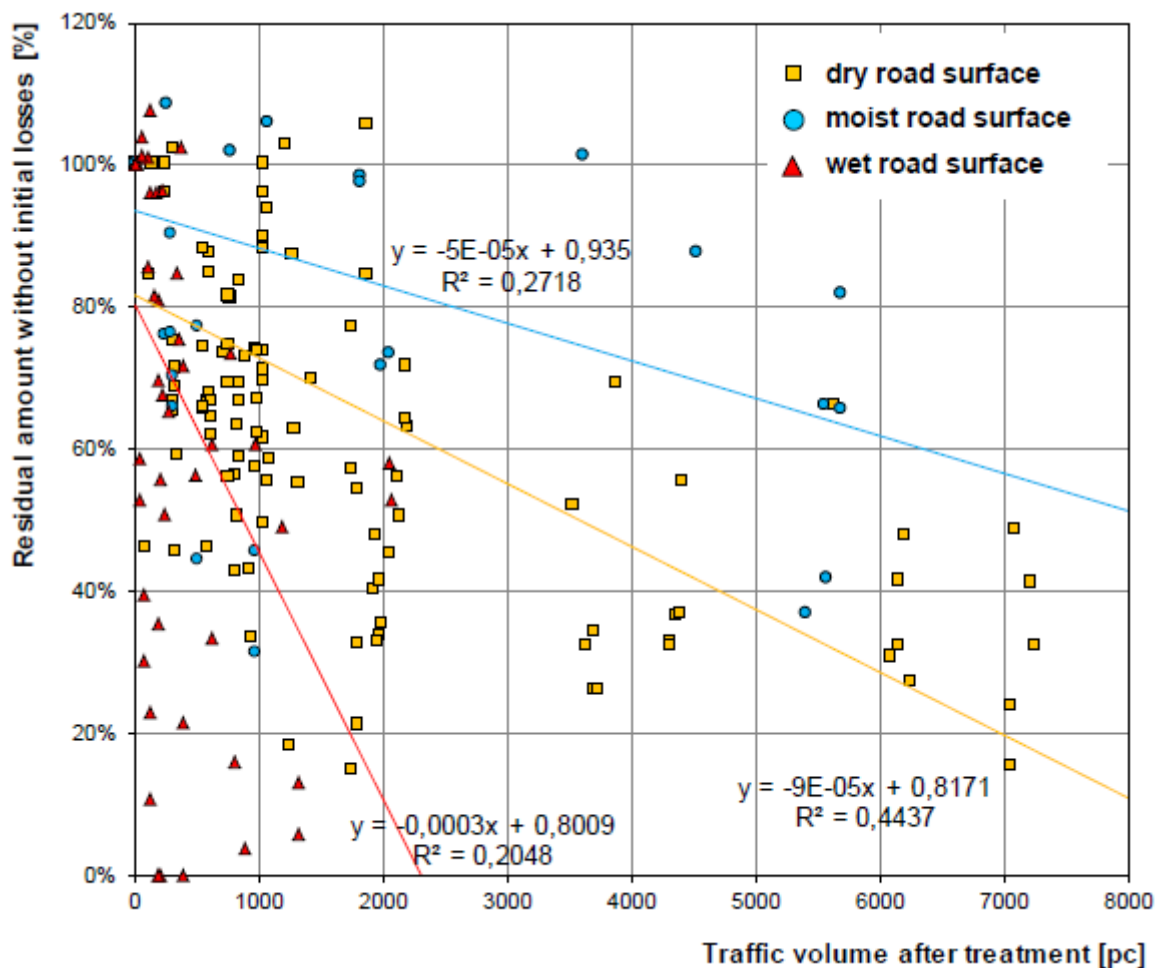


Figure 93: Residual salt quantities in different road conditions - empirical assessments of TU Wien [92].

- on average, residual salt has demonstrated to be only about the 40% of the amount used during the application process, caused by discharge losses and traffic and surface conditions (Figure 93);
- with a preventive treatment and a salt application rate of 10 [g/m²] timed prior to hoarfrost, a slippery road surface can be in most cases avoided; if the physical limited thaw capability of salt is exceeded due to the amount of snow between two treatment cycles and the remaining snow after the first snow ploughing, the development of **snow slush** cannot be avoided; in this conditions, the skid resistance is lower than to snow-covered roads. A preventive application of 10 [g/m²] is usually sufficient to form a release coating out of salt and first precipitation, that must be renewed after each ploughing operation;
- at **very low temperatures** the melting capacity of salt is very low leading to no further improvements of road condition with appropriate ploughing being a sufficient treatment;
- a delayed treatment addresses a situation where snow is already compressed by traffic and frozen onto the road surface with no release coating present. In such cases the quality of snowploughing is very low leaving high amounts of residual snow

on the road. Any thawing attempt will create a slippery brine film on top of the snow layer, with the possibility to even lower skid resistance if compared to doing nothing.

A comprehensive picture of the physical mechanism associated to delayed and preventive treatments, the suggested application rates depending on precipitation, traffic and temperature as well as a full set of recommendations for road maintainers and drivers is given in the figures below.

Picture documentary	Road condition	Treatment recommendation	Treatment recommendation
	Dry road: ----- No slickness expected Surface temperature: -30°C to +60°C High skid resistance, $\mu = 0,6 - 1,0$ ----- Hoarfrost possible or expected (usually at 2 - 4 am)	Minimal salting only at hoarfrost: ----- No treatment required ----- Preventive treatment 5 – 10* g/m ² with beginning hoarfrost	Minimal salting only at hoarfrost: ----- No restrictions due to weather based road conditions needed. ----- Reduction of the speed by at exposed road sections (e.g. bridges)
	Moist or wet road: ----- Road surface temperature > 0° C Moderate skid resistance, $\mu = 0,4 - 0,7$ ----- Road surface temperature ≤ 0° C Moist road Moderate skid resistance, $\mu = 0,2 - 0,6$ ----- Road surface temperature ≤ 0° C Wet road Very low skid resistance, $\mu = 0,1 - 0,6$	Salting at temperatures below 0° C: ----- No treatment required (Watch temperature!) ----- Preventive treatment with 5 – 10* g/m ² Before beginning freezing ----- Treatment with 20 to 40* g/m ² before freezing critical Warning messages if black ice forms!	Local ice at sub-zero temperatures: ----- Reduction of speed in case of lane grooves ----- Caution, black ice possible, Reduction of the speed by 50% at exposed road sections ----- Caution, black ice possible, Reduction of the speed by 70% at exposed road sections
	Snow next to wheel tracks: ----- No snowfall Wheel tracks free of snow Moderate skid resistance, $\mu = 0,3 - 0,5$ ----- Snowfall less than 0,5 cm/interval Low skid resistance, $\mu = 0,2 - 0,4$ ----- Snowfall more than 0,5 cm/interval Snow in wheel tracks Low skid resistance, $\mu = 0,2 - 0,4$	Ploughing and salting: ----- Ploughing and salting with 10 – 20* g/m ² , to remove remaining snow ----- Ploughing and salting with 10 – 20* g/m ² ----- Ploughing and salting 10 g/m ² (release coating!) until end of snowfalls, then ploughing and salting with 10 – 20* g/m ²	Adapted driving: ----- Adapted driving, Reduction of the speed by 20 to 30% ----- Adapted driving to road conditions, Reduction of the speed by 30 to 40% Consider restricted visibility!
	Snow in wheel tracks: ----- No snowfall Road covered with snow Low skid resistance, $\mu = 0,2 - 0,3$ ----- Snowfall less than 0,5 cm/interval Low skid resistance, $\mu = 0,2 - 0,3$ ----- Snowfall more than 0,5 cm/interval Very low skid resistance, $\mu = 0,1 - 0,3$	Ploughing and salting: ----- Ploughing and salting with 20 – 30* g/m ² , to remove remaining snow ----- Ploughing and salting with 10 – 20* g/m ² ----- Ploughing and salting 10 g/m ² (release coating!) until end of snowfalls, then ploughing and salting with 20 – 30* g/m ²	Adapted driving:: ----- Adapted driving, Reduction of the speed by 40 to 50% ----- Adapted driving to road conditions, Reduction of the speed by 60 to 70% Consider restricted visibility!
	Very low skid resistance ----- No precipitation Road surface temperature ≤ 0° C. Very low skid resistance, $\mu = 0,05 - 0,2$ ----- Black ice and further precipitation (Snow or rain) Very low skid resistance, $\mu = 0,05 - 0,2$	Salting as required: ----- Preventive treatment if possible, Maximum treatment at critical/icy Spots, Further treatments as necessary ----- Maximum treatment until ice is cleared Closure of road sections as necessary. Opening after closure only if skid resistance is sufficient	Particular caution, walking pace: ----- Follow driving restriction until clearance of road. Pass dangerous areas with walking pace ----- Caution, ice beneath snow layer is not visible and therefore dangerous. Adapted driving to road conditions, Reduction of the speed to walking pace

Figure 94: Recommendations' summary to road operators and drivers from TU Wien research study [92].

Physical mechanism „Preventive treatment“	
	<p>1. Preventive treatment just before snowfall event e.g. 10 g/m² immediately prior to snowfall of about 1 cm/h Road surface temperature = -5°C Treatment interval = 3 h 3 cm snow height during interval</p>
	<p>2. Dilution and forming of 2 phases 1. Phase snow/ice (about 0% salt) 2. Phase brine below (8% salt) The applied salt is dissolved gradually, until an equilibrium concentration is reached at 8% and -5°C</p>
	<p>3. Snowploughing and salting The brine prevents adhesion of the snow on the road surface and relieves further snowploughing. For salt application applies: remaining snow + applied salt = brine > 8% (Salt consumption depends on quality of ploughing and road condition)</p>
	<p>4. Thaw residual snow (continue with 2) Thaw of the remaining snow and brine formation > 8%; ongoing development according to 2 until end of snowfalls (discharge loss due to traffic and mixing not considered)</p>

Figure 95: Preventive treatments – reference physical mechanism [92].

Physical mechanism „Delayed treatment“	
	<p>1. Snowfall and ice formation Snowfall of 1cm/h adds up to 3cm during the interval which are discharged or compressed by traffic. Possibility of ice formation due to high pressure or freezing of snow to the road surface</p>
	<p>2. Snowploughing and salting Increased Ploughing energy needed due to absence of release coating, higher remaining snow volume= higher salt rates needed Residual snow + salt = brine > 8% (Salt consumption depends on quality of ploughing and road condition)</p>
	<p>3. Icy conditions during melting process (2 phases) 1. Phase brine on top (>8% salt) 2. Phase snow/ice (about 0% salt) During the melting process >15 - 30 minutes vehicles drive on a layer of ice</p>
	<p>4. (Partial) Thawing of remaining snow With adequate ploughing and salting remaining snow thaw under formation of brine > 8% concentration Otherwise further development as in point 2 of the preventive treatment. With insufficient salting threatens icy conditions.</p>

Figure 96: Delayed treatments – reference physical mechanism [92].

Precipitation 0,0 mm to 0,25 mm - Snow height 0,0 cm to 0,25 cm Hoarfrost or slightly visible snowfall										
Application rate [g/m ²]	Road surface temperature [°C]									
	-1	-2	-3	-4	-5	-6	-7	-8	-9	-10
Traffic during interval	250	5	16	26	36	10	10	10	10	10
	500	6	16	27	37	10	10	10	10	10
	1.000	6	17	28	39	10	10	10	10	10
	1.500	6	18	30	10	10	10	10	10	10
	2.000	6	19	31	10	10	10	10	10	10
	2.500	7	20	33	10	10	10	10	10	10
	3.000	7	21	35	10	10	10	10	10	10
	3.500	8	23	37	10	10	10	10	10	10
	4.000	8	24	40	10	10	10	10	10	10

Precipitation 0,25 mm to 0,5 mm - Snow height 0,25 cm to 0,5 cm Very light snowfall										
Application rate [g/m ²]	Road surface temperature [°C]									
	-1	-2	-3	-4	-5	-6	-7	-8	-9	-10
Traffic during interval	250	11	32	10	10	10	10	10	10	10
	500	11	33	10	10	10	10	10	10	10
	1.000	12	34	10	10	10	10	10	10	10
	1.500	12	36	10	10	10	10	10	10	10
	2.000	13	38	10	10	10	10	10	10	10
	2.500	14	10	10	10	10	10	10	10	10
	3.000	14	10	10	10	10	10	10	10	10
	3.500	15	10	10	10	10	10	10	10	10
	4.000	16	10	10	10	10	10	10	10	10

Precipitation 0,5 mm to 0,75 mm - Snow height 0,5 cm to 0,75 cm Light snowfall										
Application rate [g/m ²]	Road surface temperature [°C]									
	-1	-2	-3	-4	-5	-6	-7	-8	-9	-10
Traffic during interval	250	16	10	10	10	10	10	10	10	10
	500	17	10	10	10	10	10	10	10	10
	1.000	17	10	10	10	10	10	10	10	10
	1.500	18	10	10	10	10	10	10	10	10
	2.000	19	10	10	10	10	10	10	10	10
	2.500	20	10	10	10	10	10	10	10	10
	3.000	22	10	10	10	10	10	10	10	10
	3.500	23	10	10	10	10	10	10	10	10
	4.000	24	10	10	10	10	10	10	10	10

Precipitation 0,75 mm to 1,0 mm - Snow height 0,75 cm to 1,0 cm Light/moderate snowfall										
Application rate [g/m ²]	Road surface temperature [°C]									
	-1	-2	-3	-4	-5	-6	-7	-8	-9	-10
Traffic during interval	250	22	10	10	10	10	10	10	10	10
	500	22	10	10	10	10	10	10	10	10
	1.000	23	10	10	10	10	10	10	10	10
	1.500	24	10	10	10	10	10	10	10	10
	2.000	26	10	10	10	10	10	10	10	10
	2.500	27	10	10	10	10	10	10	10	10
	3.000	29	10	10	10	10	10	10	10	10
	3.500	31	10	10	10	10	10	10	10	10
	4.000	33	10	10	10	10	10	10	10	10

Figure 97: Application rates suggested for different road weather conditions [92].

4.1.2 Dynamic maintenance activities control

RWIS-driven winter maintenance methods do not only limit to the decision-making process as pointed above, but can also cover directly the maintenance operations as well. An example of this approach is provided in [94], in which Meteo Group presented an innovative approach to link route-based forecasts with **dynamic gritting operations**, which is actually carried out in the Netherlands. The use of route-based forecasts has been motivated by the results of several thermal mapping surveys, which demonstrated the very large RST variations that may occur in case of covered (trees/building covered roads) and uncovered (open locations) areas. In practice, road treatments are typically carried out on the whole road network based on the conditions at cold hotspots, where static RWIS stations are located, with a relevant amount of resources waste.

The reference architecture of the proposed RWIS is illustrated in Figure 98; a combination of physical / statistical road weather modelling tools as well of static and mobile observations (including initial geographical assessments, e.g. sky view) is proposed. Maintenance vehicles take RST mobile measurements as well for verification purposes of the forecast. Gritting operations are optimized in two directions:

- **dynamic gritting**, i.e. the amount of salt depends on the variable road conditions, and is thus regulated accordingly;
- **dynamic routes**, i.e. treatment operations are defined a priori in order to treat critical points first.

First empirical tests have demonstrated that in normal winter seasons (i.e. without exceptional snowfalls), dynamic gritting operations can be applied in about the 50% of the cases.

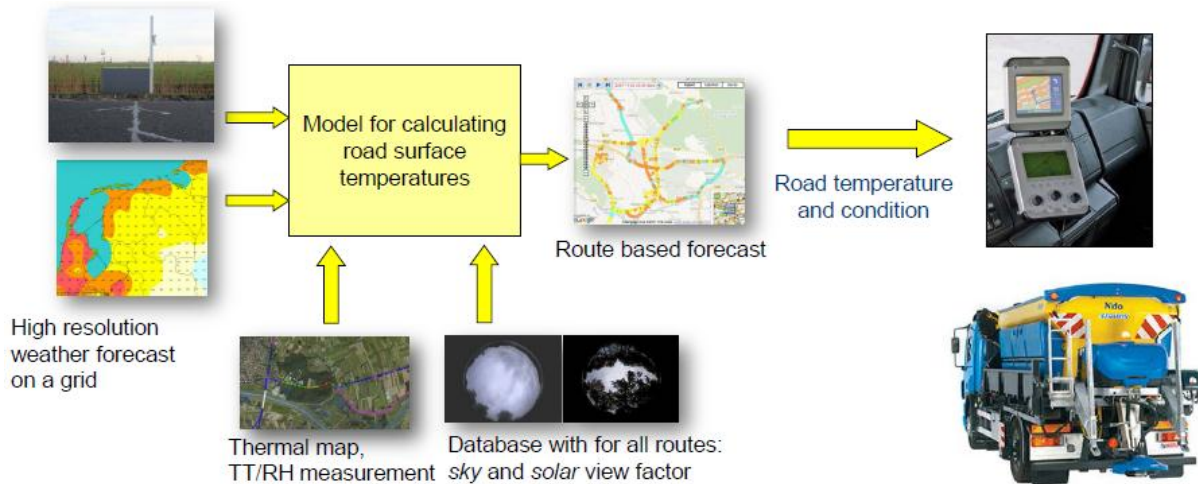


Figure 98: Recommendations' summary to road operators and drivers from TU Wien research study [92].

4.1.3 Real-time information services

A final aspect that RWIS may take in consideration is **information to drivers**. Road maintenance services must involve road travelers in the loop in order to minimize road safety risks caused by a weather event; the use of a variety of real-time travel information services must be typically considered for this goal. But how are these channels be efficiently used in order to induce the expected reaction by drivers and travelers? This is typically a very challenging task, since (i) all this is strictly linked with the hot topic of responsibility attribution, and (ii) the interaction between these services and the end-user is still an unknown topic, which can significantly vary as a function of a variety of factors (mobility need, user background, type of HMI used, pre-trip / en-route information, alternatives availability, just to cite a few).

A nice research was recently carried out by the Finnish Meteorological Institute (FMI), which defined a so-called **weather service chain analysis** (WCSA), i.e. an approach that tries to improve the traditional cost-loss approach in order to better estimate the social-economic benefits of improvements in weather services [95]. Several studies have already demonstrated that (i) the largest factor in accident reduction when adverse weather is expected is traffic volume reduction, in particular of less skilled drivers; and (ii) the road accidents are typically higher during the summer, when the road conditions are typically "ideal". In the RWIS domain, the cost-loss approach suffers in particular of the following limitations:

- the costs for weather information production are not considered;
- all users of weather information services all perfectly informed;
- prevention costs are zero;

- uncertainty range around the forecast is constant over time and “sufficiently” reduced;
- information level given by 3rd parties services does not affect the final decisions.

For this reason, the entire chain from the forecast generation to the realized benefit for the end-user has been considered. The chain is made up of seven stages that can reduce the potential benefits that a perfect weather information system could realize, namely:

1. the extent to which weather forecast information is accurate;
2. the extent to which weather forecast information contains appropriate data for a potential user;
3. the extent to which a decision maker has (timely) access to weather forecast information;
4. the extent to which a decision maker adequately understands weather forecast information;
5. the extent to which a decision maker can use weather forecast information to effectively adapt behavior;
6. the extent to which recommended responses actually help to avoid damage due to unfavorable weather information;
7. the extent to which benefits from adapted action or decision are transferred to other economic agents.

Specific researches made within the FP7 **EWENT** project (see following paragraph) have demonstrated that in Finland only 14% of the theoretical potential is currently realized, and brings benefits estimated in about 36 million €; and more interesting raising forecast accuracy only would generate an additional 3 million € at most. Figure 99 provides a specific overview of the efficiency of the above stages; stage n.7 was not considered here.

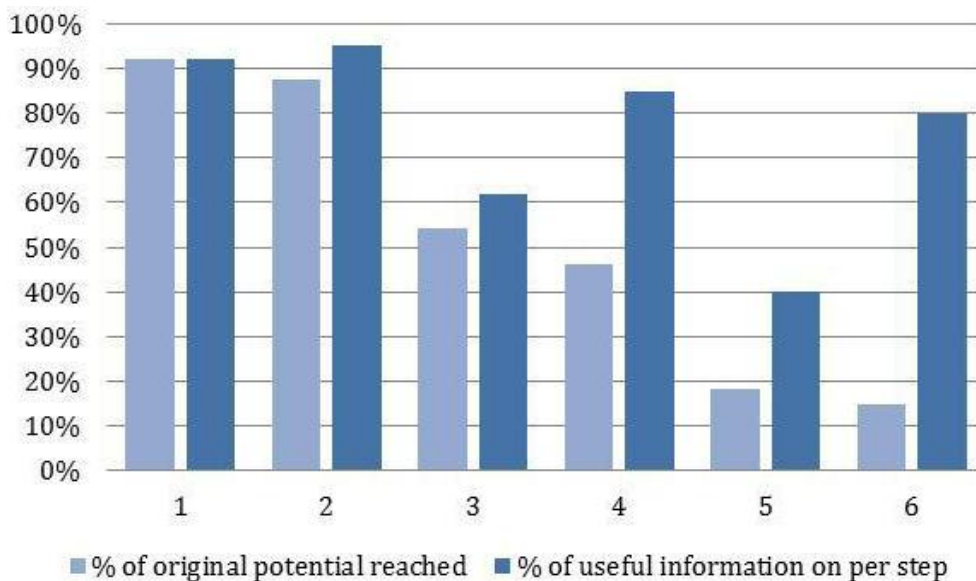


Figure 99: Application of WCSA approach to Finland [95].

Another interesting study completed in the scope of the EWENT project by VTT Technical Research Centre of Finland was related to the assessment of the potential benefits of winter road weather information in Europe [96]. The study demonstrated the **high potential of RWIS-based services in the alpine chain** (in particular in Italy), as a consequence of the existing environment in terms of driving population / road infrastructure / meteorological conditions (expressed in terms of weather accident risks indicator – see Figure 100); it's interesting to see how this potential is much lower in the Nordic area of Europe, despite the harsher conditions of winter seasons.

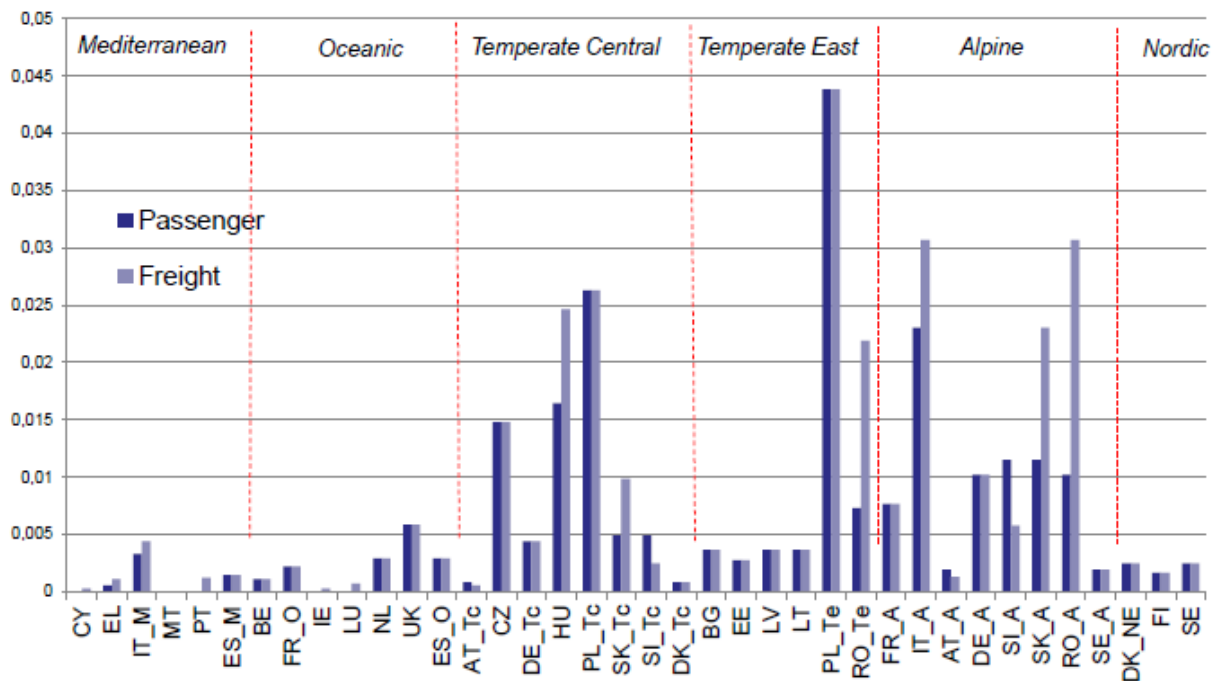


Figure 100: Winter road weather information – potential market in the EU [96].

This study put also in evidence the need for increasing research in the field of the **logistic sector** and **vulnerable road users**, and demonstrated how the **safety impacts** have been already extensively demonstrated - as for example in the US state of Idaho, in which it has been estimated that thanks to several investments in the creation of a network of static RWIS stations it has been possible to generate about 180 million \$ cost savings, with further litigation costs saved of something in the order of 58 million \$ each year [97]. A detailed assessment of the economic savings that a road administration can achieve through a RWIS is furthermore possible through the **Economic Value Tool** (EVT) developed by the international company Vaisala [98].

As already mentioned, different channels can be considered for spreading road weather real-time information. **Online channels** and **on-board telematic services** (typically integrated with real-time traffic information services –see Figure 101) will probably be the dominant market in the near future, and will present self-explaining, unambiguous and consistent messages tailored to the needs of different users. Another typical application destined to road travelers is the use of **Variable Message Signs** (VMSs). In some cases they can be

used also in order to inform drivers that current driving regulations have been currently changed, e.g. **speed limits**.

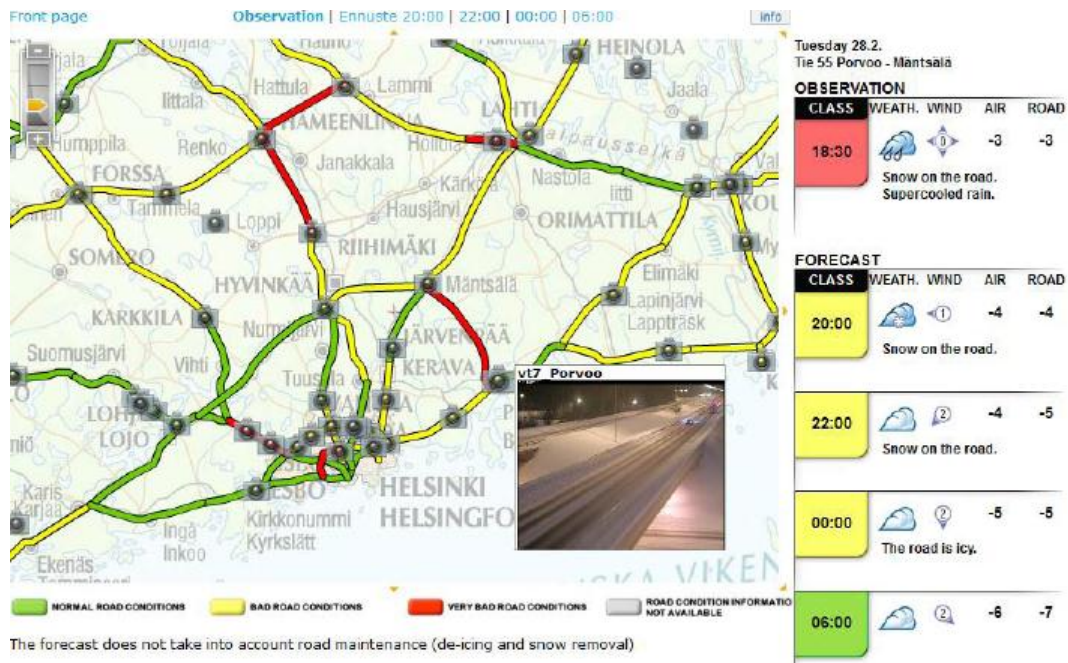


Figure 101: Real-time road weather online service example in Finland [99].

A similar pilot project recently carried out in Sweden, in correspondence of twenty roads characterized by a plenty of intersections, dense populated areas and vulnerable road users, and typical road conditions hazards, demonstrated how this traffic measure can determine less accidents, lower speeds and improved accessibility of these areas [100]. Moreover, about 80% of the local drivers have revealed to be more observant of road conditions if variable speed limits are in use. A dynamic Bayesian network with Markovian prediction for taking in consideration the previous traffic intensity and friction coefficient state was furthermore investigated in order to estimate the optimal speed to recommend drivers as a function of the uncertainty in the road conditions assessment and with the aim to smooth speed updates. Further pilot activities were recently carried out on Germany highways, where the possible impacts of different traffic control strategies have been empirically assessed [101]. Advanced services can be created by properly merging traffic flows and road weather information, as suggested in [102], where a traffic jam predictor based on forecasts coming from both domains has been presented (Figure 102).

4.2 Best-practices overview

A lot of RWIS initiatives are actually place in Europe, US and Japan. The following pages provide a short summary of the most relevant pilot initiatives and R&D international projects.

4.2.1 Pilot initiatives

The East of Europe is one of the most active macro-regions in the world where RWIS have been increasingly spread in the last years. For example, **Latvia** has today a network of 53

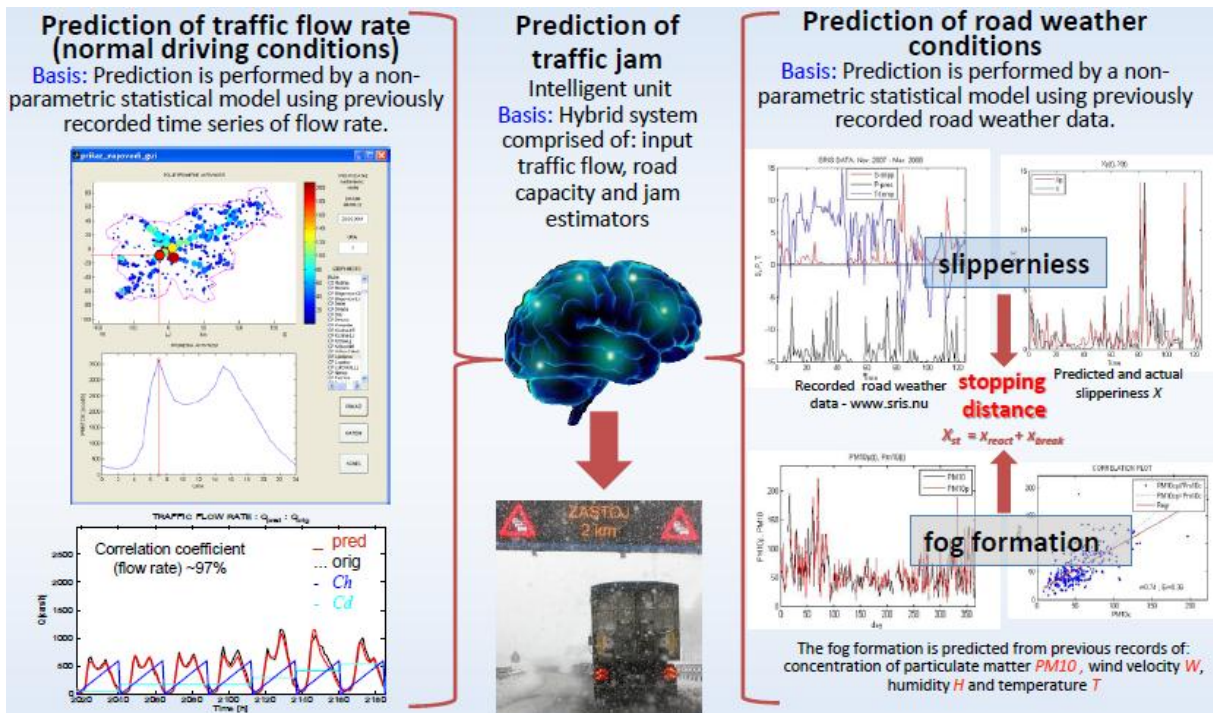


Figure 102: Traffic jam predictor based on traffic flows and road weather forecasts [102].

static RWIS stations covering the 1600-road network (Figure 103), with an average inter-station distance of 20-50 [km]. The stations are typically combined with other traffic detection systems (e.g. weather cameras, traffic counters) and their maintenance is typically outsourced.

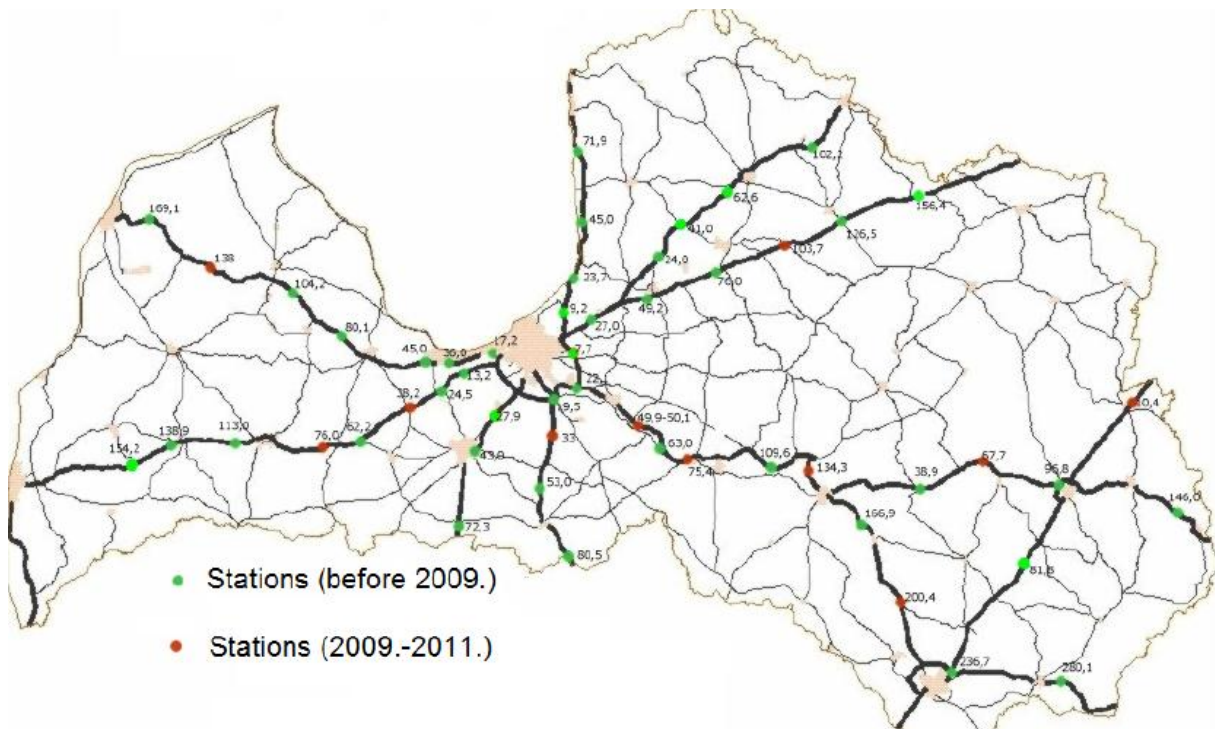


Figure 103: The static RWIS stations' network in Latvia [103].

The central software for data processing and dissemination has been however internally developed and continuously improved by the road administration.

The RWIS is used not only during the winter season, but also in other periods of the year (e.g. spring and summer) for road construction planning purposes. A lot of extensions are actually in place, the most important being (i) the introduction of an automatic decision support tool, and (ii) the creation of an end-to-end open ITS integrated architecture for the dissemination of traffic information (Figure 104).

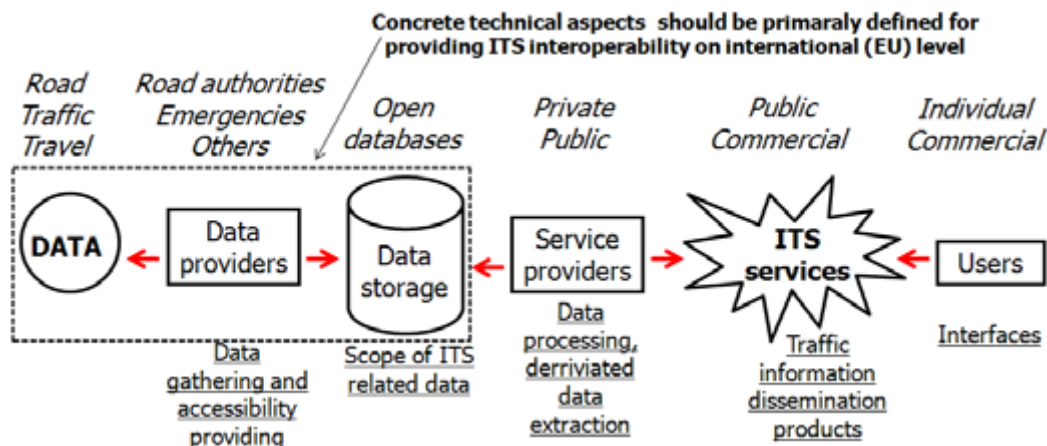


Figure 104: The integrated open ITS business model chain in Latvia [103].

Another active region in Europe in the field of RWIS is **Slovenia**, which has managed in the last years to create a network of about 100 static stations in the whole nation (Figure 105). A road weather model based on **METRo** and **INCA/ALADIN** meteorological forecasts as well a MDSS are actually in use in order to efficiently support winter maintenance activities [104].

METRo is run once every hour, with a forecast horizon of 12 [hours]. Empirical validations have demonstrated that the accuracy of the model is about 1,6 [°C] in case of 6h nowcasts and 2,2 [°C] in case of 12h forecasts, but different results are obtained as a function of the daytime in which the model is executed. The inclusion of INCA/ALADIN meteorological forecasts have demonstrated to improve a lot the accuracy of the outputs, but a real step forward will be possible once some advanced functionalities will be included in METRo, e.g. sky-view factor and statistical approaches for the pre- and post-processing of input and output variables.

Similar road weather models are in use even in **Slovakia**, where a network of 115 static RWIS stations is available [105]. Road maintainers have at disposal a GUI where they can easily check the road stretches with risky situations. At present predictions can reach an error of up to 4 [°C], and current improvement activities are therefore focused on the modeling capabilities of models through an extended evaluation of radiation fluxes components.



Figure 105: The static RWIS stations' network in Slovenia [104].

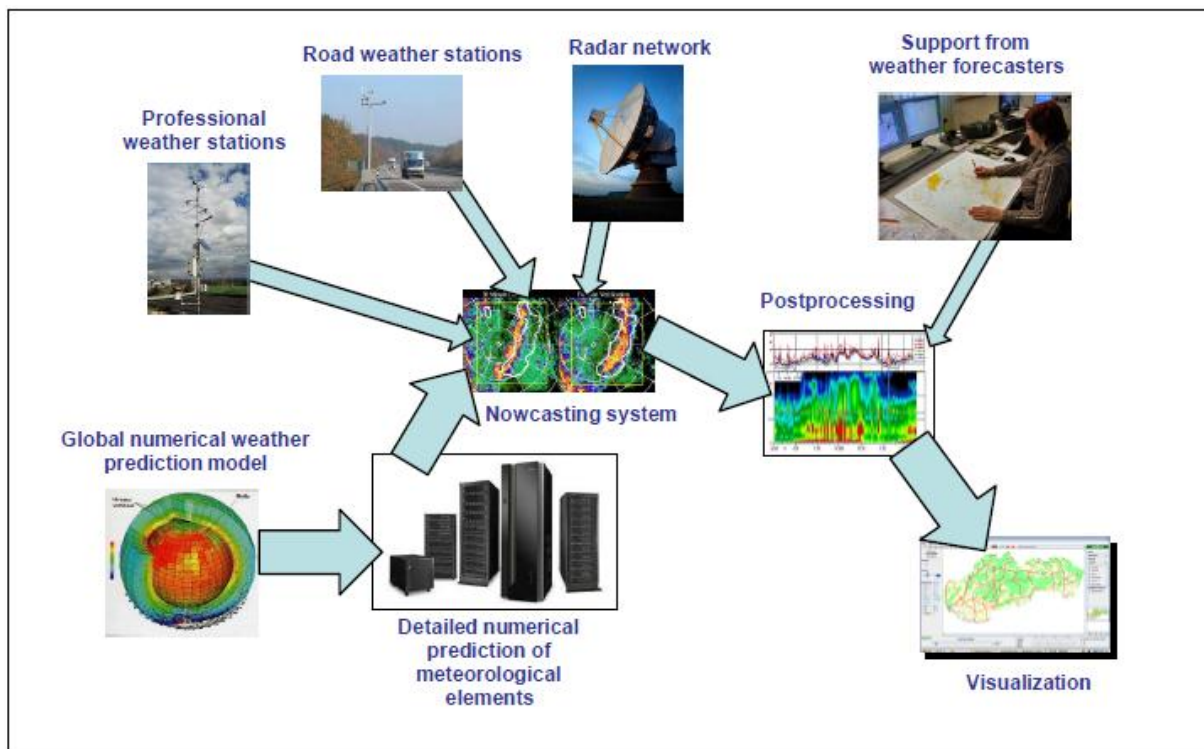


Figure 106: The RWIS in use in Slovakia [105].

A relevant pilot experience is the one carried out by **ASFINAG**, the main highway operator in Austria. ASFINAG manages a road network of about 2.000 [km], with about 1.500 employees on duty 24/7 [106]. A complete MDSS has been introduced in partnership with the private company Boschung GmbH in order to simplify winter road maintenance activities (Figure 107).

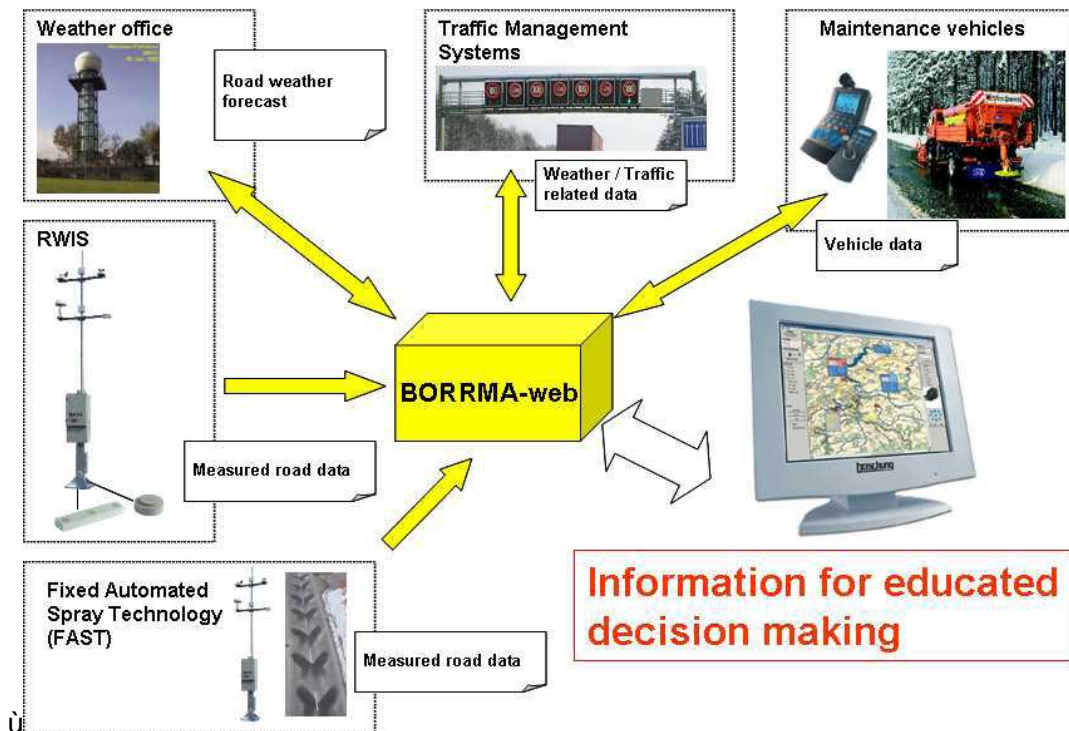


Figure 107: The RWIS used by ASFINAG [106].

Mobile data provided by the fleet of maintenance vehicles are considered in the system as well for visualization and route-based forecasts purposes. In fact, the RWIS includes a 1D road weather forecast model which is spatially extended by means of those (historical) mobile measurements. Special focus has been devoted to **HMIs** and **involvement of road maintenance staff** in order to understand how to best present the plenty of available information (Figure 108).

A very high importance to RWIS is given in **the North America** as well. Considering that that the different Department of Transportation (DOT) in the USA's snow-belt states spend typically more than US\$2 billion a year for winter operations (about 25% of their entire maintenance budget), even minor improvements in road weather operations have the potential to determine very significant savings. An evidence of what is possible to achieve in this part of the world thanks to a RWIS is given by the best practice carried out by the **Indiana DOT (INDOT)**, which decided to introduce a MDSS in 2008-2009 as part of a three year pilot project in partnership with the private company **Meridian Environmental Technology**, owned by Iteris. This action allowed INDOT to save US\$12 millions in year one by reducing salt by 40,9% (228.470 [tons]), while saving further US\$1.4 million by reducing overtime payments to staff by 25,7% [107].

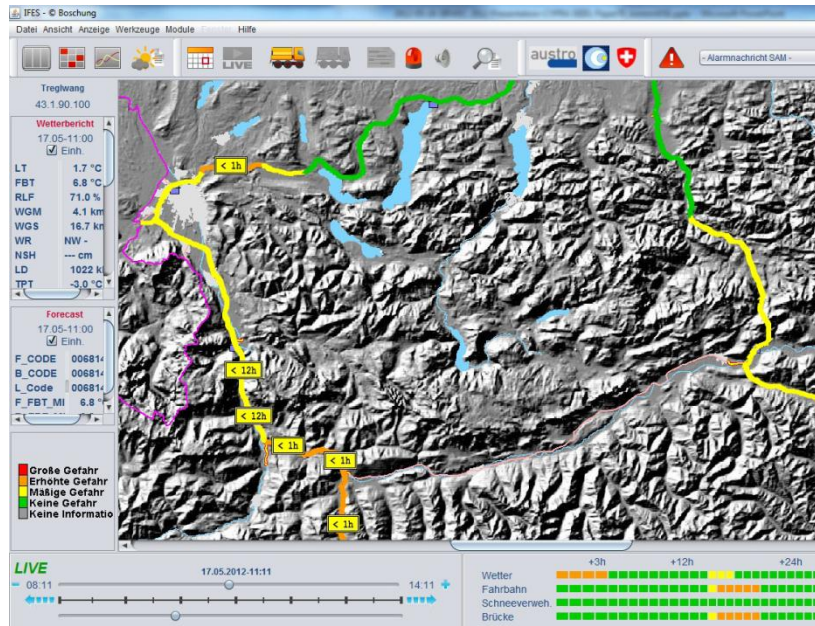


Figure 108: The MDSS HMI used in ASFINAG RWIS [105].

The **U.S. Department of Transportation (DOT) Federal Highway Administration (FHWA) Road Weather Management Program** started already in 1999 in introducing a federal MDSS prototype, in strong partnership with all interested state maintenance managers. In 2004, in partnership with the **Intelligent Transportation Systems Joint Program Office (ITS-JPO)**, the **Clarus** initiative was started, with the goal to create a robust data assimilation, quality checking, and data dissemination system that could provide near real-time atmospheric and pavement observations from the collective state's investments in RWIS. The system was supposed not only to include data from static stations, but also mobile observations collected by the Automated Vehicle Location (AVL) systems of equipped trucks (Figure 109).



Figure 109: The multiple application domains of the Clarus system (source: <http://www.its.dot.gov/clarus/>).



The main goal of the FHWA was to give at disposal of state maintenance managers a common instrument for proactive transportation systems management, but also to create a virtual environment opened to the private sector and academic organizations for the creation of new and improved road weather services. In the last part of this initiative, a two-year regional demonstration was organized with the purpose of deploying the Clarus-enabled services. Five use case scenarios were defined, one focused on the forecasting capabilities of road weather models and the other four on the optimization of maintenance operations; an independent evaluation of these Field Operational Tests (FOTs) was finally carried out in 2011. This empirical experience showed the potential of Clarus in aggregating, integrating, and exchanging data and provided accurate, quality data. State and local agencies that have connected to Clarus recognized the benefits and a growing interest in connecting to Clarus from additional agencies raised up. At the end of 2012, there were 37 states, five local agencies and four Canadian provinces feeding their data into the Clarus system, for a total of 2.253 sensor stations and 81 vehicles [108]. Today, Clarus has been becoming part of the connected vehicle research, and the focus is in understanding how C-ITS can produce significant benefits for the RWIS community. Several local initiatives are on-going in the US states, the most important being:

- an automatic fog detection and warning system in the Caltrans district of California;
- an advanced wind speed monitoring in Florida;
- a weather-responsive traffic management system in Minnesota;
- an automatic weight restriction tool based on RST measurements in Alaska;
- the introduction and continuous assessment of different winter maintenance performance measures in Idaho;
- a weather-driven variable speed limit system in Colorado;
- a performance tool for the assessment of winter maintenance effectiveness in Michigan;
- an automatic dust monitoring system in Arizona;
- an economic assessment of the benefits of RWIS in South Dakota.

Another relevant USA initiative is **MoPED** (*Mobile Platform Environmental Data*), which aims at creating an observation network for the National Oceanic and Atmospheric Administration National Weather Service (NOAA-NWS) [109]. The first prototype of the system was established in 2009, and about 1.500 of “weather boxes” (as they are called) were installed on a fleet of trucks nationwide. These boxes contain various sensors to gather atmospheric conditions at a very high sampling (10 [s]), including temperature, pressure, relative humidity, ozone, precipitation and skylight data. This data is merged with vehicle data available on the CANbus before they are remotely transmitted. Analysis of the data samples reveal how third-party instrumentation on board available in the weather box provide much more accurate and meaningful data than from CANbus, and the quality of this data is unexpectedly good if compared with the one collected by static RWIS stations.

4.2.2 Research projects

Various research activities are in place all around the world in this application domain. As far as European research is concerned, the most interesting activities are located in the North Europe, where most of the attention is devoted to the exploration of the future monitoring capabilities of mobile probes and their integration in “hybrid” observing systems.

In Sweden, probably the most important project initiative is the **BiFi** project (*Bearing information through vehicle intelligence*), which has been investigating the possibility to map the load/bearing strength of roads by a vehicle-based method. The basic idea is to combine vehicular data with weather observations and forecasted weather data in order to model and forecast the road status according to bearing strength. This is a requirement of particular importance for the Swedish environment, since in spring when the ground frost thaws load bearing capacity of the forest roads is greatly reduced, and force road maintainers to close them. This is however a damage for companies which need for example to transport heavy goods such as lumber, with the need to find more expensive alternatives to transport it; in Sweden these alternative measures have demonstrated to generate additional costs for 650 million Euros [110]. By introducing an automatic system capable to evaluating the load-bearing capacity of the road network in a detailed and dynamic way it would be possible to significantly reduce these costs. The technology to use vehicles to detect the bearing strength of gravel roads has revealed to be very promising. An algorithm based on collected real-time data from a vehicle’s standard sensors aided by additional accelerometers has been developed and extensively validated through field trials and reference measurements; the results of the surveys are finally presented to the operator through a user friendly web interface (Figure 110).

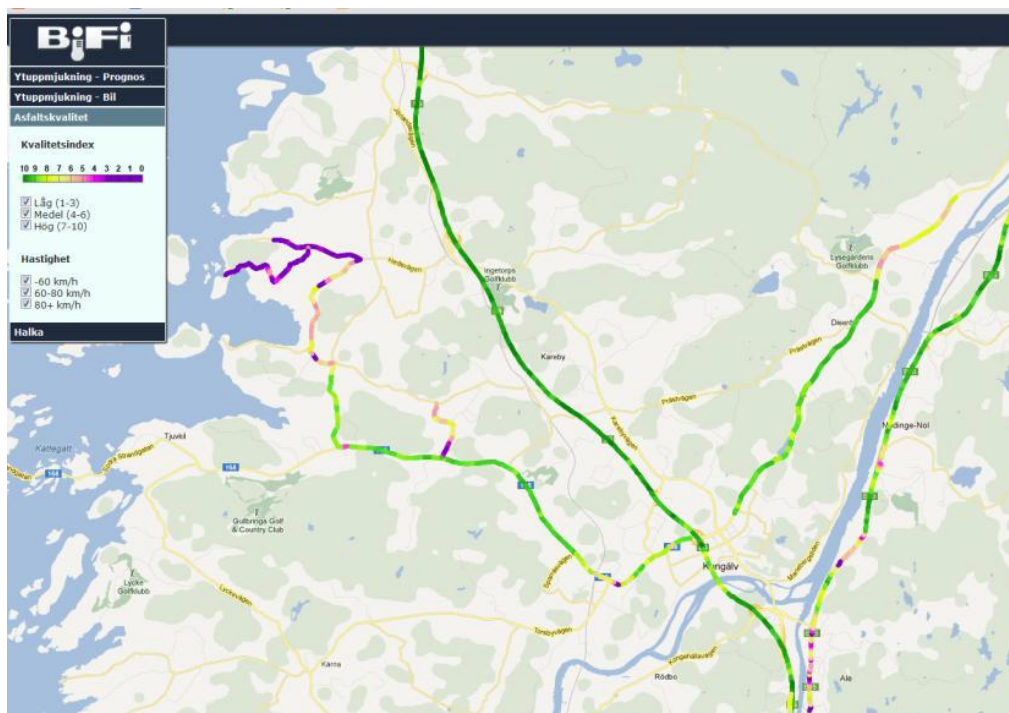


Figure 110: An example of the elaborated information from the BiFi system [110].

Further research activities carried out in Sweden on the use of in-vehicle data for RWIS applications are the **SRIS** (*Slippery Road Information System*) and **SSWM** (*Support System for Winter Maintenance*) projects. In the SRIS project data provided by existing sensors in vehicles about the road condition (ESP, ABS) and other useful information (temperature, windshield wipers etc.), were collected and transmitted to a central database, where data fusion approaches with other road weather data (e.g. coming from static stations) and information (e.g. produced by models) have been specifically investigated (Figure 111).

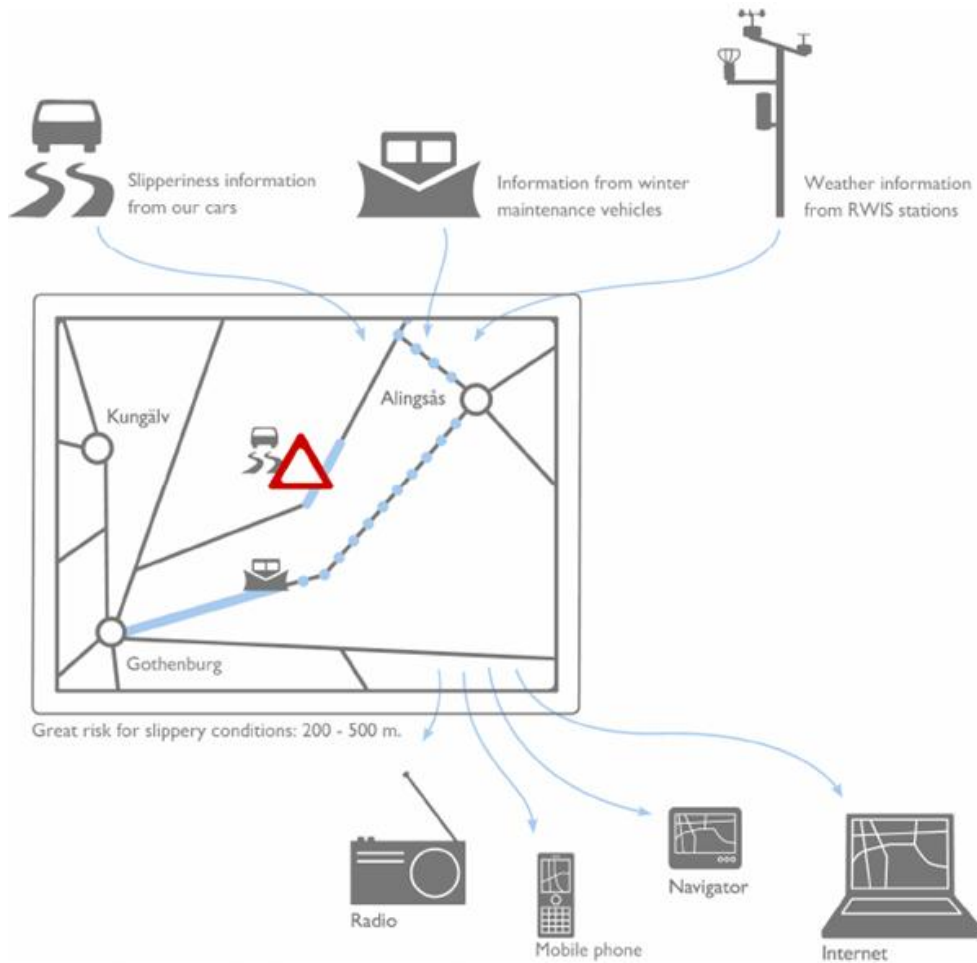


Figure 111: The architecture of the SRIS project [111].

This approach has proven to significantly increase the amount of information and detail concerning the road conditions' assessment; the main advantages have shown to be in terms of (i) spatial extensibility and (ii) higher temporal resolution. The SRIS system was tested in a big FOT during the winter 2007/2008 with 100 among company cars and taxis (90 in Gothenburg and 10 in Stockholm) produced by Volvo and Saab; empirical results demonstrated the elaborated route-based condition map was correspondent to the actual observed conditions, and moreover it has been possible to detect much more alarms than the ones that would have been generated by the static stations only.



Finally, research activities have been carried out by the University of Göteborg in order to understand how information produced by an RWIS could be a valuable input for road maintainers, who actually need a quick and simplified assessment of the overall road network situations based on the plenty of data that today is available. This topic, as well as advancing the available road weather forecasts model, has been the focus of the SSWM project; the interesting part of this research has been the idea to combine an energy-balance model together with a statistical approach based on neural network for accomplishing this task. A prototype of such a MDSS was tested in the Czech Republic during the winter 2007/2008 including first and second class roads, and demonstrated to generate effective cost savings.

Finland is also a EU state where lot of R&D activities are carried out in the field of RWIS by private/public industrial and academic organizations. A wide overview of the numerous EU projects carried out in this European area, in particular in the field of hybrid observing systems is given by **Foreca Consulting** in [112]. The first national initiative in the field of mobile road condition observing was the project **ColdSpots** (2005-2007), initiated after a very serious road accident caused by a very small scale super-cooled rain shower, with the specific aim to improve the state-of-art weather and road condition forecast models by establishing and utilizing a novelty database containing detailed local information on problematic road sections in Finland, which was at the time collected and maintained in a disaggregate way. Mobile observations of road surface state started in 2006, initially by simply mounting optical remote sensors typically installed at the roadside on mobile probes. Having an observation time of about 5 [m], it was possible to have a spatial resolution for this data in the order of 100 [m]. The data collected by the sensor were transmitted on-board through Bluetooth connection. Initial field tests immediately revealed the great potential of mobile observations, with the possibility to assess the spatial variations of RST, but also the need of research in order to guarantee the possibility to make high-quality measurements with little maintenance effort. The accumulation of dirt and slush droplets on instrument lenses pushed researchers to mount the instrument on the car roof; a second set of field measurement with this system configuration (Figure 112) were carried out in the field of the FP7 project **ROADIDEA**, started with the purpose to start developing new and intelligent services and techniques for the transport and traffic sector, including solutions for road weather management. One of the novelties introduced by the project was a friction model combined with a slipperiness-warning system called "*Pulp Friction*" [113], based on statistical assumptions made on top of a variety of different correlation analysis among observed friction and meteorological parameters, as well as to additional mobile observations which were used in order to improve the understanding of road variability patterns.

Research on hybrid observing systems continued with the EU project **GalileoCast**, which aimed at innovating new GNSS-enabled services and in particular, study the feasibility of the Galileo satellite system for road weather services. In the project, the combination of the optimal set of fixed and mobile measurements was also studied, and their specific detection capability of meteorological phenomena that can cause slipperiness or other risks to drivers was assessed, which are typically classified depending on their size (synoptic – 100 [km], mesoscale - [10 km] or microscale – 1 [km]) and life time (typically 24 [h], 6 [h] and 1 [h]).



Figure 112: The evolution of mobile road conditions observations [112].

A nice comparison of the detection capabilities of pure static, pure mobile and hybrid RWIS (i.e. static and mobile) is reported in [112], and is highlighted in Table 14 for the purpose of CLEAN-ROADS project.

Indicator	Static	Mobile	Hybrid
Measurement unit	Equipped masts	Equipped cars with GNSS	Masts and cars
Total units	80	10	90
Spatial resolution	60 [km]	100 [m]	60 [km] & 100 [m]
Temporal resolution	30 [min]	3 [s]	30 [min] & 3 [s]
Observations / day	3.840	172.800	176.640
Detection capability synoptic 100 [km]	100%	100%	100%
Detection capability meso-scale 10 [k]	40%	15%	55%
Detection capability micro-scale [km]	1%	5%	6%
Detection capability topographic effects	No	Yes	Yes
Detection capability lanes (GPS)	No	No	No
Detection capability lanes (Galileo)	No	Yes	Yes

Table 14: Detection capabilities of pure static, pure mobile and hybrid RWIS.

Further researches are now ongoing in numerous new projects, one of which is a European ERA-NET Road project called “Mobi-Roma” (*Mobile Observation Methods for Road Maintenance Assessments*), which started in late 2011. In this project, the idea is to collect mobile data directly from the CAN-bus vehicular network in order to measure the quality of the road surface (roughness, cracks, holes) and the strength of the road bed.

All this sequence of research initiatives have allowed to demonstrate that optimal hybrid observing network could be the best achievable compromise in terms of road weather phenomena detection capabilities and costs: a fixed network can be very significantly extended through a number of mobile observing drives, targeting in particular risky weather



situations and road stretches that are known for their large variability.

Other two EU projects are worth to be mentioned for the scope of this best-practice analysis. The first one is the **INCA-CE** (*Integrated nowcasting for the Central European area*) project, which is concluded INTERREG Central-Europe project aiming at *reducing adverse effects of weather-related natural disasters by establishing a state-of-the-art, high-resolution, real-time analysis and forecast system on atmospheric, hydrological, and surface conditions* [114]. In particular, a high-resolution road weather model has been experimented by combining the analysis and nowcasting system INCA (*Integrated Nowcasting through Comprehensive Analysis*) [115] with METRo. INCA combines station observations, NWP model output as well as remote sensing data (satellite and radar images). High-resolution meteorological analysis and nowcasts for a large number of parameters are produced in output (temporal resolution of 5 [min] and spatial resolution of 1 [km]). The project has in particular focused on generating automatic warnings for delayed ice formation due to falling temperatures after a precipitation event, and for slippery roads due to hoar frost formation; an INCA visibility module has been proposed as well.

The second project is **EWENT**, a FP7 initiative aiming at studying the impacts of hazardous weather on the European transportation system by taking into account the changing climate [116]. An overview of changes in the extreme and adverse winter weather events that are most likely to affect the European transport system, with special consideration for road network, focusing on the observed present climate (1970-2000) and the projected future climate (2040-2070) have been investigated. Individual phenomena, such as heavy snowfall, freezing temperatures, strong wind gusts have been moreover specifically considered. The analysis of the observed changes have revealed some common patterns on a European-wide level: high frequency of winter extremes in Northern Europe and Alpine regions, and a strong continental effect in the frequency of cold spells. A decline has been however observed in the probability of frost days and cold spells during the period studied, with a tendency towards wetter winters in Scandinavia and Eastern Europe. In terms of projected future climate the winter extremes are predicted to moderate by 2050s. Cold extremes are expected to become rarer, with a substantial decrease in the north and less accentuated over southern Europe in moderate cold extremes. The projected changes as well as large natural variability in weather extremes on transportation network will have impacts of both signs. The decline in the frequency of extreme cold and snowfall over most of the continent involves a positive impact on road transportation, e.g. reducing the cost of maintenance and also the frequency of days with slipperiness, thus the accident rate. On the other hand in northern Europe not only the heavy snowfall events are expected to become more frequent but the probability of slippery road conditions may also increase due to the more frequent near 0 [°C] temperatures. The expectedly more frequent freeze-thaw cycle will have a significant negative impact also on the road infrastructure, accelerating road deterioration and resulting in higher maintenance costs and higher life-cycle costs.



5. A glance to cooperative ITS

Before concluding this report, it is of fundamental importance to give an insight about the future connected perspectives in the transportation domain. The so-called cooperative intelligent transportation systems, which aim to put in connection always and everywhere road transport elements through a new generation of vehicular communication technologies (*vehicle-to-vehicle*, V2V and *vehicle-to-infrastructure*, V2I), promise to generate a real revolution in the transportation sector. Giving a complete overview of what is currently moving in this domain is impossible and out of the scope of this report; the aim here is to give some insights of C-ITS basic elements and highlight the first step of the international RWIS community towards these topics.

5.1 Cooperative Vehicle Infrastructure technologies

If it's possible to identify an initiative that kicked-off all the C-ITS attention worldwide, than this has to be related to the FP6 CVIS (*Cooperative Vehicle Infrastructure Systems*) project, which designed, developed and test the core technologies which are needed to allow cars to communicate with each other and with the nearby roadside infrastructure, and thus to enable a wide range of potential cooperative services to run on an open application framework in the vehicle and roadside equipment [117]. The project introduced an open architecture and system concept which is the basis of all the first C-ITS standards, and firstly addressed potential issues such as user acceptance, data privacy and security, system openness and interoperability, risk and liability, public policy needs, cost/benefit and business models, as well as roll-out plans for implementation.

The work done in CVIS was the base of the standardization work that was initiated at ETSI, and which produced the first specifications of the high-level architecture illustrated in Figure 113. Four main sub-systems are identified:

- the **personal ITS subsystem**, i.e. the applications and functionalities running on a personal mobile device;
- the **vehicle ITS subsystem**, i.e. the connected telematic elements located within the a vehicle;
- the **roadside ITS subsystem**, which is made up by the networked components installed in correspondence of the roadside;
- the **central ITS subsystem**, i.e. all the centralized equipment, typically localized in correspondence of traffic management centers.

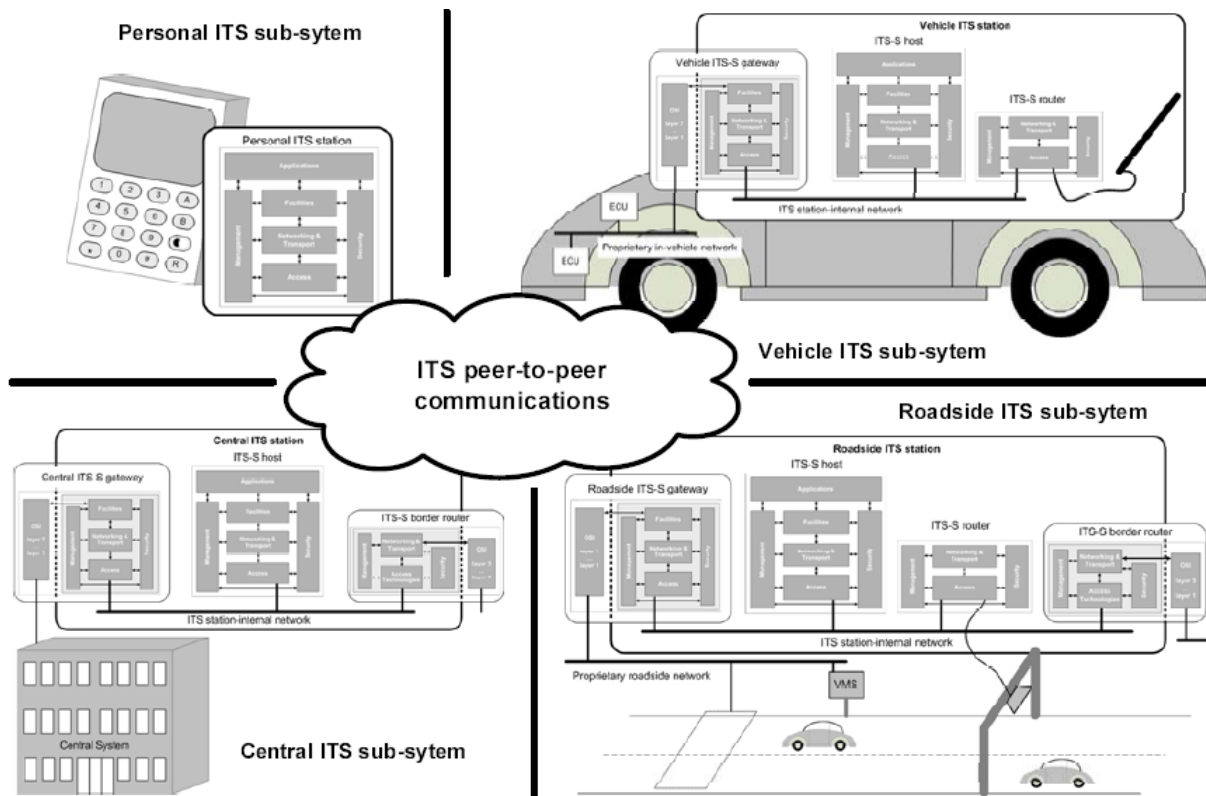


Figure 113: The architecture of a C-ITS system [118].

5.2 C-ITS projects in the RWIS domain

The initiatives worldwide trying to link C-ITS systems and technologies and RWIS are actually still limited; apart from the ambitious programs that the FHWA is carrying on, only a couple of EU projects are actually covering this gap. The details of these projects are briefly presented in the following paragraphs.

5.2.1 WiSafeCar

WiSafeCar is a project funded by the CELTIC Plus funding program which was carried out on top of an initial project initiative called CarLink by nine companies and research centers across Europe and Asia which first investigated the possibility to use a complete C-ITS architecture for putting connected cars in the conditions to exchange e.g. warnings about poor road conditions, and let drivers to adapt their itineraries and driving behavior accordingly [119]. The advantages of these future connected scenarios are in particular relevant in case of sudden and unavoidable events, which need to be directly addressed through ad hoc communications between vehicles and/or roadside equipment. The focus of the project was in particular on the enabling of a set of preliminary services belonging to three categories: (i) accident and incident warnings, (ii) driving convenience info services, and (iii) road weather alerts.

The platform considered in WiSafeCar is made up of vehicles, roadside units acting as system base stations and local weather stations, with the host systems as a linking point

beyond the base station network, linking data transfer between regular Internet and the WiSafeCar network. The V2V communication environment is in line with the ETSI standardization choices; all vehicles form a VANET (*vehicular area network*), compatible with IEEE 802.11p standard, i.e. they do not have continuous connectivity but operate in an ad-hoc manner with each other whenever possible, typically when two cars pass each other. A vehicle will get up-to-date traffic platform service data always when passing the vicinity of a roadside unit through the linking point located in the fixed network.

The system was piloted in off-line operation since the autumn of 2011 in the Tampere region in Finland. Five pilot vehicles were equipped with measurements for temperature, wipers on/off, emergency lights on/off, fog lights on/off, ABS (*Anti-lock Braking System*), ESC (*Electronic stability control*), high beam on/off and 3D-accelerations. A public pilot was conducted on January 25th 2012, in which the online services of road weather warnings, accident and incident warnings and approaching emergency vehicle warnings were delivered to four pilot vehicles and one advanced road side unit.

5.2.2 CoMoSeF

CoMoSeF is the follow-up project of WiSafeCar, giving natural continuity to the early investigations done in this first research initiative. This project has started recently (July 2012) and is expected to close in mid 2015. The consortium has further broadened if compared with the previous one, and pilot activities are expected to take place in Finland, Luxembourg, Poland, Romania, Sweden, Spain, Turkey and Republic of Korea. An external pilot is going to be organized in Russia as well during the the Sochi Winter Olympics in 2014.

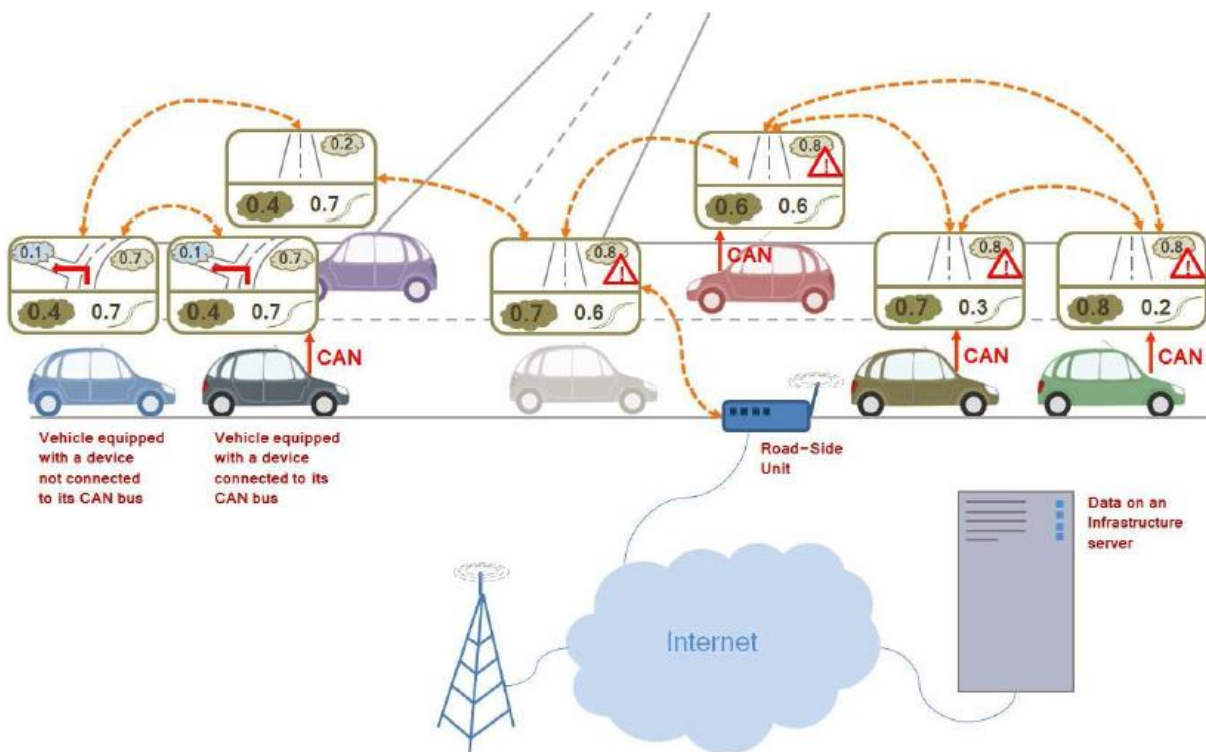


Figure 114: The architecture of the CoMoSeF project [120].

The project will cover in broader term the potential of cooperative mobility solutions, in the perspective of the large scale deployments that many Member States are actually about to start; a specific cooperation is going to be activated with the FP7 DRIVE-C2X project [120]. Sensor units, service platforms and communication technologies that will be used will be closer to market, and detailed business models will be started to be analyzed. The expectation of project partners is to use the CoMoSeF as a basic platform for the creation of a nationwide platform for Finland, to be linked to existing commercial vehicles' fleets, with and without access to the CAN-bus network (Figure 114).

5.3 Early commercial connected products for RWIS

A couple of “connected” products specifically destined for RWIS applications are starting being commercialized. In this work of analysis, the following products have been discovered:

- a **next generation roadside ITS subsystem** developed by the Swedish company Combitech, based completely on FOSS components [122];
- an **on-board assisted road condition monitoring system** called AVL Genius aided by machine vision and artificial intelligence technologies, commercialized by the Canadian company Viaesys.

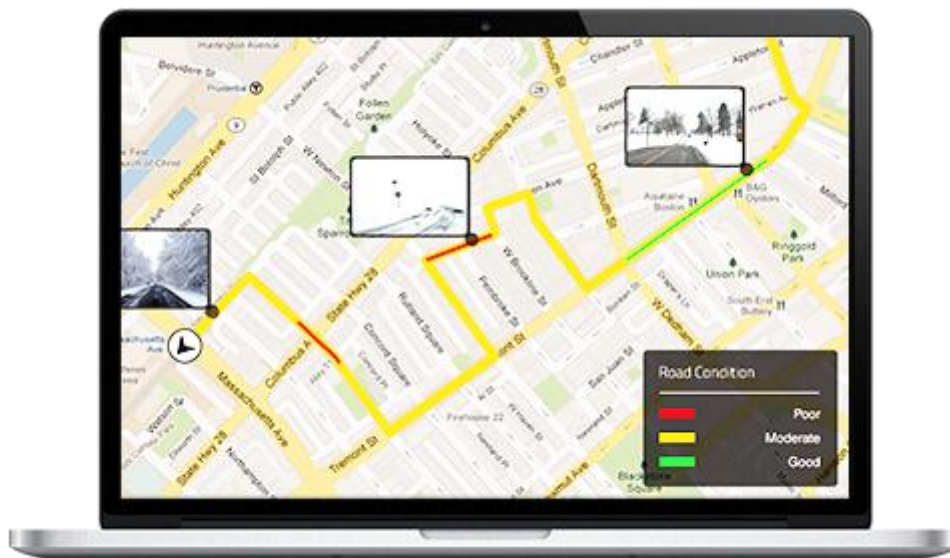


Figure 115: A screenshot of the AVL Genius application (source: www.viaesys.com).



Conclusions

The deliverable has offered a comprehensive glance of the state-of art of RWIS and its enabling technologies. Significant steps forward have been carried out in the last years, and several pilot initiatives are now in place in different parts of the world, in particular in North America and in North Europe where the winter seasons are harsher. The evolution of computing and web-based technologies, as well the future development of fully-connected scenarios offer today new perspectives for RWIS, which is now rapidly moving from 2D state-of-art route-based forecast system to N-dimensional systems in which the decision support systems is enriched by a plenty of detailed information layers (e.g. salting routing optimization techniques, probabilistic approaches, etc.). The role of mobile RWIS station is becoming increasingly higher, and the combination of these novel monitoring sources with traditional static roadside stations has been already demonstrated in several research projects. The focus of research is now moving from classic road weather models improvement to other domains of interest, ranging from low-cost mobile road conditions sensors to proper HMIs able to efficiently present the big amount of information that RWIS are now in the condition to collect. All these elements are properly taken in consideration in the definition of the CLEAN-ROADS system, so that it can not only fully match the expectations of the target user groups but also to contribute to the technical development of RWIS solutions worldwide.



Bibliography

- [1] L. Chapman, J. E. Thornes and A. V. Bradley, "Modelling of road surface temperature from a geographical parameter database. Part 1: Statistical," *Meteorological Applications*, vol. 8, no. 4, pp. 409-419, 2001.
- [2] Wikipedia, "Sub-base (pavement)," [Online]. Available: [http://en.wikipedia.org/wiki/Subbase_\(pavement\)](http://en.wikipedia.org/wiki/Subbase_(pavement)). [Accessed 2012].
- [3] SIRWEC International Road Weather Commission, "A Guide to Road Weather Systems," 2010.
- [4] L. Chapman, D. Hammond and J. Thornes, "Parameterizing road construction in road weather models - Is Ground Penetrating Radar the way forward?," in *SIRWEC Conference*, Quebec City, 2010.
- [5] Università di Napoli, "Il comfort negli spazi esterni," [Online]. Available: http://www.architettura.unina2.it/docenti/areaprivata/43/documenti/6_4.pdf. [Accessed 2012].
- [6] L. Chapman, J. E. Thornes and A. V. Bradley, "Modelling of road surface temperature from a geographical parameter database. Part 2: Numerical," *Meteorological Applications*, vol. 8, no. 4, pp. 421-436, 2001.
- [7] D. Cornford and J. E. Thornes, "A comparison between spatial winter indices and expenditure on winter road maintenance in Scotland," *International Journal of Climatology*, vol. 16, p. 339–357, 1996.
- [8] T. R. Oke, *Boundary layer climates*, Routledge, 1992.
- [9] L. Kumar, A. Skidmore and E. Knowles, "Modelling topographic variation in solar radiation in a GIS environment," *International Journal of Geographical Information Science*, vol. 11, no. 5, pp. 475-497, 1997.
- [10] J. Thornes, "Thermal mapping and road-weather information systems for highway engineers," *Highway Meteorology*, pp. 39-67, 1991.
- [11] M. Eriksson and J. Norrman , "Analysis of station locations in a road weather information system," *Meteorological Applications* , vol. 8, p. 437–448, 2001.
- [12] A. K. Andersson, T. Gustavsson, J. Bogren and B. Holmer, "Geographical distribution of road slipperiness in Sweden, on national, regional and county scales,"



Meteorological Applications, vol. 14, p. 297–310, 2007.

- [13] R. Tabony, "Relations between minimum temperature and topography in Great Britain," *Journal of Climatology*, 1985.
- [14] J. Shao, J. Swanson, R. Patterson, P. Lister and A. McDonald, "Variation of winter road surface temperature due to topography and application of thermal mapping," *Meteorological Applications*, vol. 4, pp. 131-137, 1997.
- [15] J. Bogren and T. Gustavsson, "Nocturnal air and road surface temperature variations in complex terrain," *International Journal of Climatology*, vol. 11, no. 4, pp. 443-455, 1991.
- [16] B. W. Thompson, "Small-scale katabatics and cold hollows," *Weather*, vol. 41, no. 5, pp. 146-153, 1986.
- [17] K. Keen, "The development of a nocturnal warm air layer within a shallow valley," *South African Geographical Journal*, vol. 57, pp. 135-138, 1968.
- [18] T. Gustavsson, "Variation in road surface temperature due to topography and wind," *Theoretical Applications of Climatology*, vol. 41, pp. 227-236, 1990.
- [19] L. Chapman, "Assessing topographic exposure," *Meteorological Applications*, vol. 7, pp. 335-340, 2000.
- [20] T. Gustavsson and J. Bogren, "Evaluation of a local climatological model – test carried out in the county of Halland, Sweden," *Meteorological Magazine*, vol. 122, pp. 257-266, 1993.
- [21] J. Bogren, T. Gustavsson, M. Karlsson and U. Postgard, "The impact of screening on road surface temperature," *Meteorological Applications*, vol. 7, no. 2, pp. 97-104, 2000.
- [22] T. Gustavsson, "A study of air and road surface temperature variations during clear windy nights," *International Journal of Climatology*, vol. 15, pp. 919-932, 1995.
- [23] T. Gustavsson, M. Karlsson, J. Bogren and S. Lindqvist, "Development of temperature patterns during clear nights," *Journal for Applied Meteorology*, vol. 37, pp. 559-571, 1998.
- [24] M. Karlsson, "Nocturnal temperature variations between forest and open areas," *Journal of Applied Meteorology*, vol. 39, pp. 851-862, 2000.



- [25] D. G. Steyn, "The calculation of view-factors from fisheye lens photographs: research note," *Journal of Atmospheric Oceanic Sciences*, vol. 18, no. 3, pp. 254-263, 1980.
- [26] D. Marks and J. Dozier, "A clear-sky longwave radiation model for remote alpine areas," *Theoretical and Applied Climatology*, vol. 27, no. 2-3, pp. 159-187, 1979.
- [27] T. R. Oke, G. T. Johnson, D. G. Steyn and I. D. Watson, "Simulation of surface urban heat islands under 'ideal' conditions at night. Part 2: Diagnosis of causation.," *Boundary Layer Meteorology*, vol. 56, pp. 339-358, 1991.
- [28] A. V. Bradley, J. E. Thornes and L. Chapman, "Variation and prediction of urban canyon geometry from sky-view factor transects," *Atmospheric Science Letters*, pp. 1-11, 2001.
- [29] Postgard and Nunez, "Continuous measurement of sky-view factors along roads and their relationships to air and road surface temperature," *Università di Goteborg*, 2000.
- [30] L. Barring, J. O. Mattson and S. Lindqvist, "Canyon geometry, street temperatures and urban heat island in Malmö, Sweden," *Journal of Climatology*, vol. 5, pp. 433-444, 1985.
- [31] I. Eliasson, "Urban nocturnal temperatures, street geometry and landuse," *Atmospheric Environment*, vol. 30, pp. 379-392, 1996.
- [32] H. Upmanis, "The influence of sky-view factor and land-use on city temperatures. Personal communication," *University of Gothenburg, Sweden*, 1999.
- [33] C. S. Grimmond, S. K. Potter, H. N. Zutter and C. Souch, "Rapid methods to estimate sky-view factors applied to urban areas," *International Journal of Climatology*, vol. 21, pp. 903-913, 2001.
- [34] D. B. Johnson, "Urban modification of diurnal temperature cycles in Birmingham, UK," *Journal of Climatology*, vol. 5, pp. 221-225, 1985.
- [35] E. Graham, "The urban heat island of Dublin city during the summer months," *Irish Geography*, vol. 26, pp. 45-57, 1993.
- [36] R. G. Barry and R. J. Chorley, *Atmosphere, Weather & Climate*, Routledge, 1992.
- [37] A. Fujimoto, A. Saida, T. Fukuhara and T. Futagami, "Heat Transfer Analysis on Road Surface Temperature Near a Traffic Light," in *ITS World Congress, Busan (Korea)*, 2010.



- [38] L. Chapman and J. E. Thornes, "Small-scale road surface temperature and condition variations across a road profile.," in SIRWEC, Praga, 2008.
- [39] B. S. Parmenter and J. E. Thornes, "The use of a computer model to predict the formation of ice on road surface," Transport and Road Research Laboratory Research Report, vol. 1, pp. 1-19, 1986.
- [40] T. Gustavsson, J. Bogren and C. Green, "Road climate in cities: a study of the Stockholm area, south-east Sweden," Meteorological Applications, vol. 8, pp. 481-490, 2001.
- [41] J. M. Prusa, M. Segal, B. R. Temeyer, W. A. Gallus and E. S. Takle, "Conceptual and scaling evaluation of vehicle traffic thermal effects on snow/ice covered roads," Journal of Applied Meteorology, vol. 41, pp. 1225-1240, 2002.
- [42] L. Chapman and J. E. Thornes, "The influence of traffic on road surface temperatures: implications for thermal mapping studies," Meteorological Applications, vol. 12, no. 4, pp. 371-380, 2005.
- [43] J. Shao, "A winter road surface temperature prediction model with comparison to the others," University of Birmingham (unpublished Phd thesis), 1990.
- [44] J. E. Thornes and J. Shao, "A comparison of UK ice prediction models," Meteorological Magazine, vol. 120, pp. 51-57, 1991.
- [45] S. Lindqvist, "Local climatological modelling for road stretches and urban areas," Geografiska Annaler, vol. 74, pp. 265-274, 1992.
- [46] M. Lawrence, "The Relationship between Relative Humidity and the Dewpoint Temperature in Moist Air," 2005. [Online]. Available: <http://journals.ametsoc.org/doi/pdf/10.1175/BAMS-86-2-225>.
- [47] M. Erpicum, M. Frederic, G. Mabilie, T. Nyssen and S. Litt, "Real-time regional automatic mapping of nocturnal road temperatures: application of methodology of analogous situations, the case of Walloon region (Belgium)," 2005.
- [48] SFC Energy AG, "Power Anywhere and Anytime for Road Weather Stations," 2011. [Online]. Available: http://www.efoy-pro.com/sites/default/files/download/130411_traffic_roadweatherstations.pdf.
- [49] New Energy Technologies Inc., "Motion Power," [Online]. Available: <http://www.newenergytechnologiesinc.com/technology/motionpower>.



- [50] C. Chen, "Evaluation of resistance-temperature calibration equations for NTC thermistors," *Measurement*, vol. 42, no. 7, pp. 1103-1111, 2009.
- [51] Aanderaa Data Instruments, "Road Condition Sensor," [Online]. Available: <http://www.aanderaa.com/media/pdfs/Road-Condition-Sensor-3565-3565E.pdf>.
- [52] K. Sarabandi, E. S. Li and A. Nashashibi, "Modeling and Measurements of Scattering from Road Surfaces at Millimeter-Wave Frequencies," *IEEE TRANSACTIONS ON ANTENNAS AND PROPAGATION*, vol. 45, no. 11, pp. 1679-1689, 1997.
- [53] R. Finklele, "Detection of ice layers on road surfaces using a polarimetric millimetre wave sensor at 76 GHz," *Electronics Letters*, vol. 33, no. 13, pp. 1156-1154, 1997.
- [54] J. Fraden, *Handbook of Modern Sensors: Physics, Designs and Applications*, San Diego (USA), Advanced Monitors Corporation, 2004.
- [55] W. P. Cheng, Z. G. Zhao, X. W. Liu, Z. X. Zhang and C. G. Suo, "A Capacitive Humidity Sensor based on Multi-Wall Carbon Nanotubes (MWCNTs)," *Sensors*, vol. 9, pp. 7431-7444, 2009.
- [56] Mumirel, "HS110/HS1101 Technical Data Sheet," 2002.
- [57] K. Hwan Kim, "A noncontact intraocular pressure measurement device using a micro reflected air pressure sensor for the prediagnosis of glaucoma," *Journal of Micromechanics and Microengineering*, vol. 22, no. 3, 2012.
- [58] Y. Zhang, S. Massoud-Ansari, G. Meng, W. Kim and N. Najafi, "A Ultra-Sensitive High-Vacuum Absolute Capacitive Pressure Sensor," Interlaken (Switzerland), 14th IEEE International Conference on Micro Electro Mechanical Systems (2001).
- [59] D. B. DeGraaff and J. K. Eaton, "A high-resolution laser Doppler anemometer: design, qualification and uncertainty," *Experiments in Fluids*, vol. 30, no. 5, pp. 522-530, 2001.
- [60] N. Hautiere and A. Boubezoul, "Combination of Roadside and In-Vehicle Sensors for Extended Visibility Range Monitoring," in *Sixth IEEE International Conference on Advanced Video and Signal Based Surveillance*, Genova (Italy), 2009.
- [61] P. T. Martin and Y. Feng, "Detection Technology Evaluation," Department of Civil and Environmental Engineering, University of Utah (Traffic Lab), 2003.
- [62] W. Huber, M. Lädke and R. Ogger, "Extended Floating Car Data," in *Proceedings of the 4th World Congress on Intelligent Transport Systems*, Berlin, 1997.

- [63] S. Messelodi, C. Modena, M. Zanin, F. De Natale, F. Granelli, E. Betterle and A. Guarise, "Intelligent extended floating car data collection," *Expert Systems with Applications*, vol. 36, no. 3, pp. 4213-4227, 2009.
- [64] M. Malmivuo, "Friction Meter Comparison Study 2011," in *SIRWEC Conference 2012*, Helsinki, 2012.
- [65] L. Chapman, D. S. Hammond and J. E. Thornes, "Parameterizing road construction in route-based road weather models: can ground-penetrating radar provide any answers?," *Measurement Science and Technology*, vol. 22, no. 5, 2011.
- [66] R. Buizza, "Ensemble forecasting: why is it valuable?," in *International Summer School on Atmospheric and Oceanic Services (ISSAOS)*, L'Aquila, 2013.
- [67] Finnish Meteorological Institute, "Model serves its purpose," [Online]. Available: <http://en.ilmatieteenlaitos.fi/model-serves-its-purpose>. [Accessed 2013].
- [68] J. Kukkonen, T. Olsson, D. M. Schultz, A. Baklanov, T. Klein, A. I. Miranda, A. Monteiro, M. Hirtl, V. Tarvainen, M. Boy, V. H. Peuch, A. Poupkou, I. Kioutsioukis, S. Finardi, M. Sofiev, R. Sokhi, K. E. Lehtinen, K. Karatzas, R. San José, M. Astitha, G. Kallos, M. Schaap, E. Reimer, H. Jakobs and K. Eben, "A review of operational, regional-scale, chemical weather forecasting models in Europe," *Atmospheric Chemistry and Physics*, vol. 12, pp. 1-87, 2012.
- [69] Consortium for Small-Scale Modelling, "A Description of the Nonhydrostatic Regional COSMO-Model," [Online]. Available: <http://www.cosmo-model.org/content/model/documentation/core/default.htm>. [Accessed 2013].
- [70] European Centre for Medium-Range Weather Forecasts, "Scientific and technical documentation of the ERA-40 ECMWF Integrated Forecast System," [Online]. Available: http://www.ecmwf.int/research/ifsdocs_old/. [Accessed 2013].
- [71] CISMA s.r.l., "WRF weather forecasts," [Online]. Available: <http://www.cisma.bz.it/wrf-alpha/00Z/main.html>. [Accessed 2013].
- [72] S. Pecora, "A federated global national regional hydrologic data sharing by the CUAHSI HIS architecture," in *CUAHSI Conference on Hydroinformatics and Modeling*, Logan (Utah) - USA, 2013.
- [73] Bundesamt für Meteorologie und Klimatologie (MeteoSchweiz), "MAP-NWS – an Optional EUMETNET Programme in Support of an Optimal Research Programme," 2006.



- [74] L. Chapman and H. Handa, "Robust Route Optimization for Gritting/Salting Trucks: A CERCIA Experience," *IEEE Computational Intelligence Magazine*, no. February, pp. 6-9, 2006.
- [75] J. E. Thornes, "The prediction of ice formation on motorways in Britain," Unpublished PhD thesis, 1984.
- [76] J. E. Thornes and B. S. Parameter, "The use of a computer model to predict the formation of ice on road surfaces," Transport and Road Research Laboratory Research, 1986.
- [77] J. Shao and S. A. Jones, "Area Forecast Model for Winter Road Maintenance over a Road Network," in *Convegno SIRWEC*, Helsinki, 2012.
- [78] L. P. Crevier and Y. Delage, "METRo: A New Model for Road-Condition Forecasting in Canada," *Journal of Applied Meteorology*, vol. 40, pp. 2026-2037, 2001.
- [79] Canadian Meteorological Center, "METRo: Model of the Environment and Temperature of Roads," [Online]. Available: <http://home.gna.org/metro/>. [Accessed 2013].
- [80] D. Chen, T. Gustavsson and J. Bogren, "The applicability of similarity theory to a road surface," *Meteorological Applications*, vol. 6, pp. 81-88, 1999.
- [81] S. Frankenstein and G. Koenig, "Fast All-season Soil STrength (FASST)," U.S. ARMY CORPS OF ENGINEERS, 2004.
- [82] US Army Corps of Engineers, "FASST (Fast All-season Soil STrength) Model," [Online]. Available: <https://webcam.crrel.usace.army.mil/FASST/>. [Accessed 2013].
- [83] Geotop.org, "GEOtop: a distributed hydrological model with coupled water and energy balance," University of Trento, [Online]. Available: <http://www.geotop.org>. [Accessed 2013].
- [84] J. Shao and P. J. Lister, "An Automated Nowcasting Model of Road Surface Temperature and State for Winter Road Maintenance," *Journal of Applied Meteorology*, vol. 35, pp. 1352-1361, 1996.
- [85] D. S. Hammond, "The validation and improvement of route-based road weather forecasts," School of Geography, Earth & Environmental Sciences, University of Birmingham, 2011.
- [86] P. J. Brockwell and R. A. Davis, *Introduction to Time Series and Forecasting*, Second



Edition, Colorado State University: Springer, 2001.

- [87] S. Hertl and G. Schaffar, "An autonomous approach to road temperature prediction," *Meteorological Applications*, vol. 5, pp. 227-238, 1998.
- [88] L. Chapman and J. E. Thoners, "A blueprint for 21st century road ice prediction," in 11th SIRWEC Conference, Sapporo, 2002.
- [89] National Center for Atmospheric Research, Research Applications Laboratory, "A Comparison of Road Temperature Models: FASST, METRo and SNTHERM," Boulder, Colorado (USA), 2007.
- [90] L. Chapman, "Probabilistic Road Weather Forecasting," in SIRWEC conference, Helsinki, 2012.
- [91] R. Hagendorn, "A road map towards implementing a probabilistic road weather information system," in SIRWEC conference, Helsinki, 2012.
- [92] M. Hoffmann, P. Nutz and R. Blab, "New findings in winter maintenance and their implementation in Austria," in SIRWEC conference, Helsinki, 2012.
- [93] P. Nutz and M. Hoffmann, "Towards real-time skid resistance forecast," in SIRWEC conference, Helsinki, 2012.
- [94] I. W. Smeding, M. J. Wokke, M. F. Jonker, M. Noort and M. Mimpfen, "Use a route based forecast for dynamic gritting," in SIRWEC conference, Helsinki, 2012.
- [95] A. Perrels, P. Nurmi and V. Nurmi, "Weather service chain analysis (WSCA) - An approach for appraisal of the social-economic benefits of improvements in weather services," in SIRWEC conference, Helsinki, 2012.
- [96] E. Pilli-Sihvola, P. Leviäkangas and R. Hautala, "Better winter road weather information saves money, time, lives and environment," in SIRWEC conference, Helsinki, 2012.
- [97] K. Greening, D. Johns, P. Bridge and R. Koeberlein, "A study to determine the effects of employing a well maintained RWIS network on accident rates on major highways in the US state of Idaho," in SIRWEC conference, Helsinki, 2012.
- [98] P. Bridge and D. Atallah, "Road Weather Information System (RWIS) & Maintenance Decision Support System (MDSS) - Economic Value Tool (EVT)," in SIRWEC conference, Helsinki, 2012.



- [99] T. Dubrovin and Y. Pilli-Sihvola, "Automated Road Condition Forecasts on a Public Map Service," in SIRWEC conference, Helsinki, 2012.
- [100] P. Jonsson, "Decision support system for variable speed regulation," in SIRWEC conference, Helsinki, 2012.
- [101] S. Grosanic, A. Dinkel and S. Piszczek, "Optimized traffic control with benchmarked road weather data," in SIRWEC conference, Helsinki, 2012.
- [102] I. Grabec and F. Švegl, "Forecasting of traffic jams on high-ways caused by adverse weather," in SIRWEC conference, Helsinki, 2012.
- [103] B. Jelisejevs and I. Brivulis, "Further development of RWIS and it's new potential marketplaces in Latvia," in SIRWEC conference, Helsinki, 2012.
- [104] R. Kršmanc, A. Šajn Slak, S. Čarman and M. Korošec, "METRo Model Testing at Slovenian Road Weather Stations and Suggestions for Further Improvements," in SIRWEC conference, Helsinki, 2012.
- [105] M. Benko, "Road weather forecasts and MDSS in Slovakia," in SIRWEC conference, Helsinki, 2012.
- [106] T. Cypra and W. Seidl, "Maintenance Decision Support System (MDSS) ASFINAG / Austria – Experience of a Comprehensive Winter Maintenance Management System," in SIRWEC conference, Helsinki, 2012.
- [107] T. McClellan, M. Coleman, P. Boone and K. Carpenter, "Implementing a Winter Maintenance Decision Support System," 2009.
- [108] P. Pisano, R. M. Alfelor and G. N. Guevara, "Road Weather Management – Recent Research Results from the United States," in SIRWEC conference, Helsinki, 2012.
- [109] P. Heppner, B. Bell and A. Orrego, "Real-Time Mobile Platform Environmental Data," in 92nd American Meteorological Society Annual Meeting, New Orleans, 2012.
- [110] T. Gustavsson and J. Bogren, "BiFi - Bearing information through vehicle intelligence," in SIRWEC conference, Helsinki, 2012.
- [111] SRIS project consortium, "SRIS Report first season," 2007.
- [112] P. Saarikivi, "Development of mobile optical remote road condition monitoring in Finland," in SIRWEC conference , Helsinki, 2012.



- [113] ROADIDEA consortium, "Project final report," 2010.
- [114] B. Bica, A. Kann and I. Meirold-Mautner, "Enhanced Road Weather Warnings and Improved Communication Strategies within Central Europe as part of the INCA-CE project," in SIRWEC conference, Helsinki, 2012.
- [115] T. Haiden, A. Kann, C. Wittmann, G. Pistotnik, B. Bica and C. Gruber, "The Integrated Nowcasting through Comprehensive Analysis (INCA) System and Its Validation over the Eastern Alpine Region," *Weather and Forecasting*, vol. 26, pp. 166-183, 2011.
- [116] A. Vajda, H. Tuomenvirta and P. Jokinen, "Observed and future changes of extreme winter events in Europe with implication for road transportation," in SIRWEC conference, Helsinki, 2012.
- [117] CVIS consortium, "CVIS - Cooperative Vehicle Infrastructure systems," [Online]. Available: <http://www.cvisproject.org/>. [Accessed 2012].
- [118] ETSI, "ETSI EN 302 665: Intelligent Transport Systems (ITS): Communications Architecture," 2010.
- [119] T. Sukuvaara and P. Nurmi, "Connected vehicle safety network and road weather forecasting – the WiSafeCar project," in SIRWEC conference, Helsinki, 2012.
- [120] CoMoSeF consortium, "Project information: "CoMoSeF: Co-operative Mobility Services of the Future"," Celtic-Plus, 2012.
- [121] European Center for Information and Communication , "DRIVE C2X Project," [Online]. Available: <http://www.drive-c2x.eu>.
- [122] M. Töyrä and J. Ericson, "Intelligent road side platform for future applications," in SIRWEC conference, Helsinki, 2012.
- [123] K. A. Makinwa and J. Huijsing, "A smart wind sensor using thermal sigma-delta modulation techniques," *Sensors and Actuators*, Vols. 97-97, pp. 15-20, 2002.
- [124] K. A. Makinwa and J. H. Huijsing, "A wind-sensor interface using thermal sigma delta modulation techniques," *Sensors and Actuators*, vol. 92, no. 1-3, pp. 280-285, 2011.